THE MECHANISM OF MODULATION OF THE *ESCHERICHIA COLI* DNA HELICASE II (UVRD) UNWINDING ACTIVITY, A STUDY OF THE 2B SUBDOMAIN

Matthew J. Meiners

A dissertation submitted to the faculty of the University of North Carolina at Chapel Hill in partial fulfillment of the requirements for the degree of Doctor of Philosophy in the Department of Biology.

Chapel Hill
2014

Approved by:

Steve Matson

Dorothy Erie

Jeff Sekelsky

Greg Copenhaver

Tom Kunkel

ABSTRACT

Matthew J. Meiners: The mechanism of modulation of the *Escherichia coli* DNA Helicase II (UvrD) unwinding activity, a Study of the 2B subdomain
(Under the direction of Steve Matson)

Helicases are ubiquitous motor proteins which catalyze the separation of double stranded DNA into single stranded DNA for the purposes of replication, recombination and repair. *Escherichia coli* DNA helicase II, also known as UvrD, is a Superfamily 1 helicase involved in post-replicative mismatch repair, nucleotide excision repair and conjugative recombination. These roles that UvrD fills in the cell require dramatically different unwinding activities to be performed accurately. Nucleotide excision repair only requires a 12-13 bp section of DNA to be unwound for efficient repair, while methyl-directed mismatch repair and recombination can require upwards of 1 kilobase of DNA to be traversed for the processes to be faithfully completed. These contrasting activity requirements are even more confusing when one examines the *in vitro* processivity of UvrD, which has been measured to be on the order of 40 of bp unwound in a single event. This begs the question how is the activity of UvrD regulated to perform these roles which require converse activity levels in the cell?

This dissertation offers evidence that the 2B subdomain of UvrD is involved in modulating the activity of the helicase. Mutations within this subdomain have been linked to dramatically stimulated helicase activity which I have shown is due to an increase in the processivity of the unwinding reaction. In addition, the data presented here suggest that this

subdomain is the interaction site between UvrD and other proteins which have been shown to have a stimulatory effect on the unwinding activity of UvrD. However, deletion of this subdomain in its entirety does not seem to stimulate the helicase activity of UvrD as it has been shown to do in other Superfamily 1 helicases.

It can be concluded that the 2B subdomain plays a poorly understood role in regulating the unwinding activity of UvrD and this work offers an exploratory look in to the roles this subdomain performs in the regulation of the helicase.

For Mom and Dad

ACKNOWLEDGEMENTS

I would like to thank my advisor, Steve Matson, for all the effort and work he has dedicated to my graduate career. Without doubt, I could not have asked for a better advisor, collaborator, and friend. I fully realize how fortunate I have been to benefit from his years of experience and excellence in the field. Likewise, I want to offer my deepest feelings of appreciation to my committee for their tireless efforts. Your valuable input has shaped me into a better scientist capable of more than I ever thought possible.

I also want to thank my family, specifically my parents and sisters who always believed in and never doubted my capabilities. This work represents the fruition of my formal education process to this date and I want to thank you all for your help and guidance these last 25 years of my scholastic endeavors.

All of my accomplishments would not be possible without the love and support of my best friend, Cassidy Rupp. She has been on this journey with me for near its entirety and has been a source of unwavering strength through the highs and lows of the graduate school process. Every success was shared and every set back was overcome with her help and support. I would not be where I am today without her. Thank you.

TABLE OF CONTENTS

LIST OF TABLES

LIST OF FIGURES

LIST OF ABBREVIATIONS

AMP-PNP	Adenosine-5′-(β,γ-imido) triphosphate
ATP	Adenosine-5′- triphosphate
ATP-γ-S	Adenosine-5′-O-(3-thiotriphosphate)
BER	Base excision repair
BSA	Bovine serum albumin
bp	base pair
CBD	Chitin binding domain
D403A	403rd amino acid, aspartic acid, changed to alanine
D404A	404th amino acid, aspartic acid, changed to alanine
DNA	Deoxyribonucleic acid
DSBR	Double strand break repair
dsDNA	Double-stranded deoxyribonucleic acid
DTT	Dithiothreitol
E. coli	Escherichia coli
EDTA	Ethylenediamine tertaacetic acid
EGTA	Ethylene glycol tetraacetic acis
FRET	Fluorescence resonance energy transfer
HEPES	N-[2-hydroxyethel] piperazine -N′-[2-ethanesculfonic acid]
IDL	Insertion/deletion loops
IPTG	Isopropyl-β-D-thiogalactopyranoside
LB	Luria-Bertani broth
MMR	Methyl-directed mismatch repair
NaPi	Sodium Phosphate
NER	Nucleotide excision repair

NTP	Nucleotide triphosphate
OD	Optical density
PCR	Polymerase chain reaction
PMSF	Phenylmethanesulfonyl fluoride
PNK	Polynucleotide kinase
rATP	Riboadenosine triphosphate
SDS	Sodium dodecyl sulfate
SDS-PAGE	Sodium dodecyl sulfate polyacrylamide gel electrophoresis
SF	Superfamily
ssDNA	Single-stranded deoxyribonucleic acid
TBE	Tris base, boric acid, and EDTA
TE	Tris-HCl (pH8.0) EDTA
Tris	Tris [hydroxymethyl] aminomethane
ZY	1% N-Z-amine, 0.5% yeast extract
ZYM5052	1% N-Z-amine, 0.5% yeast extract, 50mM phosphate, 0.5% glycerol, 0.05% glucose, 0.2% lactose
α-[^{32}P]ATP	Adenosine-5′- triphosphate ^{32}P labeled on the α phosphate
α-[^{32}P]dCTP	2′Deoxycytidine-5′-triphosphate ^{32}P labeled on the α phosphate
β-ME	2-mercaptomethanol
γ-[^{32}P]ATP	Adenosine-5′- triphosphate ^{32}P labeled on the γ phosphate
Δ2B	Deletion of the UvrD 2B subdomain

CHAPTER 1: DNA HELICASES

Helicases are a class of motor proteins defined by their ability to catalyze the separation of complementary strands of a duplex nucleic acid. The "unwinding" of these substrates is powered by the energy derived from the hydrolysis of nucleoside 5′-triphosphates (NTPs) (1-4). Helicases are ubiquitous and found in nearly every organism, from prokarya to ekuarya and in viruses. Helicases have been demonstrated to be required for a wide array of cellular events, from DNA replication and repair to RNA processing (5-7). Regardless of the specific task the helicase performs, this class of enzymes shares a common similarity, the NTP hydrolysis-driven disruption of hydrogen bonds between complementary base pairs of a duplex nucleic acid.

The first helicase discovered was purified from *Escherichia coli* and was shown to catalyze the separation of double stranded DNA (dsDNA) (8). DNA helicase I, as this enzyme was named, was subsequently found to be involved in the transfer of the F plasmid between *E. coli* cells (9). Since the discovery of the first helicase, hundreds of new helicases have been identified in nearly all forms of life. The universal presence of helicases reflects their importance in many fundamental nucleic acid metabolic processes, such as replication, recombination, DNA repair, and transcription. One common element these processes share is the need for double stranded nucleic acids to be separated into their respective single strands to provide the template or intermediate required for these cellular events.

Though the basic reaction these enzymes catalyze may be similar, there are many different types of helicases with very specific roles and functions. Some helicases, such as *E.*

coli DnaB can processively unwind thousands of base pairs in a single binding event (10). Others, such as UvrD, the subject of this dissertation, possess a processivity on the order of 40 base pairs unwound in a single event (11). In addition, the functional form of the enzyme can vary widely from one helicase to another. Some helicases, such as the T7 bacteriophage gene 4 protein, have been shown to function as hexamers of identical subunits (12). Others such as *E. coli* Rep helicase unwind DNA as a dimer or higher order oligomer (2, 13). Still others, such as *E. coli* RecQ, appear to unwind DNA as a monomer (14).

These differences, as well as similarities in amino acid sequence, have formed the basis of the classification of these enzymes into groups called superfamilies. Initially the delineation segmented helicases into three distinct groups based predominantly on amino acid sequence similarity (15-18). This initial classification proved to be insufficient to differentiate between bona fide helicases, which physically separate the duplex into its component strands and "putative" helicases, which couple the hydrolysis of NTPs to movement along nucleic acids but do not facilitate duplex separation. More recent investigations have expanded the number of categories to six: Superfamilies 1 (SF1), 2 (SF2), 3 (SF3), 4 (SF4), 5 (SF5), and 6 (SF6) (15, 19).

SF1 and SF2 are the largest and most closely related of the groups, containing members from viral, prokaryotic and eukaryotic species. These two families of helicases share seven conserved amino acid motifs, all of which are required for the biological function of these enzymes (18). The high degree of similarity within these motifs would suggest that these regions are directly involved in fundamental activities required for helicase function. Structure-function studies have shown this to be the case (16, 18).

In SF1 helicases, studies of the seven motifs have clarified many of the roles played by these highly conserved regions of the proteins. Motifs I and II, which are the most highly conserved across all six superfamilies, are described as the Walker A and B motifs present in many NTP binding proteins (20). In helicases, these two motifs were shown to be crucial for the binding and hydrolysis of NTPs in order to unwind duplex nucleic acids. The mutation of the invariant lysine in motif I in the SF1 helicase UvrD resulted in a helicase with a large decrease in the rate of ATP hydrolysis and an inability to catalyze duplex DNA unwinding. (21). Additional mutations within UvrD motifs I and II did not impact ATP or DNA substrate binding, but directly affected the ability of the enzyme to hydrolyze ATP (22, 23). Mutations within motif III resulted in helicases that were unable to bind ATP or DNA ligands (24). Additionally, one point mutation in motif III of UvrD resulted in the loss of the ability of the helicase to initiate unwinding from a nicked DNA duplex, the biological substrate for UvrD (25). Studies in the SF1 helicases Rep and UvrD suggest that motif IV greatly decreases the helicases ability to bind ATP (26, 27). Motif V in Rep helicase was shown to interact with the DNA backbone of the substrate (28) and motif V of UL5, a SF1 helicase from herpes virus, was shown to have a role in ssDNA binding (29). Lastly, even though motif VI in the Rep helicase crystal structure was not observed to make contacts with either the nucleotide or ssDNA substrate, it was seen to make contacts with motifs IV and III. These data may indicate that motif VI is involved in the coupling of the energy derived from ATP hydrolysis to the unwinding of the duplex substrate.

SF2 is the single largest single superfamily, including both DNA and RNA helicases. These enzymes have a diverse number of roles in the cell (17, 18). Similar to SF1 helicases, this class of enzyme also possesses the seven conserved helicase motifs, which all appear to

be required for proper *in vivo* function of these helicases (30-33). There has been some evidence to suggest that even though these motifs are conserved between SF1 and SF2, there are some differences in their functions. Motifs I and II were seen to be functionally similar to their counterparts in SF1 helicases, while the other motifs were quite different. Motifs III and IV seem to share little, if any, sequence similarities between SF1 and SF2 helicases. Additionally, motifs III and IV from SF2 NS3 helicase from the hepatitis C virus and SF1 helicase such as Rep and UvrD appear to be located in different relative positions (34) and perform different tasks (28, 35). Motif V exhibits limited sequence similarity between SF2 and SF1 proteins, but mutations within this motif exhibit similar defects to those previously mentioned in SF1. Mutations within the NS3 helicase motif V have demonstrated DNA binding defects (36, 37). Motif VI is the third most conserved motif between SF2 and SF1 helicases. Defects within this motif in SF2 helicases resulted in nucleic acid binding defects (38). Studies (35, 39) suggested that motif VI in NS3 helicase is part of the energy transduction mechanism, coupling NTP hydrolysis to DNA unwinding, as described above for motif VI in SF1 helicases. These studies indicate that most, if not all, of the seven conserved motifs are associated with the NTPase activity of helicases. It would appear that the conserved motifs act as a functional unit and have been thought of as the components that form the NTP hydrolysis-driven motor of the helicase.

Of all the SF1 helicases, the best studies are the Rep and UvrD helicases from gram negative bacteria and the PcrA helicases from gram positive bacteria. These helicases exhibit a high degree of similarity, sharing approximately 40% overall amino acid sequence identity and about 90% within the conserved motifs (3). In addition to their amino acid similarities, crystal structure analysis has revealed that all three helicases contain two structural domains

(1 and 2), each further divided into two subdomains (A and B) (28, 40-42). These helicases have been shown to play roles in DNA repair and genome maintenance, and will be discussed in more detail below. Eukaryotes contain SF1 helicases as well, but less in number than are found in bacteria. *Saccharomyces cerevisiae*, contains the well-studied Srs2 helicase, which is thought to have a role in regulating homologous recombination via Rad51 filament disruption (43). Humans contain Fbh1, which appears to be the functional analogue of Srs2 and is also involved in regulating homologous recombination (44, 45) .

One subset of SF2 is the RecQ protein family, consisting of RECQL1, BLM, WRN, RECQL4 and RECQL5 in most mammals. This group of helicases has been referred to as the "guardians of the genome" (5, 46) and defects within these helicase-encoding genes has been linked to premature aging disorders such as Werner's Syndrome and Bloom's Syndrome. These data suggest that RecQ helicases are vital for proper development, and additionally it has been shown that these helicases are active in many forms of DNA repair, including base excision repair (BER) (47-49), double strand break repair (DSBR) (50-53), and DNA replication restart (54, 55).

Superfamilies 3-6 consist of proteins which form hexameric rings and are structurally similar (Reviewed in 12). These classes of helicases are commonly responsible for replicative unwinding and possess the capability of unwinding megabase lengths of DNA in some cases (56). Superfamily 3 helicases were initially identified from viruses, form hexameric or double hexameric rings, and all members unwind their substrates with a 3′ to 5′ directionality (57, 58). Superfamily 4 helicases were first identified in bacteria and bacteriophage (59, 60). Superfamily 5 contains the Rho helicases from bacteria responsible for halting transcription and unwinding DNA/RNA hybrids (61, 62). Lastly, Superfamily 6

contains the mini chromosome maintenance helicase, the main replicative helicase in eukaryotes, and is essential for replication in humans (63).

This disertation will examine the activity of one member of SF1, *E. coli* DNA helicase II, also known as UvrD. This 82 kDa helicase exhibits a well characterized 3′ to 5′ directionality as both a translocase and a helicase (1, 64-66). It has been suggested that UvrD is involved in regulating recombination by hindering RecA filament formation, as well as having well documented roles in both methyl-directed mismatch repair and nucleotide excision repair (67-72)

Methyl-Directed Mismatch Repair and UvrD

DNA polymerases are highly efficient molecular machines and are capable of effectively replicating DNA with minimal errors. However, polymerases occasionally incorporate the incorrect base or create insertion/deletion loops (IDL). *E. coli* DNA polymerase III holoenzyme exhibits an error rate on the order of 10^{-7}-10^{-8} errors per bases synthesized (73). Given the size of the *E. coli* chromosome and the doubling time for a single cell, the absence of a mechanism to recognize and correct errors which escape the polymerase proofreading activity could result in the accumulation of errors. Any unrepaired deleterious mutations within essentials genes would ultimately result in cell death. The methyl-directed mismatch repair pathway (MMR) is a post replicative repair pathway which can recognize and remove non-complementary base pairs and IDLs. The efficiency of this repair pathway coupled with the fidelity of the proofreading polymerase, results in an apparent error occurrence of one uncorrected mismatch in every 10^{10} bases synthesized (73) and maintains the integrity of the *E. coli* genome.

Successful MMR requires two different types of detection within the cell. The machinery must be able to find the mispaired bases in a very large population of base pairs and it must be able to distinguish which of the two strands of DNA contains the wrong information. The strand discrimination signal in *E. coli* is a hemi-methylation of a newly synthesized DNA duplex in which only the parental DNA has been marked via deoxyadenine methyl-transferase (74). This signal is conveyed by the addition of a methyl group to the N6 of the Ade in a d(GATC) sequence on the template DNA, while the daughter DNA remains transiently unmethylated (75). The asymmetric methylation of the duplex DNA targets repair to the newly synthesized, error-containing daughter strand. The second mechanism of detection, the identification of mismatched bases, is performed by the repair protein MutS (76). The mismatched base pairs can generate distortions in the DNA backbone due to the poor stacking of the incorrectly incorporated bases (77). These distortions can be recognized by the MutS homodimer which will bind these mismatches and initiate the repair process. Structural and biochemical studies including atomic force microscopy and total internal reflection microscopy have shown the ability of MutS to interact with mismatched DNA specifically at the site of the base-base mispair (78-80).

In *E. coli* MMR, once the MutS homodimer detects and binds to a mismatch, a MutL homodimer is recruited to the repair site in an ATP-dependent manner (76). This MutL molecule is thought to be the coordinator of MMR, interacting with MutS as well as downstream repair proteins (81-84). MutL induces the sequence/methylation specific endonuclease, MutH, to induce a nick on the daughter DNA strand 5′ to the d(GATC) sequence (85). MutL has been shown to stimulate the MutH nickase activity *in vitro* (86). Repair is bidirectional and can be carried out from either side of the mismatch. After the

daughter strand of DNA is cleaved by MutH, MutL facilitates the loading of UvrD onto the DNA in order to catalyze the separation of the duplex (81). The length of DNA that must be unwound by UvrD for repair is variable depending on the location of the d(GATC) site relative to the mispair but can be in excess of 1 kilobase from the nick induced by MutH. An inverse correlation has been observed between increasing distance of the mismatch from the site of unwinding initiation and the efficiency of repair (87). After the error containing nascent strand of DNA has been displaced by UvrD, it will be degraded by appropriate exonucleases. Finally, DNA polymerase III, assisted by ssDNA binding protein, will fill in the resulting gap and DNA ligase seals the nicked strand completing the repair event (Fig. 1) (88).

It has been suggested that defects in the MMR pathway are directly linked with the emergence of antibiotic resistant strains of bacteria (Reviewed in 89). Strains of bacteria have been isolated from clinical settings which seem to possess a 1000-fold increase in mutation frequency (90, 91). "Mutator" strains found in pathogenic *E. coli* and *Salmonella typhimurium* have been categorized as having defects in *mutS, mutL*, and *uvrD* genes (91-93), and even isolates of vancomycin resistant *Staphylococcus aureus* have been shown to contain frameshifts within the *mutS* gene (94). Any research into the effectiveness of the MMR pathway could elucidate new techniques for countering the increase in emergence of antibiotic resistant strains of bacteria.

In vitro, UvrD can unwind a modest ~40 bases in a single unwinding event (11). It is curious that a helicase with such a modest processivity has evolved to play a role in which it must unwind DNA of much greater lengths than its intrinsic processivity. It has been shown that MutL stimulates the unwinding activity of UvrD, but it is unclear as to how the MutL

stimulation of UvrD-catalyzed unwinding is accomplished (81, 86). The work in this dissertation seeks to clarify the relationship between UvrD and MutL to arrive a better understanding of the mechanism by which MutL stimulates the unwinding activity of UvrD.

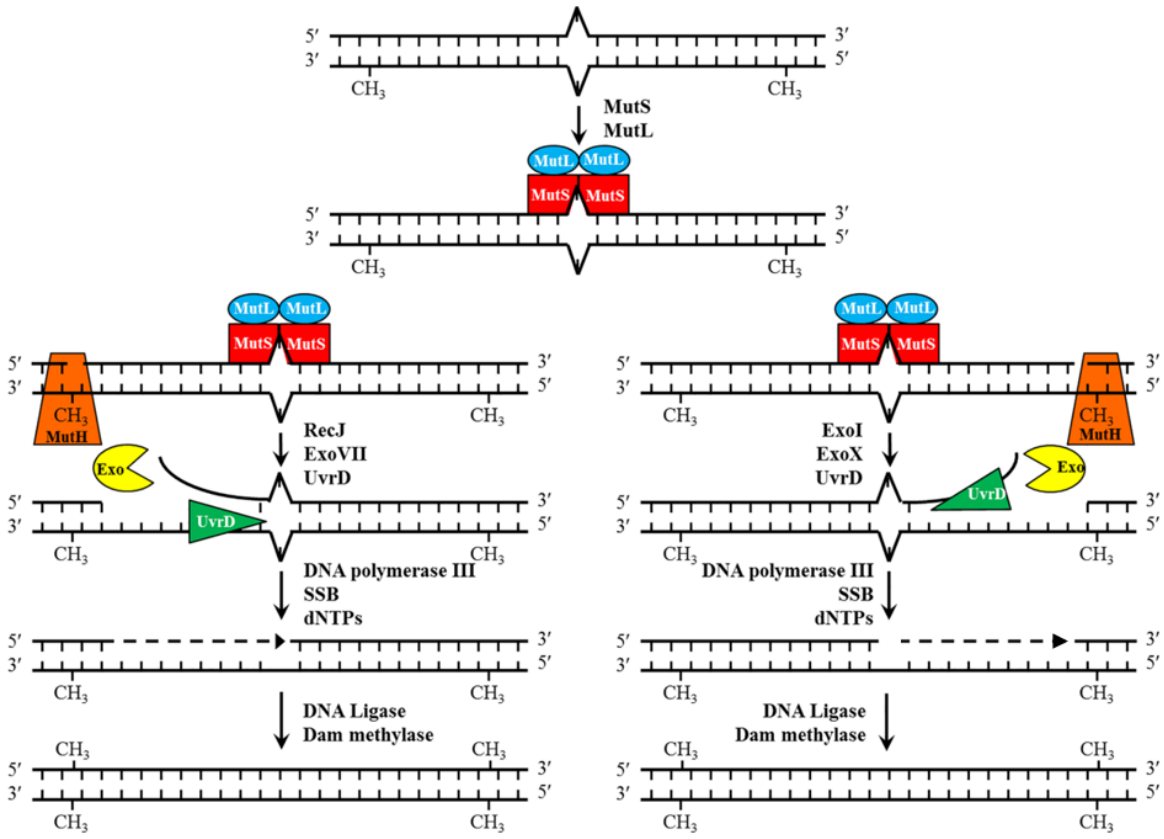

Figure 1. Model of the *Escherichia coli* methyl-directed mismatch repair pathway.

MutL

The *E. coli* MutL protein is a homodimer exhibiting a weak DNA-stimulated ATPase activity, is a member of the GHL ATPase family (95-99), and is required for MMR (81, 83, 95, 100, 101). MutL is comprised of two domains linked by a proline-rich flexible region of ~100 amino acids: an N-terminal ATPase domain and a C-terminal domain (102), referred to

as LN40 (MutL N-terminal 40 kDa) and LC20 (MutL C-terminal 20 kDa), respectively. Both the N –terminal and the C-terminal region of MutL are essential for dimerization of the protein (95). Using size exclusion chromatography in the presence of adenine nucleotides MutL exhibits a more compact structure, suggesting that the N-terminal regions dimerize in response to nucleotide occupancy (96). The MutL-mediated stimulation of UvrD and MutH is dependent on nucleotide binding but not hydrolysis (81, 103, 104). It has been suggested that the two subunits of a MutL dimer come together to form a ring containing a large central channel capable of encompassing duplex DNA (102). This, in turn, may suggest the ability of MutL to increase the processivity of a UvrD-DNA complex, by constraining the helicase on the DNA. If this were the case, MutL could be envisioned to act as a clamping processivity factor for UvrD similar to the beta clamp that increases the processivity of DNA polymerase III. It will be one of the aims of this thesis to examine if MutL is capable of increasing the processivity of UvrD and, if so, to determine how this increase is being conveyed.

Nucleotide Excision Repair and UvrD

Ultraviolet radiation-induced damage in DNA must be recognized and repaired for the stability of the genome and the survivability of the cell. In *E. coli*, one method of repairing this type of damage is the nucleotide excision repair (NER) pathway. In NER, the damaged bases are removed as part of a contiguous oligonucleotide 12-13 nucleotides in length (105, 106). In this pathway, the UvrABC excision nuclease complex induces single strand breaks at the 8^{th} phosphodiester bond 5′ and the 4^{th} /5^{th} phosphodiester bond 3′ to the site of DNA damage. UvrD helicase is recruited to remove the 12-13-mer from the DNA and the resultant gap is then filled in by DNA polymerase I and sealed by DNA ligase (107).

The damage induced by ultraviolet radiation causes a distortion in the DNA backbone which can be recognized and targeted for repair. In order to facilitate efficient repair, the UvrA protein must recognize the DNA damage. Upon binding to the DNA, the UvrA dimer recruits UvrB (108). Recent atomic force microscopy studies suggest that as the UvrAB complex is searching for damage, the complex contains two molecules of both UvrA and UvrB (109). After the UvrAB complex has identified DNA damage, the UvrA dimer exits the complex allowing UvrC to be recruited (108, 110). UvrC is a dual nuclease and, incises the damaged DNA strand 3′ to the lesion using it N-terminal nuclease domain and 5′ to the lesion using its C-terminal nuclease domain (111, 112). UvrD then enters the process in a step that is not well understood, possibly recruited by UvrB (113), and displaces the 12-13-mer containing the DNA damage as stated above. It has been reported that UvrD exhibits a lower unwinding activity when unwinding from a nick, than from its preferred substrate of duplex DNA with a 3′ ssDNA tail. However, *in vitro* work has presented evidence for the UvrAB complex having a stimulatory effect on the helicase activity of UvrD (104, 114). As the unwinding processivity of UvrD has been well documented to be approximately 40 bases unwound in a single event (11), UvrD seems ideally suited to perform of performing the role it plays in NER.

The Structure of SF1 Helicases and the 2B subdomain

The activity of UvrD *in vitro* suggests the helicase is well suited for unwinding short regions of duplex DNA such as the 12-13 base oligonucleotide that must be removed in the NER pathway. What is not clear is how or why a helicase with limited processivity has recruited for the completion of a repair process where, in some cases, long patches of DNA must be replaced. UvrD seems to lack the required processive activity to perform such a

task. Yet studies have shown that the MMR system is capable of increasing the fidelity of the replication process by as much as 1000-fold, indicating that UvrD is proficient in this repair process (91). How then might UvrD be regulated to exhibit both controlled short length unwinding activity and long processive unwinding?

SF1 helicases have been shown to contain 2 domains, each with 2 subdomains: 1A, 1B, 2A, and 2B. Subdomains 1A and 2A contain part, if not all, of the seven conserved amino acid motifs described above to form a binding pocket for the hydrolysis of ATP. The energy derived from ATP hydrolysis forces the tyrosine separation pin in the 2A subdomain between the bases of duplex DNA, facilitating their separation. The 1B subdomain has been thought of as a site for ssDNA binding and contains a conserved phenylalanine residue which lies outside of the conserved motifs (42). In UvrD, as the duplex is unwound, one strand of the DNA is extruded though a channel between the 1A and 1B subdomains called the gating helix. The 1B subdomain has been shown to make contacts with the ssDNA as it passes through the gating helix (Fig. 2) (42).

The role of the 2B subdomain has been the subject of debate in the field for several years. Some have claimed the 2B subdomain interacts with the duplex DNA and is required for helicase activity (42). Others have demonstrated, using the Rep helicase as a model, that the 2B subdomain is not required for helicase activity (115, 116). Indeed, recent studies have shown that deletion of this subdomain in Rep actually *increases* the activity of the helicase as well as activating the helicase activity of the monomeric form of Rep (115, 116). Mutations within the 2B subdomain in UvrD have been shown to increase the helicase activity by as much as ten-fold *in vitro* (117). Genetic studies have also shown that cells expressing the same mutant allele of UvrD exhibited a decreased the rate of spontaneous mutation by as

much as 80% (117). However, a direct examination of the role of the 2B subdomain in UvrD, as was performed in Rep, was not possible as the deletion of the 2B subdomain appeared to be lethal to the cell upon expression (116). Ultimately, the role of the 2B subdomain in SF1 helicases is still not well understood.

As discussed above, there are many similarities between SF1 and SF2 helicases in their sequence, and there are similarities in their structures, as well. The crystal structures of SF1 helicases UvrD, Rep, and PcrA and SF2 helicase NS3 have been reported. (39, 41, 42, 116, 118). A common feature of these structures is the nucleotide binding pocket formed between domains 1A and 2A in SF1 helicases and between domains 1 and 2 in the SF2 helicase. In the UvrD crystal structure all seven conserved motifs are present in the 1A and 2A subdomains and make contacts with the ATP binding and hydrolysis pocket. The crystal structure of NS3 shows a nucleotide binding pocket nearly identical to that of the SF1 helicases. In fact, domains 1 and 2 from NS3 are structurally homologous to the 1A and 2A subdomains of UvrD and five (motifs I, Ia, II, V, and VI) of the seven conserved amino acid motifs appear to occupy the same relative position and function in both SF1 and SF2 helicases.

Perhaps the most noticeable difference between the two structures is that the SF1 helicases possess the 2B subdomain while the SF2 NS3 helicase does not (Fig. 3). The SF2 helicase is able to function without this subdomain of the protein. Even though this structure is shared among the SF1 helicases, none of the seven conserved motifs are found in this subdomain of the helicase. The lack of a conserved motif in this subdomain may suggest that this region of the helicase fulfills some other role. The 2B subdomain in Rep helicase has been shown to have a regulatory role instead of, or possibly in addition to, a role in DNA

Figure 2. Ribbon diagram of UvrD bound to partial duplex DNA in the closed conformation (Protein Data Bank Code 2IS2). The 1A subdomain is shown in yellow, the 1B subdomain is shown in green, the 2A subdomain is shown in red, the 2B subdomain is shown in blue, Y621 shown in stick model and colored cyan. Molecular images were generated with the PyMOL Molecular Graphics System, Version 1.3, Schrödinger, LLC

unwinding (115, 116). When the 2B subdomain was deleted from Rep helicase, the helicase activity of the monomeric form of Rep was activated. These studies suggest that the 2B subdomain in Rep helicase exhibits an autoregulatory control over the unwinding activity of the helicase. The crystal structures of the structurally similar UvrD and PcrA helicase monomer bound to a dsDNA/ssDNA junction show the 2B subdomain in contact with the duplex DNA. Although this 2B subdomain/duplex DNA interaction has been suggested to facilitate DNA unwinding (41, 42), the data from the Rep helicase studies clearly show that the 2B subdomain is not required for unwinding activity. An alternate interpretation is that the 2B subdomain might inhibit the DNA unwinding activity of the monomeric form of the helicase. Self-assembly into dimers or higher order oligomers might relieve this inhibition through the movement of the 2B subdomain (4). These hypotheses may present a new, but poorly understood mechanism by which SF1 helicases regulate their unwinding activity.

This dissertation will investigate the potential of the 2B subdomain to act as a regulatory region to modulate the helicase activity of UvrD. Previous studies of the 2B subdomain in Rep helicase and the work presented here suggest that the activity of UvrD may be modulated by the 2B subdomain. Chapter 2 will describe a mutation within the 2B subdomain that increases the processivity of the unwinding reaction catalyzed by UvrD. I speculate this may be achieved by forcing the helicase to adopt a translocation-based unwinding mechanism. Chapter 3 will address the mechanism by which the MutL stimulates the unwinding activity of UvrD by a direct interaction with the helicase. Chapter 4 will address how a 2B subdomain deletion in UvrD decreases the activity of UvrD as a helicase and disrupts the ability of UvrD to function in mismatch repair. The final chapter will

discuss the impact the 2B subdomain has on the activity of UvrD and propose experiments and future research directions.

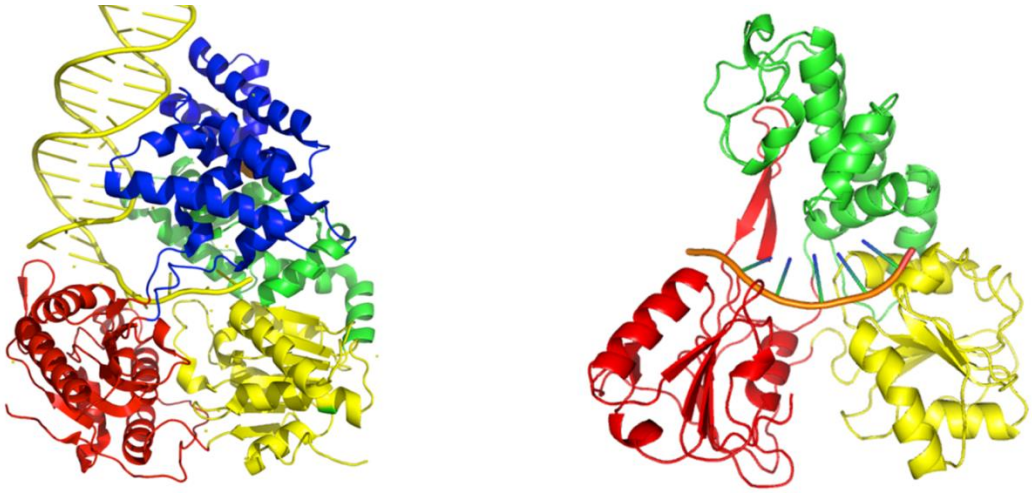

Figure 3. The presence of a 2B subdomain in SF1 helicases. Ribbon diagram of UvrD bound to partial duplex DNA in the closed conformation (Protein Data Bank Code 2IS2). The 1A subdomain is shown in yellow, the 1B subdomain is shown in green, the 2A subdomain is shown in red, the 2B subdomain is shown in blue. Ribbon diagram of NS3 helicase bound to single stranded DNA (Protein Data Bank Code 1A1V). Molecular images were generated with the PyMOL Molecular Graphics System, Version 1.3, Schrödinger, LLC

REFERENCES

1. Matson SW, George JW. DNA helicase II of Escherichia coli. characterization of the single-stranded DNA-dependent NTPase and helicase activities. J Biol Chem 1987 Feb 15;262(5):2066-76.

2. Lohman TM. Helicase-catalyzed DNA unwinding. J Biol Chem 1993 Feb 5;268(4):2269-72.

3. Hall MC, Matson SW. Helicase motifs: The engine that powers DNA unwinding. Mol Microbiol 1999 Dec;34(5):867-77.

4. Lohman TM, Tomko EJ, Wu CG. Non-hexameric DNA helicases and translocases: Mechanisms and regulation. Nat Rev Mol Cell Biol 2008 May;9(5):391-401.

5. Larsen NB, Hickson ID. RecQ helicases: Conserved guardians of genomic integrity. Adv Exp Med Biol 2013;767:161-84.

6. Chu WK, Hickson ID. RecQ helicases: Multifunctional genome caretakers. Nat Rev Cancer 2009 Sep;9(9):644-54.

7. Bachrati CZ, Hickson ID. RecQ helicases: Guardian angels of the DNA replication fork. Chromosoma 2008 Jun;117(3):219-33.

8. Abdel-Monem M, Durwald H, Hoffmann-Berling H. Enzymic unwinding of DNA. 2. chain separation by an ATP-dependent DNA unwinding enzyme. Eur J Biochem 1976 Jun 1;65(2):441-9.

9. Frost LS, Ippen-Ihler K, Skurray RA. Analysis of the sequence and gene products of the transfer region of the F sex factor. Microbiol Rev 1994 Jun;58(2):162-210.

10. Mok M, Marians KJ. The escherichia coli preprimosome and DNA B helicase can form replication forks that move at the same rate. J Biol Chem 1987 Dec 5;262(34):16644-54.

11. Ali JA, Lohman TM. Kinetic measurement of the step size of DNA unwinding by escherichia coli UvrD helicase. Science 1997 Jan 17;275(5298):377-80.

12. Singleton MR, Dillingham MS, Wigley DB. Structure and mechanism of helicases and nucleic acid translocases. Annu Rev Biochem 2007;76:23-50.

13. Wong I, Chao KL, Bujalowski W, Lohman TM. DNA-induced dimerization of the escherichia coli rep helicase. allosteric effects of single-stranded and duplex DNA. J Biol Chem 1992 Apr 15;267(11):7596-610.

14. Zhang XD, Dou SX, Xie P, Hu JS, Wang PY, Xi XG. Escherichia coli RecQ is a rapid, efficient, and monomeric helicase. J Biol Chem 2006 May 5;281(18):12655-63.

15. Singleton MR, Dillingham MS, Wigley DB. Structure and mechanism of helicases and nucleic acid translocases. Annu Rev Biochem 2007;76:23-50.

16. Hodgman TC. A new superfamily of replicative proteins. Nature 1988 May 5;333(6168):22-3.

17. Gorbalenya AE, Koonin EV, Donchenko AP, Blinov VM. A novel superfamily of nucleoside triphosphate-binding motif containing proteins which are probably involved in duplex unwinding in DNA and RNA replication and recombination. FEBS Lett 1988 Aug 1;235(1-2):16-24.

18. Gorbalenya AE, Koonin EV. Helicases: Amino acid sequence comparisons and structure-function relationships. Curr Opin Struct Biol 1993;3(3):419 <last_page> 429.

19. Fairman-Williams ME, Guenther UP, Jankowsky E. SF1 and SF2 helicases: Family matters. Curr Opin Struct Biol 2010 Jun;20(3):313-24.

20. Walker JE, Saraste M, Runswick MJ, Gay NJ. Distantly related sequences in the alpha- and beta-subunits of ATP synthase, myosin, kinases and other ATP-requiring enzymes and a common nucleotide binding fold. EMBO J 1982;1(8):945-51.

21. George JW, Brosh RM,Jr, Matson SW. A dominant negative allele of the escherichia coli uvrD gene encoding DNA helicase II. A biochemical and genetic characterization. J Mol Biol 1994 Jan 14;235(2):424-35.

22. Washburn BK, Kushner SR. Construction and analysis of deletions in the structural gene (uvrD) for DNA helicase II of escherichia coli. J Bacteriol 1991 Apr;173(8):2569-75.

23. Brosh RM,Jr, Matson SW. Mutations in motif II of escherichia coli DNA helicase II render the enzyme nonfunctional in both mismatch repair and excision repair with differential effects on the unwinding reaction. J Bacteriol 1995 Oct;177(19):5612-21.

24. Brosh RM,Jr, Matson SW. A partially functional DNA helicase II mutant defective in forming stable binary complexes with ATP and DNA. A role for helicase motif III. J Biol Chem 1996 Oct 11;271(41):25360-8.

25. Brosh RM,Jr, Matson SW. A point mutation in escherichia coli DNA helicase II renders the enzyme nonfunctional in two DNA repair pathways. evidence for initiation of unwinding from a nick in vivo. J Biol Chem 1997 Jan 3;272(1):572-9.

26. Hall MC, Matson SW. Mutation of a highly conserved arginine in motif IV of escherichia coli DNA helicase II results in an ATP-binding defect. J Biol Chem 1997 Jul 25;272(30):18614-20.

27. Velankar SS, Soultanas P, Dillingham MS, Subramanya HS, Wigley DB. Crystal structures of complexes of PcrA DNA helicase with a DNA substrate indicate an inchworm mechanism. Cell 1999 Apr 2;97(1):75-84.

28. Korolev S, Hsieh J, Gauss GH, Lohman TM, Waksman G. Major domain swiveling revealed by the crystal structures of complexes of E. coli rep helicase bound to single-stranded DNA and ADP. Cell 1997 Aug 22;90(4):635-47.

29. Graves-Woodward KL, Weller SK. Replacement of gly815 in helicase motif V alters the single-stranded DNA-dependent ATPase activity of the herpes simplex virus type 1 helicase-primase. J Biol Chem 1996 Jun 7;271(23):13629-35.

30. Naumovski L, Friedberg EC. Analysis of the essential and excision repair functions of the RAD3 gene of saccharomyces cerevisiae by mutagenesis. Mol Cell Biol 1986 Apr;6(4):1218-27.

31. Martinez R, Shao L, Weller SK. The conserved helicase motifs of the herpes simplex virus type 1 origin-binding protein UL9 are important for function. J Virol 1992 Nov;66(11):6735-46.

32. Ma L, Westbroek A, Jochemsen AG, Weeda G, Bosch A, Bootsma D, Hoeijmakers JH, van der Eb AJ. Mutational analysis of ERCC3, which is involved in DNA repair and transcription initiation: Identification of domains essential for the DNA repair function. Mol Cell Biol 1994 Jun;14(6):4126-34.

33. Richmond E, Peterson CL. Functional analysis of the DNA-stimulated ATPase domain of yeast SWI2/SNF2. Nucleic Acids Res 1996 Oct 1;24(19):3685-92.

34. Korolev S, Yao N, Lohman TM, Weber PC, Waksman G. Comparisons between the structures of HCV and rep helicases reveal structural similarities between SF1 and SF2 super-families of helicases. Protein Sci 1998 Mar;7(3):605-10.

35. Kim JL, Morgenstern KA, Griffith JP, Dwyer MD, Thomson JA, Murcko MA, Lin C, Caron PR. Hepatitis C virus NS3 RNA helicase domain with a bound oligonucleotide: The crystal structure provides insights into the mode of unwinding. Structure 1998 Jan 15;6(1):89-100.

36. Moolenaar GF, Visse R, Ortiz-Buysse M, Goosen N, van de Putte P. Helicase motifs V and VI of the escherichia coli UvrB protein of the UvrABC endonuclease are essential for the formation of the preincision complex. J Mol Biol 1994 Jul 22;240(4):294-307.

37. Hsu DS, Kim ST, Sun Q, Sancar A. Structure and function of the UvrB protein. J Biol Chem 1995 Apr 7;270(14):8319-27.

38. Pause A, Sonenberg N. Mutational analysis of a DEAD box RNA helicase: The mammalian translation initiation factor eIF-4A. EMBO J 1992 Jul;11(7):2643-54.

39. Yao N, Hesson T, Cable M, Hong Z, Kwong AD, Le HV, Weber PC. Structure of the hepatitis C virus RNA helicase domain. Nat Struct Biol 1997 Jun;4(6):463-7.

40. Subramanya HS, Bird LE, Brannigan JA, Wigley DB. Crystal structure of a DExx box DNA helicase. Nature 1996 Nov 28;384(6607):379-83.

41. Velankar SS, Soultanas P, Dillingham MS, Subramanya HS, Wigley DB. Crystal structures of complexes of PcrA DNA helicase with a DNA substrate indicate an inchworm mechanism. Cell 1999 Apr 2;97(1):75-84.

42. Lee JY, Yang W. UvrD helicase unwinds DNA one base pair at a time by a two-part power stroke. Cell 2006 Dec 29;127(7):1349-60.

43. Macris MA, Sung P. Multifaceted role of the saccharomyces cerevisiae Srs2 helicase in homologous recombination regulation. Biochem Soc Trans 2005 Dec;33(Pt 6):1447-50.

44. Skarstad K, Katayama T. Regulating DNA replication in bacteria. Cold Spring Harb Perspect Biol 2013 Apr 1;5(4):a012922.

45. Lorenz A, Osman F, Folkyte V, Sofueva S, Whitby MC. Fbh1 limits Rad51-dependent recombination at blocked replication forks. Mol Cell Biol 2009 Sep;29(17):4742-56.

46. Bohr VA. Rising from the RecQ-age: The role of human RecQ helicases in genome maintenance. Trends Biochem Sci 2008 Dec;33(12):609-20.

47. Das A, Boldogh I, Lee JW, Harrigan JA, Hegde ML, Piotrowski J, de Souza Pinto N, Ramos W, Greenberg MM, Hazra TK, et al. The human werner syndrome protein stimulates repair of oxidative DNA base damage by the DNA glycosylase NEIL1. J Biol Chem 2007 Sep 7;282(36):26591-602.

48. Ahn B, Harrigan JA, Indig FE, Wilson DM,3rd, Bohr VA. Regulation of WRN helicase activity in human base excision repair. J Biol Chem 2004 Dec 17;279(51):53465-74.

49. Schurman SH, Hedayati M, Wang Z, Singh DK, Speina E, Zhang Y, Becker K, Macris M, Sung P, Wilson DM,3rd, et al. Direct and indirect roles of RECQL4 in modulating base excision repair capacity. Hum Mol Genet 2009 Sep 15;18(18):3470-83.

50. Cooper MP, Machwe A, Orren DK, Brosh RM, Ramsden D, Bohr VA. Ku complex interacts with and stimulates the werner protein. Genes Dev 2000 Apr 15;14(8):907-12.

51. Parvathaneni S, Stortchevoi A, Sommers JA, Brosh RM,Jr, Sharma S. Human RECQ1 interacts with Ku70/80 and modulates DNA end-joining of double-strand breaks. PLoS One 2013 May 1;8(5):e62481.

52. Nimonkar AV, Genschel J, Kinoshita E, Polaczek P, Campbell JL, Wyman C, Modrich P, Kowalczykowski SC. BLM-DNA2-RPA-MRN and EXO1-BLM-RPA-MRN constitute

two DNA end resection machineries for human DNA break repair. Genes Dev 2011 Feb 15;25(4):350-62.

53. Adams MD, McVey M, Sekelsky JJ. Drosophila BLM in double-strand break repair by synthesis-dependent strand annealing. Science 2003 Jan 10;299(5604):265-7.

54. Machwe A, Xiao L, Lloyd RG, Bolt E, Orren DK. Replication fork regression in vitro by the werner syndrome protein (WRN): Holliday junction formation, the effect of leading arm structure and a potential role for WRN exonuclease activity. Nucleic Acids Res 2007;35(17):5729-47.

55. Machwe A, Xiao L, Groden J, Orren DK. The werner and bloom syndrome proteins catalyze regression of a model replication fork. Biochemistry 2006 Nov 28;45(47):13939-46.

56. Davey MJ, O'Donnell M. Replicative helicase loaders: Ring breakers and ring makers. Curr Biol 2003 Aug 5;13(15):R594-6.

57. Hickman AB, Dyda F. Binding and unwinding: SF3 viral helicases. Curr Opin Struct Biol 2005 Feb;15(1):77-85.

58. Gorbalenya AE, Koonin EV, Wolf YI. A new superfamily of putative NTP-binding domains encoded by genomes of small DNA and RNA viruses. FEBS Lett 1990 Mar 12;262(1):145-8.

59. Singleton MR, Sawaya MR, Ellenberger T, Wigley DB. Crystal structure of T7 gene 4 ring helicase indicates a mechanism for sequential hydrolysis of nucleotides. Cell 2000 Jun 9;101(6):589-600.

60. Ilyina TV, Gorbalenya AE, Koonin EV. Organization and evolution of bacterial and bacteriophage primase-helicase systems. J Mol Evol 1992 Apr;34(4):351-7.

61. Gogol EP, Seifried SE, von Hippel PH. Structure and assembly of the escherichia coli transcription termination factor rho and its interaction with RNA. I. cryoelectron microscopic studies. J Mol Biol 1991 Oct 20;221(4):1127-38.

62. Skordalakes E, Berger JM. Structure of the rho transcription terminator: Mechanism of mRNA recognition and helicase loading. Cell 2003 Jul 11;114(1):135-46.

63. Labib K, Tercero JA, Diffley JF. Uninterrupted MCM2-7 function required for DNA replication fork progression. Science 2000 Jun 2;288(5471):1643-7.

64. Matson SW. Escherichia coli helicase II (urvD gene product) translocates unidirectionally in a 3' to 5' direction. J Biol Chem 1986 Aug 5;261(22):10169-75.

65. Maluf NK, Fischer CJ, Lohman TM. A dimer of escherichia coli UvrD is the active form of the helicase in vitro. J Mol Biol 2003 Jan 31;325(5):913-35.

66. Maluf NK, Ali JA, Lohman TM. Kinetic mechanism for formation of the active, dimeric UvrD helicase-DNA complex. J Biol Chem 2003 Aug 22;278(34):31930-40.

67. Hickson ID, Arthur HM, Bramhill D, Emmerson PT. The E. coli uvrD gene product is DNA helicase II. Mol Gen Genet 1983;190(2):265-70.

68. Centore RC, Leeson MC, Sandler SJ. UvrD303, a hyperhelicase mutant that antagonizes RecA-dependent SOS expression by a mechanism that depends on its C terminus. J Bacteriol 2009 Mar;191(5):1429-38.

69. Centore RC, Sandler SJ. UvrD limits the number and intensities of RecA-green fluorescent protein structures in escherichia coli K-12. J Bacteriol 2007 Apr;189(7):2915-20.

70. Lahue RS, Modrich P. Methyl-directed DNA mismatch repair in escherichia coli. Mutat Res 1988 Mar;198(1):37-43.

71. Modrich P, Lahue R. Mismatch repair in replication fidelity, genetic recombination, and cancer biology. Annu Rev Biochem 1996;65:101-33.

72. Husain I, Van Houten B, Thomas DC, Abdel-Monem M, Sancar A. Effect of DNA polymerase I and DNA helicase II on the turnover rate of UvrABC excision nuclease. Proc Natl Acad Sci U S A 1985 Oct;82(20):6774-8.

73. Schaaper R. Base selection, proofreading, and mismatch repair during DNA replication in escherichia coli. The Journal of Biological Chemistry 1993;268(32):23762.

74. Wagner RJ, Meselson M. Repair tracts in mismatched DNA heteroduplexes. DNA Repair (Amst) 1976;4(1):103.

75. Palmer BR, Marinus MG. The dam and dcm strains of escherichia coli--a review. Gene 1994 May 27;143(1):1-12.

76. Kunkel TA, Erie DA. DNA mismatch repair. Annu Rev Biochem 2005;74:681-710.

77. Tuteja N, Tuteja R. Unraveling DNA helicases. motif, structure, mechanism and function. Eur J Biochem 2004 May;271(10):1849-63.

78. Yang Y, Sass LE, Du C, Hsieh P, Erie DA. Determination of protein-DNA binding constants and specificities from statistical analyses of single molecules: MutS-DNA interactions. Nucleic Acids Res 2005 Aug 1;33(13):4322-34.

79. Qiu R, DeRocco VC, Harris C, Sharma A, Hingorani MM, Erie DA, Weninger KR. Large conformational changes in MutS during DNA scanning, mismatch recognition and repair signalling. EMBO J 2012 May 30;31(11):2528-40.

80. Geng H, Sakato M, DeRocco V, Yamane K, Du C, Erie DA, Hingorani M, Hsieh P. Biochemical analysis of the human mismatch repair proteins hMutSalpha MSH2(G674A)-MSH6 and MSH2-MSH6(T1219D). J Biol Chem 2012 Mar 23;287(13):9777-91.

81. Mechanic LE, Frankel BA, Matson SW. Escherichia coli MutL loads DNA helicase II onto DNA. J Biol Chem 2000 Dec 8;275(49):38337-46.

82. Cheng F, Hou J, Chen YY, Zhou Y, Zhang HT, Bi LJ, Zhang XE. Functional interaction between MutL and 3'-5' exonuclease X in escherichia coli. Arch Biochem Biophys 2010 Oct 1;502(1):39-43.

83. Grilley M, Welsh KM, Su SS, Modrich P. Isolation and characterization of the escherichia coli mutL gene product. J Biol Chem 1989 Jan 15;264(2):1000-4.

84. Lu AL, Welsh K, Clark S, Su SS, Modrich P. Repair of DNA base-pair mismatches in extracts of escherichia coli. Cold Spring Harb Symp Quant Biol 1984;49:589-96.

85. Welsh KM, Lu AL, Clark S, Modrich P. Isolation and characterization of the escherichia coli mutH gene product. J Biol Chem 1987 Nov 15;262(32):15624-9.

86. Hall MC, Matson SW. The escherichia coli MutL protein physically interacts with MutH and stimulates the MutH-associated endonuclease activity. J Biol Chem 1999 Jan 15;274(3):1306-12.

87. Bruni R, Martin D, Jiricny J. D(GATC) sequences influence escherichia coli mismatch repair in a distance-dependent manner from positions both upstream and downstream of the mismatch. Nucleic Acids Res 1988 Jun 10;16(11):4875-90.

88. Lahue RS, Au KG, Modrich P. DNA mismatch correction in a defined system. Science 1989 Jul 14;245(4914):160-4.

89. Chopra I, O'Neill AJ, Miller K. The role of mutators in the emergence of antibiotic-resistant bacteria. Drug Resist Updat 2003 Jun;6(3):137-45.

90. Russell A, Chopra I. Understanding antibacterial action and resistance. 2nd ed. Hertfordshire: Ellis Horwood Ltd; 1996. .

91. Miller JH. Spontaneous mutators in bacteria: Insights into pathways of mutagenesis and repair. Annu Rev Microbiol 1996;50:625-43.

92. Boe L, Danielsen M, Knudsen S, Petersen JB, Maymann J, Jensen PR. The frequency of mutators in populations of escherichia coli. Mutat Res 2000 Mar 14;448(1):47-55.

93. LeClerc JE, Li B, Payne WL, Cebula TA. High mutation frequencies among escherichia coli and salmonella pathogens. Science 1996 Nov 15;274(5290):1208-11.

94. Schaaff F, Reipert A, Bierbaum G. An elevated mutation frequency favors development of vancomycin resistance in staphylococcus aureus. Antimicrob Agents Chemother 2002 Nov;46(11):3540-8.

95. Ban C, Yang W. Crystal structure and ATPase activity of MutL: Implications for DNA repair and mutagenesis. Cell 1998 Nov 13;95(4):541-52.

96. Ban C, Junop M, Yang W. Transformation of MutL by ATP binding and hydrolysis: A switch in DNA mismatch repair. Cell 1999 Apr 2;97(1):85-97.

97. Dutta R, Inouye M. GHKL, an emergent ATPase/kinase superfamily. Trends Biochem Sci 2000 Jan;25(1):24-8.

98. Guarne A, Junop MS, Yang W. Structure and function of the N-terminal 40 kDa fragment of human PMS2: A monomeric GHL ATPase. EMBO J 2001 Oct 1;20(19):5521-31.

99. Hu X, Machius M, Yang W. Monovalent cation dependence and preference of GHKL ATPases and kinases. FEBS Lett 2003 Jun 5;544(1-3):268-73.

100. Cheng F, Hou J, Chen YY, Zhou Y, Zhang HT, Bi LJ, Zhang XE. Functional interaction between MutL and 3'-5' exonuclease X in escherichia coli. Arch Biochem Biophys 2010 Oct 1;502(1):39-43.

101. Modrich P, Lahue R. Mismatch repair in replication fidelity, genetic recombination, and cancer biology. Annu Rev Biochem 1996;65:101-33.

102. Guarne A, Ramon-Maiques S, Wolff EM, Ghirlando R, Hu X, Miller JH, Yang W. Structure of the MutL C-terminal domain: A model of intact MutL and its roles in mismatch repair. EMBO J 2004 Oct 27;23(21):4134-45.

103. Robertson A, Pattishall SR, Matson SW. The DNA binding activity of MutL is required for methyl-directed mismatch repair in escherichia coli. J Biol Chem 2006 Mar 31;281(13):8399-408.

104. Robertson AB, Pattishall SR, Gibbons EA, Matson SW. MutL-catalyzed ATP hydrolysis is required at a post-UvrD loading step in methyl-directed mismatch repair. J Biol Chem 2006 Jul 21;281(29):19949-59.

105. SETLOW RB, CARRIER WL. The disappearance of thymine dimers from dna: An error-correcting mechanism. Proc Natl Acad Sci U S A 1964 Feb;51:226-31.

106. BOYCE RP, HOWARD-FLANDERS P. Release of ultraviolet light-induced thymine dimers from dna in E. coli K-12. Proc Natl Acad Sci U S A 1964 Feb;51:293-300.

107. Sancar A, Rupp WD. A novel repair enzyme: UVRABC excision nuclease of escherichia coli cuts a DNA strand on both sides of the damaged region. Cell 1983 May;33(1):249-60.

108. Orren DK, Sancar A. The (A)BC excinuclease of escherichia coli has only the UvrB and UvrC subunits in the incision complex. Proc Natl Acad Sci U S A 1989 Jul;86(14):5237-41.

109. Verhoeven EE, Wyman C, Moolenaar GF, Goosen N. The presence of two UvrB subunits in the UvrAB complex ensures damage detection in both DNA strands. EMBO J 2002 Aug 1;21(15):4196-205.

110. Moolenaar GF. The role of ATP binding and hydrolysis by UvrB during nucleotide excision repair. J Biol Chem 2000;275(11):8044 <last_page> 8050.

111. Karakas E, Truglio JJ, Croteau D, Rhau B, Wang L, Van Houten B, Kisker C. Structure of the C-terminal half of UvrC reveals an RNase H endonuclease domain with an argonaute-like catalytic triad. EMBO J 2007 Jan 24;26(2):613-22.

112. Truglio JJ, Rhau B, Croteau DL, Wang L, Skorvaga M, Karakas E, DellaVecchia MJ, Wang H, Van Houten B, Kisker C. Structural insights into the first incision reaction during nucleotide excision repair. EMBO J 2005 Mar 9;24(5):885-94.

113. Pakotiprapha D, Jeruzalmi D. Small-angle X-ray scattering reveals architecture and A_2B_2 stoichiometry of the UvrA-UvrB DNA damage sensor.. Proteins 2013;81(1):132.

114. Atkinson J, Guy CP, Cadman CJ, Moolenaar GF, Goosen N, McGlynn P. Stimulation of UvrD helicase by UvrAB. J Biol Chem 2009 Apr 3;284(14):9612-23.

115. Brendza KM, Cheng W, Fischer CJ, Chesnik MA, Niedziela-Majka A, Lohman TM. Autoinhibition of escherichia coli rep monomer helicase activity by its 2B subdomain. Proceedings of the National Academy of Sciences 2005;102(29):10076.

116. Cheng W, Brendza KM, Gauss GH, Korolev S, Waksman G, Lohman TM. The 2B domain of the escherichia coli rep protein is not required for DNA helicase activity. Proc Natl Acad Sci U S A 2002 Dec 10;99(25):16006-11.

117. Zhang G, Deng E, Baugh L, Kushner SR. Identification and characterization of escherichia coli DNA helicase II mutants that exhibit increased unwinding efficiency. J Bacteriol 1998 Jan;180(2):377-87.

118. Kim JL, Morgenstern KA, Griffith JP, Dwyer MD, Thomson JA, Murcko MA, Lin C, Caron PR. Hepatitis C virus NS3 RNA helicase domain with a bound oligonucleotide: The crystal structure provides insights into the mode of unwinding. Structure 1998;6(1):89 <last_page> 100.

CHAPTER 2: THE UVRD303 HYPER-HELICASE EXHIBITS INCREASED PROCESSIVITY

Abstract

DNA helicases use energy derived from nucleoside 5′-triphosphate hydrolysis to catalyze the separation of double stranded DNA into single stranded intermediates for replication, recombination, and repair. *Escherichia coli* helicase II (UvrD) functions in methyl-directed mismatch repair, nucleotide excision repair, and homologous recombination. A previously discovered two amino acid substitution of residues 403 and 404 (both D→A) in the 2B subdomain of UvrD (*uvrD303*) confers an antimutator and UV sensitive phenotype on cells expressing this allele. The purified protein exhibits a "hyper-helicase" unwinding activity *in vitro*. Using rapid quench, pre-steady state kinetic experiments we show the increased helicase activity of UvrD303 is due to an increase in the processivity of the unwinding reaction. We suggest that this mutation in the 2B subdomain results in a weakened interaction with the 1B subdomain, allowing the helicase to adopt a more open conformation. This is consistent with the idea that the 2B subdomain may have an autoregulatory role. The UvrD303 mutation may enable the helicase to unwind DNA via a 'strand displacement' mechanism, which is similar to the mechanism used to processively translocate along single-stranded DNA, and the increased unwinding processivity may contribute directly to the antimutator phenotype.

Introduction

DNA helicases are ubiquitous motor proteins that transiently convert duplex DNA into single-stranded DNA (ssDNA) using energy derived from nucleoside 5'-triphosphate (NTP) hydrolysis for a wide variety of biological processes including DNA replication, repair and recombination (1-5). Thus, helicases are vital for the maintenance of the genome and mutations within helicase-encoding genes in humans have been linked to both cancer and aging disorders (6-8). In *E. coli*, the product of the *uvrD* gene, DNA helicase II (UvrD), has been shown to function in two fundamental DNA repair processes – nucleotide excision repair (NER) (9) and methyl-directed mismatch repair (MMR) (10, 11). In NER, UvrD acts in conjunction with the UvrABC excision nuclease and DNA polymerase I to remove short 12-13 base oligonucleotides containing a wide variety of bulky lesions including pyrimidine dimers (9). UvrD also participates in the MMR pathway by initiating unwinding at the nicked d(GATC) site created by MutH to displace the nascent error-containing strand of DNA which is degraded by appropriate exonucleases. The resulting gap is subsequently resynthesized by DNA polymerase III (10, 12). UvrD has been suggested to have a role in other cellular processes, such as displacement of RecA protein from ssDNA during homologous recombination (13). However, this role for UvrD is not as well understood. The *uvrD* gene encodes a 720 amino acid, 82 kDa Superfamily 1A (SF1A) helicase with well characterized 3' to 5' unwinding and translocase directionality. Consistent with other SF1 helicases, UvrD contains seven conserved amino acid motifs and two structural domains (1 and 2) each with two subdomains (A and B) (14-21).

Crystal structures for both UvrD (14, 22) and the structurally related (38% amino acid identity) Rep helicase (20) have been reported (see Fig. 4 for UvrD). Each protein is capable

of adopting two conformations – open and closed – with the major difference between the two conformations being the orientation of the 2B subdomain. In the 'open' conformation the 2B subdomain is stacked above the 2A subdomain and no contacts are made between the 2B and 1B subdomains. To adopt the alternate 'closed' structure, the 2B subdomain rotates about a flexible hinge connected to the 2A subdomain and closes onto the 1B subdomain. The magnitude of the 2B subdomain rotation as the helicases modulate between the open and closed conformations has been reported to be 130° in Rep protein and 160° in UvrD. Although it is known that these SF1 helicases can adopt these alternate conformations, it is not clear why there are two alternate conformations. The related SF2 helicases (e.g. the hepatitis NS3 helicase) lack the equivalent of the 2B subdomain (23, 24). Consequently, the role of the 2B subdomain in SF1 helicases is not well understood.

Previous studies (25, 26) have examined what role, if any, the 2B subdomain of Rep protein plays in the activity of this helicase. It was concluded that the 2B subdomain is most likely a regulatory domain since deletion of this subdomain stimulates the unwinding and translocase activity of the protein in addition to activating the helicase activity of a RepΔ2B monomer. However, the role of the 2B subdomain in UvrD continues to be debated (14). The two prevailing hypotheses suggest that either the 2B subdomain is required to make direct double-stranded DNA interactions which allow the helicase to bind various substrates or that the 2B subdomain functions in a regulatory role, modulating helicase activity. Direct studies of a corresponding deletion of the 2B subdomain in UvrD have not been reported due to the apparent lethality of the expression of UvrDΔ2B (25).

Previous work by Zhang et al (27) isolated an allele of *uvrD* that contained two point mutations within the 2B subdomain. In this mutant form of UvrD, named UvrD303, the

native amino acids at positions 403 and 404 (both aspartic acids) were mutated to alanines (Fig. 4). When UvrD303 was expressed in place of the wild-type protein, from either the chromosome or a high copy number plasmid, cells exhibited antimutator, UV sensitive and hypo-recombinant phenotypes (27, 28). When purified and analyzed *in vitro*, UvrD303 exhibited a ten-fold increase in unwinding activity compared to its wild-type counterpart. This increased activity led to UvrD303 being referred to as a "hyper-helicase". Interestingly, neither D403A nor D404A alone were sufficient to convey this hyper-helicase activity (27).

This chapter presents a biochemical characterization of the UvrD303 mutant including a possible explanation for how the 2B subdomain mutation increases the unwinding activity of the helicase. Using single turnover, rapid quench helicase assays we have shown that the processivity of UvrD303, as a DNA helicase, is approximately ten-fold higher than that of wild-type UvrD. We speculate that the mutation alters the ability of the 2B subdomain to properly adopt a closed conformation, as referred to above. The closed conformation appears to be important for normal endogenous helicase activity of wild-type UvrD as evidenced by the phenotype of cells expressing UvrD303.

Materials and Methods

Helicase purification –The *uvrD* gene was amplified via polymerase chain reaction from genomic K12 λ^+ F^+ DNA using the following primers: forward primer 5′-CGGC GGTGCCATGGACG-3′ and reverse primer 5′-TACCGACTCCAGCCGGGC-3′. The 5′ terminus of the reverse primer was phosphorylated with T4 polynucleotide kinase to facilitate blunt end ligation. The pTYB4-His vector was digested using the restriction enzymes NcoI and SmaI (NEB) and the resulting 7.5 kb DNA fragment was purified via agarose gel

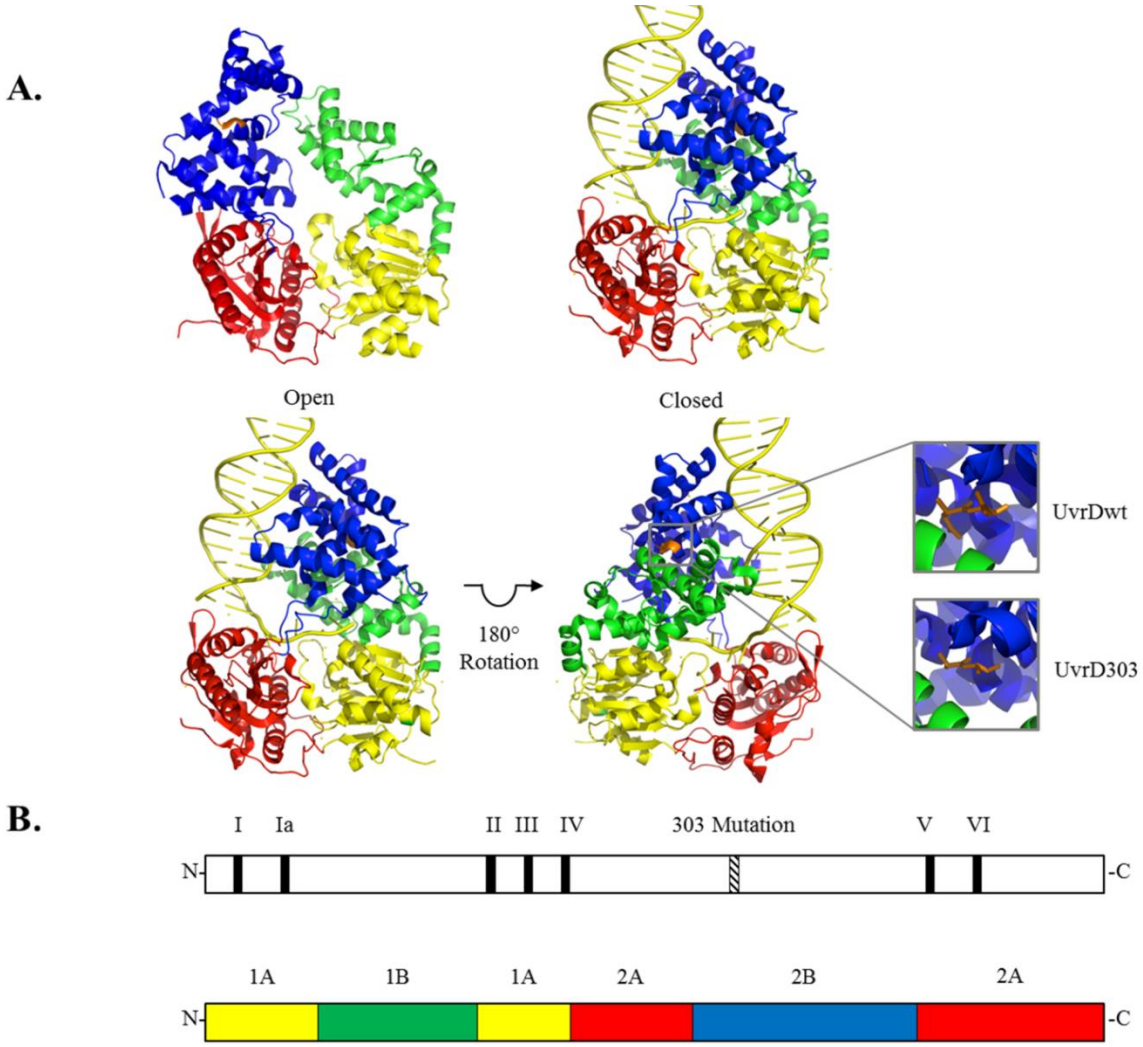

Figure 4. Models of *E. coli* UvrD and the mutant UvrD303 helicase in open and closed conformations. A. Upper panel – Ribbon diagram of the apo-structure of UvrD in the open conformation (Protein Data Bank code 3LFU) and ribbon diagram of UvrD bound to partial duplex DNA in the closed conformation. Lower panel – Ribbon diagram of UvrD bound to partial duplex DNA in the closed conformation (left side) and rotated 180^{o} (right side) (Protein Data Bank Code 2IS2)(33,14). The 1A subdomain is shown in yellow, the 1B subdomain is shown in green, the 2A subdomain is shown in red, the 2B subdomain is shown in blue. Mutated residues are denoted in orange and by the stick representation. For amino acid substitution in UvrD303 (D to A), rotamers were selected for minimum steric hindrance. Molecular images were generated with the PyMOL Molecular Graphics System, Version 1.3, Schrödinger, LLC. B. Top panel – A schematic representation of the seven conserved helicase motifs (15) of UvrD. The hashed box represents the placement of the 303 mutation. Bottom panel – A schematic representation of the four structural subdomains of UvrD. The two graphics are aligned such that the placement of the 303 mutation within the 2B subdomain can be seen.

electrophoresis and excision of the DNA followed by use of a Qiagen quick spin purification column. The purified digested vector was treated with shrimp alkaline phosphatase to reduce the likelihood of vector re-ligation in subsequent cloning reactions. The *uvrD* containing PCR product was digested with the restriction enzyme NcoI and purified in a manner similar to the vector. The resultant digested vector and PCR insert were ligated using T4 ligase. Using this cloning technique, the SmaI site in pTYB4-His is destroyed, but will ensure that only a C-terminal glycine will be added to the protein after purification, yielding essentially native protein. This construct enabled the rapid purification of the helicase as previously described (29). The *uvrD303* allele was constructed using site-directed mutagenesis. A quickchange PCR was performed using primers of the following sequence: forward 5′-CTGATTGCCAACCGCAACGACGACGCGGCCTTTGAGCGTGTG-3′ and reverse 5′-CACACGCTCAAAGGCCGCGTCGTCGTTGCGGTTGGCAATCAG-3′ to change the 403rd and 404th codons from -GACGAC- to -GCGGCC-, thus converting both the aspartic acids to alanines. This mutagenesis also introduced a silent NotI restriction site which was used to screen potential clones for the *uvrD303* allele. The resulting plasmid was sequenced to ensure no additional mutations had been introduced.

The construct, pTYB4-UvrD303-His, was transformed into *E. coli* strain BL21DE3*uvrD*::Tn5*mutL*::Tn10 and a 20 mL culture was grown overnight at 37°C in ZY media (30). The overnight culture was introduced to 1 L of ZYM5052 autoinduction media (30) and grown at 16°C for 48 hours. The cells were harvested by centrifugation, washed once with 25 mL of STE buffer (10 mM Tris-HCl (pH 8.0), 1 mM EDTA and 100 mM NaCl) and harvested again by centrifugation. The cells were stored at -80^{o}C until use. The cells were lysed and the protein was purified as previously described using a combination of Talon

(Clone-tech) and Chitin (NEB) resins to take advantage of the two affinity tags present on the overexpressed fusion protein (29). Protein that eluted from the Chitin column was dialyzed against UvrD storage buffer (31) and stored at -20^{o}C. The purified protein was greater than 95% homogeneous as determined by polyacrylamide gel electrophoresis in the presence of sodium dodecyl sulfate (SDS).

Wild-type UvrD was purified as previously described (31).

DNA Substrates – Partial duplex substrates were prepared by radiolabeling the 5'-end of oligonucleotides obtained from Integrated DNA Technologies (Coralville, Iowa) using [γ-^{32}P]ATP and T4 polynucleotide kinase (see Table 1 for sequences). A 1.1 fold excess of an unlabeled complementary oligonucleotide was annealed to the labeled strand by heating the two strands to 95°C for 5 minutes and allowing them to slow cool to 25°C overnight. The partial duplex substrate was purified from free nucleotide using a Sephadex G50 spin column and dialyzed into TEN buffer (10 mM Tris-HCl (pH 7.5), 1 mM EDTA, 50 mM NaCl). This process was used to generate the 24/64 and 90/130 partial duplex substrates. In each case the shorter DNA strand was radioactively labeled. The longer DNA strand contains a 40 base 3'-tail ssDNA to facilitate loading of UvrD.

The 243 bp partial duplex substrate was generated from a modified version of pUC19, pUC19-TS. The pUC19-TS construct was created by digesting pUC19 DNA (NEB) with BamHI and EcoRI. The insert was created by annealing the following synthetic oligonucleotides:5′-AATTCCTCAGCAATCCTCAGCCAGGCCTCAGCTGGCCTCAGCG-3′ and 5′-GATCCGCTGAGGCCAGCTGAGGCCTGGCTGAGGATTGCTGAGG-3′. The annealing reaction created compatible ends with the BamHI and EcoRI digested pUC19 vector. This

Table 1. Oligonucleotides used in the UvrD303 study

Oligonucleotide Sequence
RQ24: 5′ -GCCCTGCTGCCGACCAACGAAGGT- 3′
RQ64: 5′ -ACCTTCGTTGGTCGGCAGCAGGGC (T_{40}) -3′
RQ90: 5′ -GCCCTGCTGCCGACCAACGAAGGTTACATTCCCCGTGCTGGCCGT TTG CGGTTGTCCTGTACCACTCGAAGTAGGAGGGGTGCTCACCGA -3′
RQ130: 5′ -TCGGTGAGCACCCCTCCTACTTCGAGTGGTACAGGACAACCGCAA ACGGCCAGCACGGGGAATGTAACCTTCGTTGGTCGGCAGCAGGGC (T_{40}) -3′
Hairpin Trap: 5′ -CCTCGCTGCTTTTTGCAGCGAGGC (T_{30}) -3′
Fluorescence Anisotropy Labeled: 5′ -TATCGGCACGTCTCGAGATG-Cy5 -3′
Fluorescence Anisotropy 40b Tail: 5′ -CATCTCGAGACGTGCCGATA (T_{40}) -3′

elongated version of pUC19 was then used in a site directed mutagenic PCR (with the following primers: forward 5′-GGATCCTCAGCAGTCGACCTCAG CGCATGC-3′ and reverse 5′-GCATGCGCT GAGGTCGACTGCTGAGGATCC-3′ to create pUC19-TS, which contains a 67 bp stretch of DNA between the EcoRI and HindIII restriction sites (5′-CCTCAGCAATCCTCAGCCAGGCC TCAGCTGGCCTCAGCGGATCCTCAGCAGTCGACCTCAGCGCATG-3′) containing multiple Nt.BbvC1 nicking sites.

To produce the 243 bp partial duplex substrate 50 pmols of plasmid DNA were digested with EcoRI and SapI to completion to produce a 297 bp DNA fragment. The enzymes were heat killed at 65°C for 20 minutes and the resulting DNA was purified by gel extraction using a 1.5% (w/v) (0.75% (w/v) agarose, 0.75% (w/v) low melting agarose) agarose gel. The three nucleotide overhang generated by the SapI digest was filled in using Klenow fragment polymerase and [α-^{32}P]dCTP, dGTP and dTTP. The fill-in reaction was incubated at 37^{o}C for 30 minutes. The purified DNA fragment, which contains seven Nt.BbvCI nickase sites (CCTCAGC), was nicked with Nt.BbvCI followed by heating to 80°C for 20 minutes to denature the on-average 11 nucleotide fragments generated by the nicking reaction. The resulting DNA molecule contains a 45 base 3'-ssDNA tail preceding a 243 bp duplex region. The nicked DNA was immediately applied to Qiagen QIAquick PCR Purification spin columns for purification (1 column used per 8 pmols of DNA) and eluted in TEN buffer. The final DNA concentration was determined by scintillation counting.

DNA-dependent ATPase assays – The standard reaction mixture (40 µl) contained 25 mM Tris-HCl (pH 7.5), 3 mM $MgCl_2$, 20 mM NaCl, 5 mM 2-mercaptoethanol, 50 µg/mL bovine serum albumin, 10 ng/µL M13 ssDNA, [α-^{32}P]ATP (~60 nCi/µL) and 10 nM UvrD

or UvrD303 helicase. For *k*cat determinations, the ATP concentration was 400 μM. For *Km* determinations the ATP concentration ranged from 50 to 500 μM. All reagents except ATP were mixed and allowed to incubate on ice for 5 minutes. Then ATP was added and the reaction was incubated at 37°C for 10 minutes. Aliquots (5 μl) were removed every two minutes and 2 μL of 5 M formic acid was added to stop the reaction. 2.5 μL of this mixture was spotted onto a thin layer chromatography plate and developed in a 0.45 M ammonium sulfate solution. Results were visualized by PhosphorImaging (Molecular Dynamics).

Helicase Assays – Helicase reaction mixtures (16 μL) for steady-state experiments contained 25 mM Tris-HCl (pH7.5), 3 mM $MgCl_2$, 20 mM NaCl, 5 mM 2-mercaptoethanol (βME), 50 μg/mL bovine serum albumin, 3 mM ATP, helicase concentration as described, and approximately 0.2 nM radiolabeled partial duplex DNA substrate. The reactions were assembled on ice and the helicase was allowed to preincubate with the DNA substrate for several minutes. The reactions were initiated by the addition of ATP and incubated at 37°C for 5 minutes before addition of 8 μL of stop solution, 37.5% (v/v) glycerol, 50 mM EDTA, 0.3% (w/v) SDS, 0.5x TBE and dyes. The reactions were resolved on 12% (w/v) or 8% (w/v) non-denaturing polyacrylamide gels (19:1 crosslinking ratio), or 3% (w/v) nusieve agarose gels depending on substrate size and visualized by PhosphorImaging (Molecular Dynamics).

Rapid Quench Singe Turnover Assays and Modeling – Rapid quench single turnover assays were performed essentially as previously described (32), with minor modifications, at room temperature (~19^{o}C) using a computer controlled quenched-flow apparatus (KinTek RQF-3, University Park, PA). Helicase was allowed to incubate with the partial duplex substrate (100 nM helicase, 2 nM DNA substrate) in buffer L (25 mM Tris-HCl (pH 7.5), 200 μg/mL bovine serum albumin, 200 μM EDTA, 10% (v/v) glycerol, 5 mM βME) plus 3

mM ATP on ice for 15 min, and then loaded into the D loop. The opposite E loop was loaded with 6 mM $MgCl_2$ and 3 μM DNA hairpin trap in buffer M (25 mM Tris-HCl (pH 7.5), 25 mM NaCl, 10% (v/v) glycerol, 5 mM βME). Reactions were initiated by rapidly mixing equal volume aliquots of the solutions from loops D and E, and were quenched with 200 mM EDTA and 0.2% (w/v) SDS. Samples were resolved on non-denaturing polyacrylamide gels or 3% (w/v) nusieve agarose gels as described above and visualized by PhosphorImaging (Molecular Dynamics).

The modeled unwinding curves were fit to the data collected with each partial duplex DNA substrate using a linear regression model and the kinetic simulator Tenua (Bililite). Using the previously published step size as a starting reference, the pre-steady state kinetics were modeled using the n-step kinetic scheme (see Scheme 1). The modeled data were compared to the collected data by calculating the residuals for each collected data point at the corresponding point generated by the model. The number of steps, k_{np}, k_d and k_u were manually adjusted until a best fit was obtained. The fits which produced the smallest residuals compared to model were defined as best fits. The modeled curves were visually inspected to ensure the quality of the fit. The data for each substrate length was analyzed in this manner and best fits calculated.

DNA binding Assays – Affinities of the helicases for DNA were determined using electrophoretic mobility shift assays and fluorescence anisotropy as previously described (33-35).

Results

The *uvrD303* allele, containing amino acid substitutions at positions 403 and 404 (D403A, D404A), was originally isolated by Kushner and colleagues (27) in a screen for mutations in regions outside the conserved helicase motifs that impact biological function. Cells expressing this mutant form of UvrD from a plasmid exhibit increased sensitivity to ultraviolet light and methyl methane sulfonate as do cells containing a deletion of the *uvrD* gene. Interestingly, cells expressing *uvrD303* also exhibit an antimutator phenotype (27) whereas a *uvrDΔ* strain has a mutator phenotype (36). A strain containing *uvrD303* in the chromosome exhibits similar phenotypes (28) indicating that the phenotypes observed are not simply due to increased expression of the mutant protein. Importantly, the purified UvrD303 protein was characterized as having a slightly increased specific activity as an ATPase and unwinds partial duplex substrates 10-fold better than the wild-type enzyme (27) leading to its designation as a hyper-helicase. We have used biochemical assays, including pre-steady state, single turnover kinetic experiments, to further understand the mechanistic basis of the increased helicase activity associated with this mutant protein.

The *uvrD303* allele was constructed in an expression plasmid as described under "Materials and Methods" and the protein was purified to apparent homogeneity using a rapid two step purification procedure (29). To confirm the results presented previously (27), unwinding assays were performed using partial duplex substrates under multiple turnover conditions. All DNA substrates used for these experiments contained a 40 nucleotide poly(dT) 3'-tail and a duplex region of varying length (Table 1). Previous studies have shown that a 40 nucleotide ssDNA is optimal for UvrD-catalyzed helicase activity (32).

Either UvrD or UvrD303 was incubated with the DNA substrate and unwinding was initiated by the addition of ATP. Using a 24 base pair (bp) partial duplex, the wild-type helicase unwound approximately 6% of the substrate at a concentration of 3.7 nM as compared to unwinding of 77% of the substrate at an equal concentration of UvrD303 (Fig. 5A). This represents nearly a 13-fold increase in unwinding activity. The significant increase in unwinding activity observed with UvrD303 was also demonstrated using a 90 bp partial duplex substrate. On this longer substrate only about 4% of the DNA was unwound by the wild-type helicase at a concentration of 5 nM as compared to 59% unwound by UvrD303 at the same concentration (Fig. 5B). These data support previous work showing that UvrD303 exhibits a marked increase in helicase activity under multiple turnover conditions (27).

The multiple turnover unwinding experiments, while informative, do not yield significant new information about the mechanism by which the helicase activity is increased. The observed increase could be due to one or more of any number of properties being altered in the mutant including binding affinity for the substrate, an increase in the rate of unwinding or an increase in the processivity of the unwinding reaction.

The previous study (27) suggested that the increased helicase activity observed in multiple turnover experiments was not due to an increased affinity of UvrD303 for the DNA substrate. To confirm and extend this observation we measured the DNA binding activity of UvrD303, as compared to that of the wild-type UvrD, using both electrophoretic mobility shift assays (EMSA) and fluorescence anisotropy in the presence and absence of nucleotide. EMSA experiments using the 24 bp partial duplex ligand indicated that UvrD and UvrD303 both bound DNA, in the presence and absence of nucleotide, with very similar affinity (Fig. 6A). Fluorescence anisotropy experiments were performed using a fluorescently labeled

ligand with 20 bp of duplex DNA and a 40 nucleotide 3'-ssDNA tail to mimic the substrate used in unwinding experiments. Ten individual measurements were made at each protein concentration and the average was plotted as a function of protein concentration (Fig. 6B). These experiments yielded a K_d for UvrD of 23.5 ± 1.4 nM in the absence of nucleotide and 14.6 ± 1.4 nM in the presence of the poorly hydrolyzed ATP analog, ATPγS. These values are somewhat higher than previously reported K_d values for UvrD (37) which were determined using a different technique and a different DNA ligand. The K_d measured for UvrD303 was 15.7 ± 2.3 nM in the absence of nucleotide and 3.9 ± 0.6 nM in the presence of ATPγS. These data suggest that UvrD303 has a somewhat higher initial binding affinity for the partial duplex substrate than UvrD. However, this difference in initial DNA binding affinity alone is not likely to account for the dramatic increase in unwinding observed using UvrD303.

To investigate further the increase in UvrD303-catalzyed unwinding, single turnover pre-steady state kinetic experiments were performed. Using a rapid chemical quenched flow protocol, excess helicase (50 nM final concentration), the partial duplex substrate (1 nM final concentration) and ATP were pre-incubated to allow formation of the enzyme-substrate complex, and then rapidly mixed with $MgCl_2$ and a 1500-fold excess of a DNA hairpin trap to initiate unwinding. The excess trap ensures the sequestering of any free or dissociated helicase and prevents any reinitiation of unwinding. Control experiments have demonstrated that the hairpin trap at this concentration is effective in trapping all excess UvrD (data not shown). The time of incubation was varied from 0.075s to 65s and the fraction of DNA unwound was determined at each time point. Rapid quench flow experiments were performed using the 24 bp and 90 bp partial duplex substrates described above and a 243 bp

partial duplex substrate generated by digestion of pUC19-TS plasmid as described under "Materials and Methods". It is important to note that these unwinding assays are 'all or none' and do not detect partially unwound DNA molecules. Using the 24 bp partial duplex DNA, both UvrD and UvrD303 were capable of converting the duplex substrate to ssDNA (Fig. 7A). Under these conditions UvrD unwound approximately 40% of the substrate while UvrD303 unwound nearly 95% of the substrate. It also appears that the exponential rise trends generated by the unwinding reactions level off at very similar time points. If these trends are compared with respect to the total amount of partial duplex substrate, a simple rate describing the approximate number of base pairs unwound per second per UvrD molecule can be estimated. These rates on this 24 bp partial duplex substrate are estimated to be 0.13 bp unwound per second per UvrD and 0.19 bp unwound per second per UvrD303. These data suggest that the unwinding reaction catalyzed by UvrD and UvrD303 occurs at a similar rate but UvrD303 is able to unwind a much larger fraction of the substrate.

The similarity of the rates of unwinding prompted us to also measure the rate of ATP hydrolysis by the wild-type and mutant protein. Previous data (27) suggested there was a modest increase in ATP hydrolysis activity conveyed by the 303 mutation. However, the K_m for ATP was nearly identical for each helicase. We performed similar ATPase assays and observed the same result. UvrD303 does have a somewhat higher ATPase activity and the K_m of the protein for ATP is essentially identical to that of the wild-type enzyme (Table 2).

When rapid quench flow experiments were performed using the 90 bp partial duplex no detectable unwinding by UvrD was observed. This result was expected as previous work indicates the processivity of UvrD is 40-50 base pairs unwound per binding event (39).

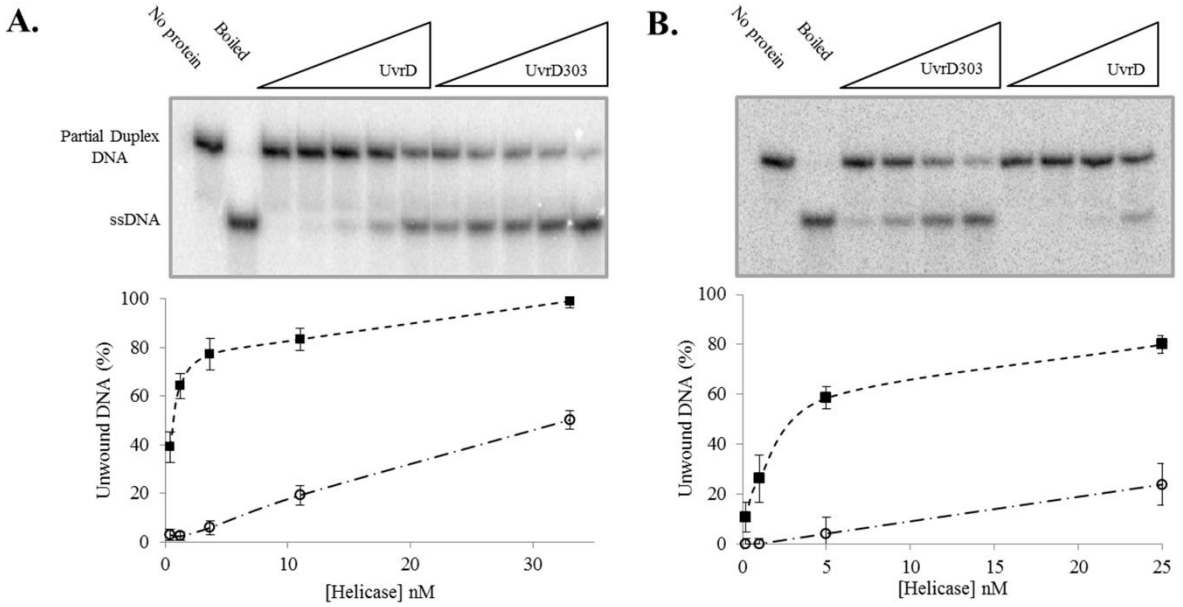

Figure 5. UvrD303 exhibits hyper-helicase activity compared to wild-type UvrD**.** Panel A – DNA helicase reactions were performed as described under "Materials and Methods" using the 24 bp partial duplex substrate and increasing concentrations of UvrD or UvrD303. The first two lanes are controls for no protein and heat denatured substrate DNA. The remaining lanes depict a protein titration of increasing concentration from 0.4 to 33 nM UvrD or UvrD303. Quantitative data from 2 experiments at the indicated concentrations of UvrD (open circles) and UvrD303 (closed squares) were plotted as the average at each protein concentration. Error bars represent the standard deviation about the mean. Panel B – DNA helicase reactions were as described under "Materials and Methods" using the 90 bp partial duplex substrate and increasing concentrations of UvrD or UvrD303. The first two lanes are controls for no protein and heat denatured substrate DNA. The remaining lanes show a protein titration of increasing concentration from 0.2 to 25 nM UvrD or UvrD303. Quantitative data from 2 experiments at the indicated concentrations of UvrD (open circles) and UvrD303 (closed squares) were plotted as the average at each protein concentration. Error bars represent the standard deviation about the mean.

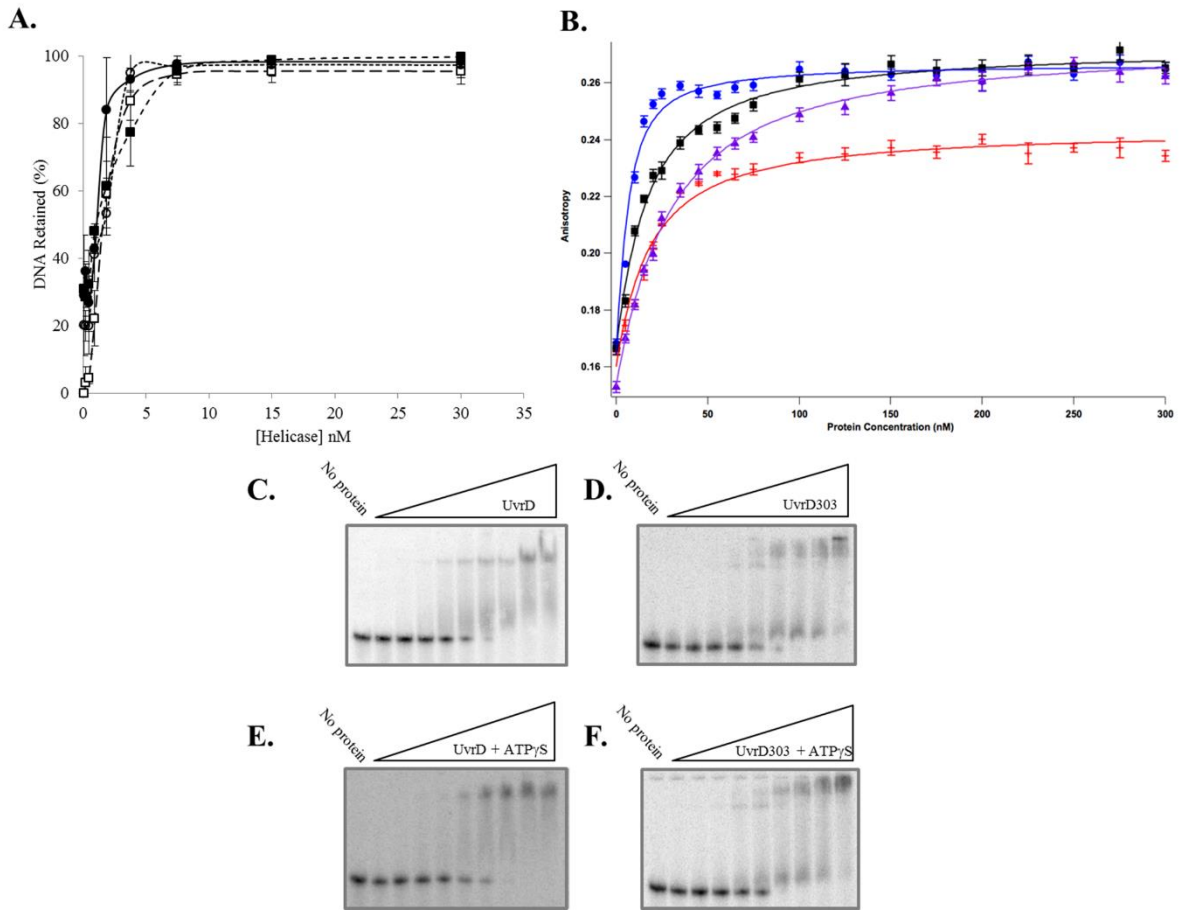

Figure 6. UvrD303 exhibits similar DNA binding properties to that of wild-type UvrD. Panel A – Electrophoretic mobility shift assays were performed as described under "Materials and Methods". Increasing concentrations of UvrD (open circles), UvrD + ATγSP (open squares), UvrD303 (closed circles) and UvrD303+ ATPγS (closed squares) were incubated with the 24 bp partial duplex substrate for 5 min prior to electrophoresis. Data represent the average of 3 experiments. Panel B – Fluorescence anisotropy was performed as described under "Materials and Methods". Each data point is an average of ten reads at each indicated protein concentration. The data were collected using a SPEX Fluorolog-3 spectrofluorometer. UvrD303 (red cross); UvrD303 +ATPγS (blue circles); wild-type UvrD (purple triangles); wild-type UvrD + ATPγS (black squares).

Therefore, UvrD is not expected to unwind a 90 bp partial duplex substrate in a single turnover experiment. UvrD303, however, was able to unwind nearly 70% of the of the 90 bp substrate (Fig. 7B).

Since UvrD303 unwound a significant fraction of the 90 bp partial duplex substrate in a single turn over we designed a longer 243 bp partial duplex molecule to begin to test the processivity limits of the mutant helicase. Wild-type UvrD was not tested on this longer substrate since it failed to unwind the 90 bp substrate under single turnover conditions. Significant unwinding activity under single turnover conditions was also observed using the 243 bp partial duplex where UvrD303 was able to unwind approximately 30% of the substrate (Fig. 7C). Taken together, these data suggest that UvrD and UvrD303 unwind duplex DNA with similar rates but the processivity of the unwinding reaction catalyzed by UvrD303 is significantly higher than that of wild-type UvrD. The augmented helicase activity observed in the single turnover experiments reported above could indicate a change in the kinetic mechanism of unwinding by the helicase. Alternatively, these data may indicate that the kinetic mechanism is essentially the same as that of wild-type UvrD but the processivity of the unwinding reaction has been significantly increased due to the mutation in the 2B subdomain. The unwinding kinetics of UvrD were previously modeled by Ali and Lohman (39) and conform to the well documented n-step model of unwinding applied to many DNA helicases (39, 40). In this model, wild-type UvrD has been shown to have a kinetic step size of approximately four base pairs and takes about 10 steps before dissociating from the DNA. Thus, the average processivity of UvrD is 40-50 base pairs unwound per binding event.

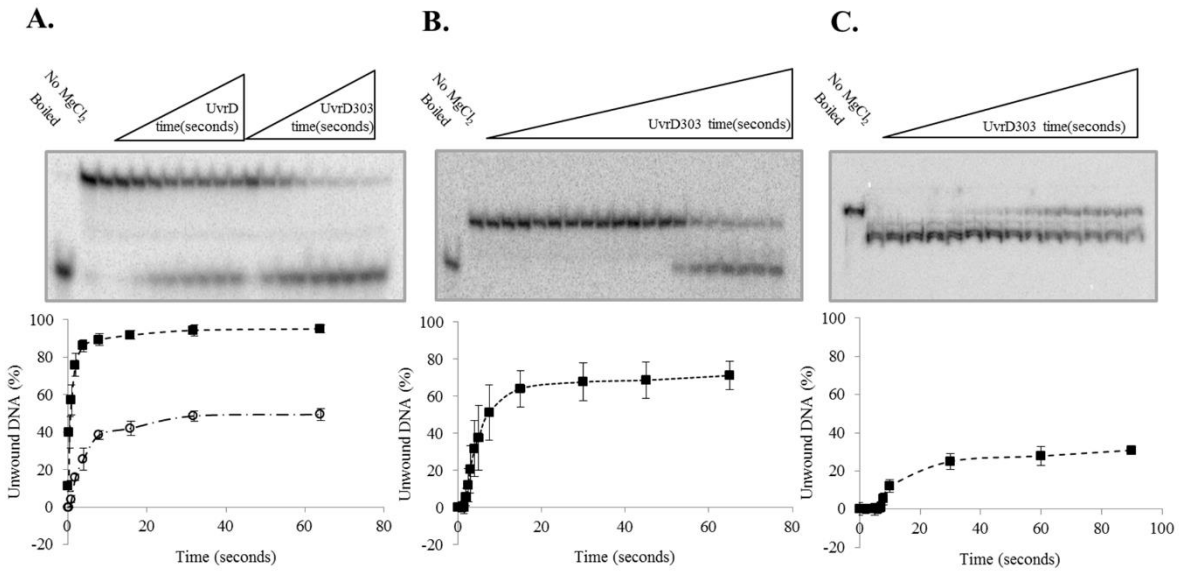

Figure 7. UvrD303 exhibits a stimulated helicase activity in single turnover rapid quench reactions. Panel A – DNA helicase single turnover rapid quench reactions were performed as described under "Materials and Methods" using a 24 bp partial duplex substrate and increasing time. The first two lanes are controls for heat denatured substrate and for no magnesium chloride ($MgCl_2$). The remaining lanes depict a time course from 0.25 to 64 seconds for both UvrD and UvrD303. Quantitative data from 3 experiments for UvrD (open circles) and UvrD303 (filled squares) were plotted as an average. Panel B – DNA helicase single turnover rapid quench reactions were performed as described under "Materials and Methods" using a 90 bp partial duplex substrate and increasing time. The first two lanes are controls for heat denatured substrate and no magnesium chloride ($MgCl_2$). The remaining lanes depict a time course from 0.075 to 65 seconds for UvrD303. Quantitative data represent the average of 3 experiments using UvrD303. Panel C – DNA helicase single turnover rapid quench reactions were performed as described in "Materials and Methods" using a 243 bp partial duplex substrate and increasing time. The first two lanes are controls for heat denatured substrate and no magnesium chloride ($MgCl_2$). The remaining lanes depict a time course from 2 to 90 seconds for UvrD303. Quantitative results from 4 experiments were averaged and plotted for UvrD303.

The n-step model is shown in Scheme 1. UvrD bound to the partial duplex DNA undergoes a poorly understood conversion from a non-productive complex to an active unwinding complex (k_{np}). It should be noted that k_{np} represents not only the conversion to a productive unwinding complex, but the lag from the initiation of unwinding to the point at which completely unwound ssDNA is detectable. Using these parameters, k_{np} "slows" with increasing substrate length (Fig. 8A). Once unwinding is initiated, the unwinding scheme assumes that UvrD has a chance to dissociate at each intermediate step (k_d) and a chance to continue unwinding (k_u). The mechanism continues with the helicase taking a size-defined "kinetic step" between each intermediate until either the duplex is unwound or the helicase dissociates from the substrate. The probability of the helicase taking another unwinding step as opposed to dissociating from the substrate is defined as the processivity. Wild-type UvrD was previously modeled to have an average step size of 4.4 bp and a processivity of 0.9. We applied this model to our data using the kinetic simulator Tenua (Bililite). The resulting best fits for the data (Fig. 8B) were used to calculate the processivity of the helicases. Using the data reported here for wild-type UvrD unwinding of the 24 bp partial duplex we observed a step size of 4.0 and a processivity of 0.87. These values are in excellent agreement with those reported previously (39) and suggest that UvrD can unwind approximately 35 bp in a single turnover. When the model is applied to the single turnover data obtained using UvrD303 for the three partial duplex substrates studied here two striking differences are observed. The average kinetic step size and processivity of UvrD303 increase to an average of 7.0 and 0.973, respectively, as shown in Table 3. This correlates to an average of 37 steps taken or 261 bp unwound before dissociation. The observed increase in the number of base pairs

unwound per binding event is an approximate eight-fold increase and accounts for the previously reported ten-fold increase in helicase activity.

Discussion

The *uvrD303* allele was discovered in a screen for mutations outside the conserved helicase motifs of UvrD that had a clear impact on the activity of the protein as measured in genetic assays (27). UvrD303 contains two amino acid substitutions (D403A, D404A) in the 2B subdomain of the protein between conserved motifs IV and V (see Fig. 4B). The impact of this mutation is remarkable both for its alteration of the biochemistry of the protein and the significantly different phenotype of cells harboring this mutation. The purified protein has been described as a "hyper-helicase" based on a steady state analysis of helicase activity.

This has been confirmed in our studies (see Fig. 5). Expression from a plasmid or the chromosome confers an antimutator phenotype on cells suggesting an altered, but still functional, role in MMR. Curiously, cells harboring the *uvrD303* mutation are UV-sensitive as are *uvrD* null mutants. Sandler and colleagues (28) have traced this phenotype to a defect in recombinational repair of UV-induced lesions rather than a defect in NER and conclude that UvrD303 is likely functional in NER. This is consistent with the fact that UvrD303 is active as a helicase and with the hypo-recombination phenotype associated with the *uvrD303* allele (27). *uvrD* null mutants exhibit a hyper-recombination phenotype that has been ascribed to the ability of wild-type UvrD to strip RecA protein from potential recombination intermediates (38). Thus, wild-type UvrD prevents unwanted recombination events from occurring and, in the absence of UvrD, there is more recombination than in wild-type cells. The hypo-recombination phenotype associated with *uvrD303* may be due to an increased ability to disrupt RecA-DNA filaments poised to undergo recombination. The experiments

reported here have shed light on the altered properties of UvrD303 and provide some insight into why cells harboring UvrD303 exhibit antimutator and hypo-Rec phenotypes.

The pre-steady state, single turnover experiments shown in Figure 7 indicate that UvrD303 has an increased processivity and an increased kinetic step size. In fact, the processivity of the mutant protein is increased by a factor of eight from approximately 40 base pairs per unwinding event to nearly 300 base pairs unwound per unwinding event. This result is sufficient to explain the increased helicase activity observed in steady state experiments (27 and Fig. 5) and, coupled with the fact that the rate of unwinding catalyzed by UvrD303 is essentially the same as for the wild-type protein, suggests that the primary biochemical alteration in the enzyme is an increase in processivity. However, we also note there is an increase in the affinity of UvrD303 as compared to wild-type UvrD for initial binding to a DNA substrate as measured using fluorescence anisotropy. Since the single turnover experiments demonstrating an increase in the processivity of the unwinding reaction are done under conditions of excess enzyme this is not likely to be a significant factor in determining the processivity of unwinding. Nonetheless, this may contribute to the observed hyper-helicase activity measured in multiple turnover experiments and could have an impact *in vivo*.

How might the two amino acid mutation within the 2B subdomain of UvrD increase the processivity of the enzyme? It has been shown that the 2B subdomain of SF1 helicases has a role in regulating the helicase activity of the enzyme (41). Deletion of the 2B subdomain in the very closely related Rep helicase has been shown to activate the helicase activity of a Rep monomer (26) consistent with the 2B subdomain having a role in regulating

helicase activity. Efforts to delete the 2B subdomain of UvrD have not been successful and it has been suggested that perhaps the unregulated activity of UvrD is lethal (25).

Table 2. DNA-stimulated ATPase activity of UvrD and UvrD303

Enzyme	ATPase Activity (pmols ADP/UvrD/sec)	K_m (μM)
UvrD	28.5 ± 8.1	64.3 ± 2.7
UvrD303	68.9 ± 27.2	71.1 ± 1.4

All ATPase assays were performed as described under "Materials and Methods" and measured the production of [^{32}P]ADP as a function of time and helicase (monomer) concentration.

Table 3. The 303 mutation confers an increased processivity and step size compared to wild-type

	UvrD	UvrD303
Processivity	0.87 ± 0.008	0.973 ± 0.003
Step Size	4 bases	7 bases
Steps Taken	8.9 ± 0.97	37.4 ± 4.8
Bases Unwound	34.9 ± 3.9	261 ± 33.5

The modeled data were used in conjunction with the following equations: $A_L=P^{(L/m)}$ and $P=(N-1)/N$ to calculate step size, processivity, and number of bases unwound where A_L is the extent of unwinding, P is processivity, L is duplex length, m is the average step size and N is the average number of steps taken in a single turnover (39).

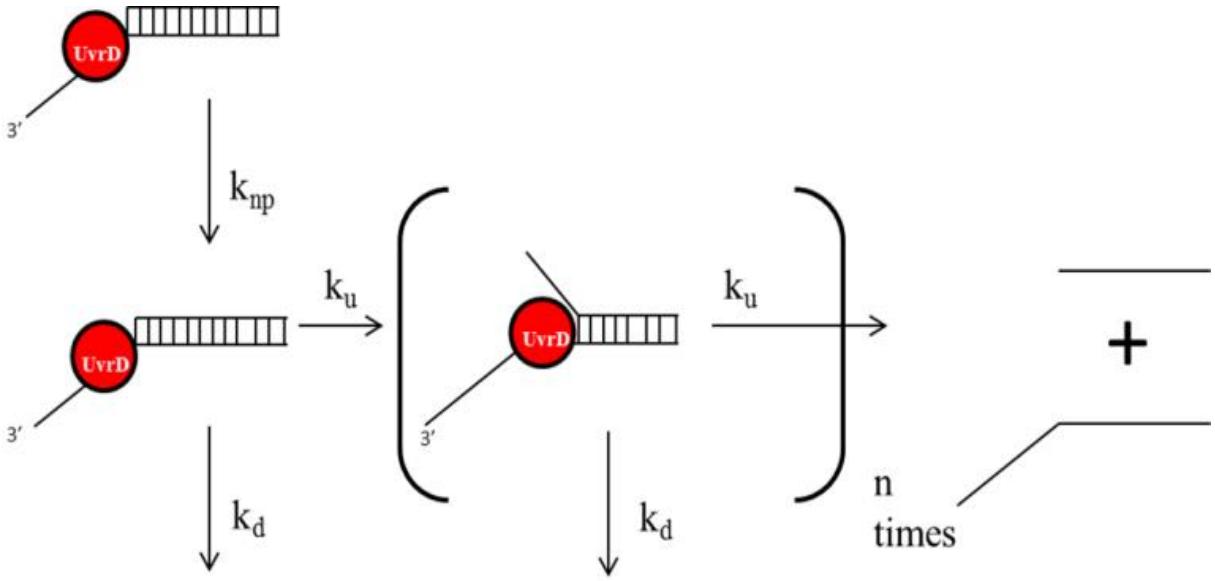

Scheme 1. The sequential n-step kinetic model**.** Preformed UvrD-DNA complexes undergo a conversion to partially unwound intermediates (see inside brackets) as the pathway progresses until a fully unwound ssDNA is generated. At each intermediate step the helicase may dissociate from the unwinding complex, k_d, or proceed with further unwinding, k_u. The processivity calculated using this model is representative of the probability that the helicase will proceed in the unwinding pathway. The model also predicts a slow, rate limiting step, k_{np}, which describes the conversion of nonproductive UvrD-DNA complexes into active unwinding complexes.

A.

	UvrD	UvrD303		
Duplex Size	24bp	24bp	90bp	243bp
Amplitude	0.48	0.93	0.71	0.28
Processivity	0.88	0.98	0.97	0.97
Step Size	5 bp	8 bp	7 bp	6 bp
k_{np}	1.09s^{-1}	1.85s^{-1}	0.23s^{-1}	0.05s^{-1}
k_u	6.70s^{-1}	5.80s^{-1}	5.55s^{-1}	6.30s^{-1}
k_d	0.41s^{-1}	0.65s^{-1}	0.58s^{-1}	0.54s^{-1}

B.

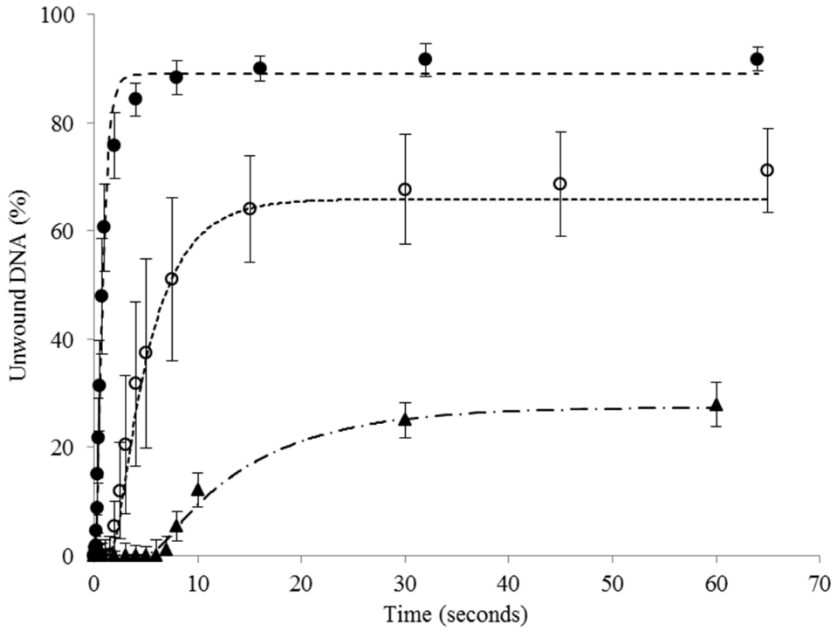

Figure 8. Modeled kinetics of UvrD303 helicase activity**.** Panel A – Compiled data for kinetic parameters of the n-step model for UvrD303 on the 24 bp partial duplex, 90 bp partial duplex or 243 bp partial duplex. Panel B – Graphical fit of modeled data versus collected data. The hashed lines represent the unwinding predicted by the model while the markers depict the average data collected from single turnover rapid quench experiments for the 24 bp partial duplex (closed circles), the 90 bp partial duplex (open circles) and the 243 bp partial duplex (closed triangles).

A possible explanation for the increase in processivity is that UvrD303 forms dimers more efficiently than the wild-type protein. The impact of more efficient dimer formation is not likely to be reflected in single turn over experiments done with an excess of enzyme since the substrate is prebound with protein prior to initiating the unwinding reaction. Alternatively, the dimers might be more stable during the course of the unwinding reaction serving to increase the processivity. We cannot formally discount this possibility.

The explanation for the increased processivity that we propose takes into account the mechanistic insights derived from various co-crystal structures and the proposal that the 2B domain plays a regulatory role. The crystal structure of UvrD with the 2B subdomain in the open conformation has been reported (22). This open conformation of UvrD differs from its closed counterpart by a 160° rotation of the 2B subdomain around the 2A subdomain. The closed conformation, as captured by Lee and Yang (14), showed that the 2B subdomain makes contacts with the duplex DNA and the newly unwound ssDNA as well as having contacts with the 1B subdomain. The two conformations of UvrD (open and closed) differ only slightly from the two conformations of Rep protein reported earlier (20). Recently it has been shown that the 2B subdomain of UvrD exists in many intermediate positions between completely open and completely closed depending on factors such as salt concentration, DNA and nucleotide binding (22). We speculate that the UvrD303 mutation prevents the helicase from adopting a fully closed conformation with respect to the 2B subdomain perhaps because the mutant 2B subdomain is unable to make or maintain contacts with the 1B subdomain. Although our current attempts at localizing the "contact points" of the 2B and 1B subdomains have not been successful (data not shown), it may be possible to construct a

helicase that exhibits UvrD303-like hyper-helicase activity via mutations in the 1B subdomain.

Yang and colleagues (14) have proposed an alternative mode of unwinding based on the translocation of the protein along one strand with the helicase acting to "plow through" and displace the partner strand as contrasted with the wrench-and-inchworm model for unwinding proposed based on structural studies of UvrD bound to varying DNA substrates and nucleotides. In the latter model, the 2B subdomain engages the duplex DNA via the so called GIG motif and, along with the ssDNA anchor of motif III, holds the DNA substrate while the separation pin and ssDNA gateway remain flexible allowing for unwinding. As the helicase cycles through the process of ATP hydrolysis these four contact points invert their roles allowing the helicase to act as a sort of "molecular ratchet" in the course of the unwinding reaction. We speculate that UvrD303 utilizes the strand displacement mode of unwinding exclusively due to the mutations in the 2B subdomain. This interpretation is consistent with the increased processivity we have measured with the mutant protein and, remarkably, the increased processivity reported here mirrors the processivity reported for UvrD as a translocase (42). In addition, an alternate mode of unwinding may account for the near doubling in kinetic step size observed for UvrD303. It is reasonable to expect a different unwinding mechanism to exhibit a different kinetic step size.

It is possible that the opening and closing of the 2B subdomain modulates the unwinding activity of UvrD and this, in turn, directs its function in some of its intracellular roles. It was reported that UvrD303 removes RecA from sites of DNA damage to a greater extent than wild-type UvrD when expressed from the chromosome (28). These data would suggest that the 303 mutation alters the function of UvrD in its role in RecA-mediated DNA

repair. Wild-type UvrD has been shown to remove RecA from RecA-ssDNA filaments and presumably this is regulated such that UvrD destroys unwanted recombination intermediates while not interfering with those intermediates that are required for appropriate recombinational repair. How this activity of UvrD is regulated is unknown. It is tempting to speculate that UvrD303 is hyperactive in this function and this leads to the hypo-Rec phenotype associated with the mutant. Indeed, if UvrD303 simply translocates along ssDNA acting as a helicase by plowing through the duplex then this mechanism might also remove bound protein, like RecA.

In addition, it has been shown that when UvrD303 is expressed from the chromosome there is a decrease in the rate of spontaneous mutation by 50-80% (27, 28). UvrD has a well described role in MMR as the helicase that unwinds the duplex DNA between the nick that initiates this repair reaction and the mismatched base pair that must be repaired. As the DNA is unwound the nascent ssDNA is removed by ssDNA exonucleases providing a gap that is filled by DNA polymerase III to complete the repair reaction. The nick that initiates MMR is located on the unmethylated strand at a hemi-methylated d(GATC) site. This site may be located at a significant distance from the mismatched base pair that must be replaced to complete repair. The efficiency of this repair reaction decreases as the distance between the hemi-methylated d(GATC) and the mismatch increases (43), perhaps due to the limited processivity of UvrD. A UvrD mutant with an increased processivity could be envisioned to improve the efficiency of mismatch repair over long distances and this may account for the antimutator phenotype associated with the *uvrD303* mutation. This hypothesis has not been directly tested.

REFERENCES

1. Matson, S.W., Dean, D.W., and George, J.W. (1994). DNA helicases: enzymes with essential roles in all aspects of DNA metabolism. *Bioessays.* **16**,13-22

2. Egelman, E.H. (1998). Bacterial Helicases. *J Struct Biol.* **124,** 123-128

3. Bochman, M.L., and Schwacha A.(2009). The Mcm complex: unwinding the mechanism of a replicative helicase. *Microbiol Mol Biol Rev.* **73**, 652-683

4. Abdelhaleem, M. (2010) Helicases: an overview. *Methods Mol Biol.* **587**, 1-12

5. Bachrati, C.Z., and Hickson, I.D. (2008). RecQ helicases: guardian angels of the DNA replication fork. *Chromosoma.* **117**, 219-233

6. Chu,W.K., and Hickson, I.D. (2009). RecQ helicases: multifunction genomic caretakers. *Nat Rev Cancer.* **9**, 644-654

7. Gupta, R., and Brosh R.M.,Jr. (2007). DNA repair helicases as targets for anti-cancer therapy. *Curr Med Chem.* **14**, 503-517

8. Brosh, R.M.,Jr., and Bohr, V.A. (2007). Human premature aging, DNA repair and RecQ helicases. *Nucleic Acids Res.* **35**, 7527-7544

9. Husain, I., Van Houten, B., Thomas, D.C., Abdel-Monem, M., Sancar, A. (1985). Effect of DNA polymerase I and DNA helicase II on the turnover rate of UvrABC excision nuclease. *Proc Natl Acad Sci USA.* **82**, 6774-6778

10. Yamaguchi, M., Dao, V., and Modrich, P. (1998). MutS and MutL activate DNA helicase II in a mismatch dependent manner. *J Biol Chem.* **273**, 9197-9201

11. Lahue, R.S., Au, K.G., and Modrich, P. (1989) DNA mismatch correction in a defined system. *Science.* **245**, 160-164

12. Dao, V., and Modrich, P. (1998) Mismatch-, MutS-, MutL-, and helicase II- dependent unwinding from the single-strand break of an incised heteroduplex. *J Biol Chem.* **273**, 9202-9207

13. Centore, R.C., and Sandler, S.J. (2007). UvrD limits the number and intensities of RecA-green fluorescent protein structures in Escherichia coli K-12. *J Bacteriol.* **189**, 2915-2920

14. Lee, J.Y., and Yang, W. (2006). UvrD helicase unwinds DNA one base pair at a time by a two-part power stroke. *Cell.* **127**, 1349-1360

15. Gorbalenya, A.E., and Koonin, E.V. (1993) Helicases: amino acid sequence comparisons and structure-function relationships. *Curr. Opin. Strut. Biol*. **3,** 419-429

16. Iyer, L.M., Leipe, D.D., Koonin, E.V., and Aravind, L. (2004). Evolutionary history and higher order classification of AAA+ ATPases. *J. Struct.Biol.***146**, 11–31

17. Hickson, I.D., Arthur, H.M., Bramhill, D., and Emmerson, P.T. (1983). The E. coli uvrD gene product is DNA helicase II. *Mol. Gen. Genet.* **190**, 265–270

18. Matson, S.W., and George, J.W. (1987). DNA helicase II of Escherichia coli. Characterization of the single-stranded DNA-dependent NTPase and helicase activities. *J. Biol. Chem.* **262**, 2066–2076

19. Velankar, S.S., Soultanas, P., Dillingham, M.S., Subramanya, H.S. ,and Wigley, D.B. (1999). Crystal structures of complexes of PcrA DNA helicase with a DNA substrate indicate an inchworm mechanism. *Cell* **97**, 75–84

20. Korolev, S., Hsieh, J., Gauss, G.H., Lohman, T.M., and Waksman, G. (1997). Major domain swiveling revealed by the crystal structures of complexes of E. coli Rep helicase bound to single-stranded DNA and ADP. *Cell* **90**, 635–647

21. Matson, SW. (1986) Escherichia coli helicase II (uvrD gene product) translocates unidirectionally in a 3′ to 5′ direction. *J Biol Chem.* **261**, 10169-10175

22. Jia, H., Korolev, S., Niedziela-Majka A., Maluf, N.K., Gauss, G.H., Myong, S., Ha, T., Waksman, G., Lohman, T.M. (2011). Rotations of the 2B sub-domain of E. coli UvrD helicase/translocase coupled to nucleotide and DNA binding. *J Mol Biol*. **411**, 633-9648

23. Yao, N., Reichert, P., Taremi, S.S., Prosise, W.W., and Weber, P.C. (1999) Molecular views of viral polyptrotein processing revealed by the crystal structure of the hepatitis C virus bifunctional protease-helicase. *Structure.* **7**, 1353-1363

24. Appleby, T.C., Anderson, R., Fedorova, O., Pyle, A.M., Wang, R., Liu, X., Brendza, K.M., and Somoza, J.R. (2011) Visualizing ATP-dependent RNA translocation by the NS3 helicase from HCV. *J Mol Biol.* **405**, 1139-1153

25. Cheng, W., Brendza, K.M., Gauss, G.H., Korolev, S., Waksman, G., Lohman, T.M. (2002). The 2B domain of the Escherichia coli Rep protein is not required for DNA helicase activity. *Proc Natl Acad Sci U S A.* **99**, 16006-16011

26. Brendza, K.M., Cheng, W., Fischer, C.J., Chesnik, M.A., Niedziela-Majka, A., Lohman, T.M. (2005). Autoinhibition of Escherichia coli Rep monomer helicase activity by its 2B subdomain. *Proc Natl Acad Sci U S A.* **102**, 10076-10081

27. Zhang, G., Deng, E., Baugh, L., and Kushner, S.R. (1998). Identification and characterization of Escherichia coli DNA helicase II mutants that exhibit increased unwinding efficiency. *J. Bacteriol.* **180**, 377–387

28. Centore, R.C., Leeson, M.C., and Sandler, S.J. (2009). UvrD303, a hyperhelicase mutant that antagonizes RecA-dependent SOS expression by a mechanism that depends on its C terminus. *J. Bateriol.* **191**, 1429-1438

29. Tahmaseb K., and Matson S.W. (2010) Rapid purification of helicase proteins and in vitro analysis of helicase activity. *Methods*. **51**, 322-328

30. Studier F.W. (2005) Protein production by auto-induction in high-density shaking cultures. *Prot. Exp. Pur*. **41**, 207-234

31. Runyon, G.T., Bear, D.G., and Lohman, T.M. (1993) Overexpression, purification, DNA binding and dimerization of the Esherichia coli uvrD gene product (helicase II). *Biochemistry*. **32**, 602-612.

32. Ali, J.A., Maluf, N.K., and Lohman, T.M. (1999) An oligomeric form of E. coli UvrD is required for optimal helicase activity. *J Mol Bio*. **293**, 815-834

33. Mechanic, L.E., Frankel, B.A., and Matson, S.W. (2000) Escherichia coli MutL loads DNA helicase II onto DNA. *J Biol Chem*. **275**, 38337-38346

34. Yang, Y., Sass, L. E., Du, C., Hsieh, P., and Erie, D.A. (2005) Determination of protein-DNA binding constants and specificities from statistical analyses of single molecules. MutS-DNA interactions. *Nucleic Acids Res.* **33**, 4322–4334

35. Geng, H., Sakato, M., DeRocco, V., Yamane, K., Du, C., Erie, DA., Hingprani, M., and Hsieh, P. (2012) Biochemical analysis of the human mismatch repair proteins hMutSa MSH2(G674A)-MSH6 and MSH2-MSH6(T1219D*). J Biol Chem.* **287**, 9777-9797

36. Washburn, B.K., and Kushner, S.R. (1991) Construction and analysis of deletions in the structural gene (*uvrD*) for DNA helicase II of *Escherichia coli. J. Bacteriol.* **173**, 2569–2575

37. Hall, M.C., Ozsoy, A.Z., and Matson S.W. (1998) Site-directed mutations in motif VI of Escherichia coli DNA helicase II result in multiple biochemical defects: evidence for the involvement of motif VI in the coupling of ATPase and DNA binding activities via conformational changes. *J Mol Biol.* **277**, 257-271

38. Veaute, X., Delmas, S., Selva, M., Jeusset, J., Le Cam, E., Matic, I., Fabre, F., and Petit, M.A. (2005) UvrD helicase, unlike Rep helicase, dismantles RecA nucleoprotein filaments in Escherichia coli. *EMBO J*. **24**, 180–189

39. Ali, J.A., and Lohman, T.M. (1997). Kinetic measurement of the step size of DNA unwinding by Escherichia coli UvrD helicase. *Science*. **275**, 377-380

40. Maluf, N.K., Ali, J.A., and Lohman, T.M. (2003) Kinetic mechanism for formation of the active, dimeric UvrD helicase-DNA complex. *J Biol Chem*. **278**, 31930-31940

41. Lohman, T.M., Tomoko, E.J., and Wu, C.G. (2008) Non-hexameric DNA helicases and translocases: mechanisms and regulation. *Nat Rev Mol Cell Biol*. **9**, 391-401

42. Tomko, E.J., Fischer, C.J., and Lohmn, T.M. (2012). Single-stranded DNA translocation of E. coli UvrD monomer is tightly coupled to ATP hydrolysis. *J Mol Biol*. **418**, 32-46

43. Bruni, R., Martin, D., and Jiricny, J. (1988) d(GATC) sequences influence Escherichia coli mismatch repair in a distance-dependent manner from positions both upstream and downstream of the mismatch. *Nucleic Acids Res*. **16**, 4875-4890

CHAPTER 3: THE MISMATCH REPAIR PROTEIN MUTL IS A PROCESSIVITY FACTOR FOR THE UVRD HELICASE

Abstract

The *Escherichia coli* UvrD helicase has well described and well studied roles in both nucleotide excision repair and methyl-directed mismatch repair. In the latter DNA repair pathway, UvrD displaces the newly synthesized strand containing the mis-incorporated base which is digested by an appropriate exonuclease. The resulting gap is filled by the replicative DNA polymerase III holoenzyme, facilitating the incorporation of the correct base into the bacterial genome. The repair tracks in mismatch repair initiate at a nick induced by the repair protein MutH at a hemi-methylated d(GATC) and can be in excess of one kilobase in length, well beyond the reported unwinding processivity UvrD exhibits *in vitro*. This apparent disconnect in between the activity required *in vivo* and observed *in vitro* is not fully understood. We previously reported a physical interaction between MutL, a protein required for mismatch repair, and UvrD. This interaction results in a dramatic stimulation of the UvrD-catalyzed unwinding reaction that requires the ATP-bound form of MutL but does not require MutL-catalyzed ATP hydrolysis. To characterize the functional implications of this interaction, a pre-steady state, single turnover kinetic analysis of MutL-stimulated UvrD-catalyzed unwinding was undertaken using partial duplex DNA substrates of increasing duplex length. The kinetic data indicate that the MutL-stimulated unwinding reaction catalyzed by UvrD is significantly more processive than the unwinding reaction catalyzed by UvrD alone. We hypothesize that the ATP-

bound form of MutL may be acting to either alter the unwinding mechanism utilized by UvrD or may clamp UvrD on the DNA thereby increasing its processivity.

Introduction

DNA helicases catalyze the energy-dependent unwinding of duplex DNA and are required in all aspects of DNA metabolism, including DNA replication, recombination and repair (1-6). These enzymes couple the disruption of the hydrogen bonds that hold the two DNA strands together to the hydrolysis of nucleoside 5'-triphosphates using a variety of mechanisms (7-10). Some helicases function as hexamers, threading one strand of DNA though a central channel while extruding the other strand to the outside of the ring-shaped structure. Others function as dimers where the leading monomer functions as a helicase while the trailing subunit functions as a translocase (11, 12). Finally, some helicases appear to function as monomers and unwind DNA using an 'inchworm-like' mechanism (13).

The UvrD helicase, which functions as a dimer (11, 12, 14), is required in methyl-directed mismatch repair (MMR) to displace the error containing nascent DNA strand to facilitate the removal of the error-containing DNA strand with an appropriate single-stranded DNA (ssDNA) exonuclease (15-17). Previous kinetic studies have shown that UvrD has a very modest processivity of 40-50 base pairs (bp) unwound per binding event (18). The low processivity of this helicase is potentially problematic in a repair pathway that requires the processing of repair tracks that can be in excess of one kilobase in length (19).

UvrD also has a direct role in nucleotide excision repair (NER). In this repair pathway UvrD removes a 12-13 base oligonucleotide containing the DNA damage after incision on both sides of the damage by the UvrABC nuclease complex (20, 21). In this role the modest processivity of UvrD makes it well suited to its task. UvrD is likely to have additional functions in recombinational repair, replication and the inhibition of homeologous recombination (20-25). The role of UvrD in each of these processes is less well understood.

A physical interaction between UvrD and the mismatch repair protein MutL was first uncovered in a yeast two hybrid study (26). Subsequent work showed that MutL dramatically stimulated the UvrD-catalyzed helicase reaction (27-29). We have proposed two models to describe the mechanism for the stimulation of UvrD-catalyzed unwinding by MutL (38; see Fig. 9). In the first model, MutL bound to the DNA near a ssDNA-duplex DNA junction is envisioned to load multiple molecules of UvrD onto the DNA. Since UvrD exhibits a processivity of ~250 bases as a translocase on ssDNA (30, 31), MutL is proposed to repeatedly load UvrD so that as one UvrD dimer dissociates from the DNA after unwinding 40-50 bp another UvrD dimer is present to continue unwinding before the partially unwound duplex reanneals. This iterative loading of UvrD is thought to occur multiple times until the duplex region is effectively unwound past the mismatch or insertion-deletion loop and is consistent with electron microcopy showing multiple molecules of UvrD associated with unwound DNA (32). The second model posits that MutL increases the processivity of UvrD, perhaps by clamping UvrD on the DNA, much like the sliding clamps that increase the processivity of DNA polymerases (33). In this case MutL would increase the number of bp unwound by UvrD in a single binding event by forming a topological clamp that effectively tethers the UvrD helicase on the DNA. This model is consistent with the closed structure of ATP-bound MutL observed by X-ray crystallography (34, 35) and the stable interaction between UvrD and MutL that has been reported (26). Alternatively, MutL could interact with UvrD to stabilize the open conformation of UvrD which was suggested to increases the processivity of the UvrD unwinding reaction (Chapter 2).

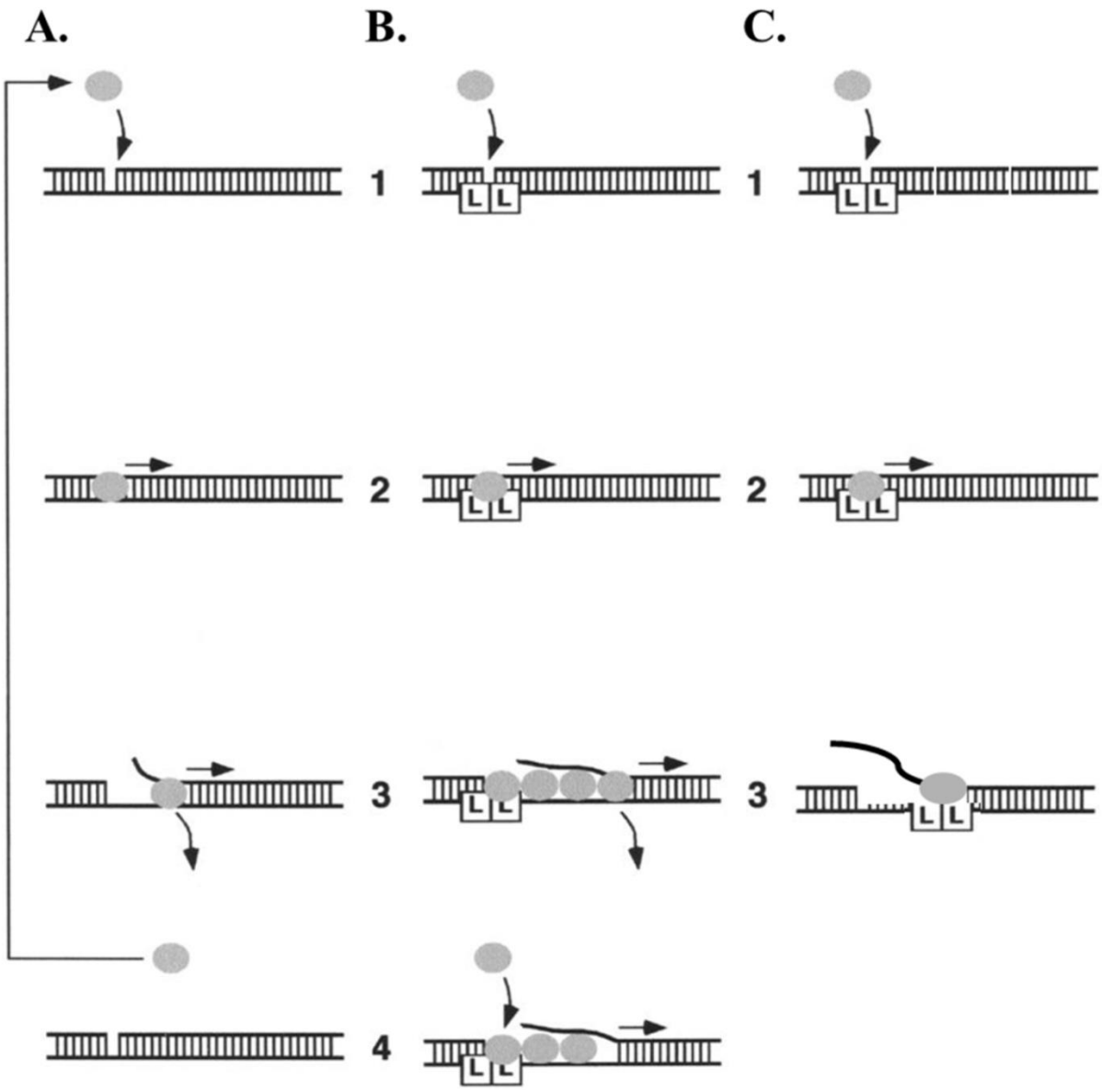

Figure 9. Representation of two models of MutL stimulated UvrD-catalyzed unwinding of DNA. Panel A – Unwinding in the absence of MutL. UvrD binds at the nick and initiates unwinding but can only unwind 40-50 bp before dissociating from the DNA, allowing the duplex to reanneal. Panel B – MutL-stimulated UvrD unwinding by continuously loading UvrD molecules onto the duplex in an iterative process. Panel C – MutL increases the processivity of UvrD by clamping UvrD on the DNA and translocating along the duplex with UvrD as it unwinds. Modified from (27).

Kinetic studies have shown that UvrD unwinds duplex DNA via a step-wise mechanism exhibiting a lag phase in which only partially unwound intermediates are produced before a completely unwound ssDNA species is detected (18). UvrD has been shown to unwind ~4-5 bp of double-stranded DNA in one 'kinetic step' and takes an average of 10 steps before dissociation (18). The distinct lag phase that exists in the pre-steady state, during which no fully unwound substrate is detected, is dependent upon the length of the duplex region. As the length of the duplex is increased, the lag phase likewise increases due to more intermediate steps being needed to fully convert the partial duplex substrate to completely unwound product (11, 14, 18).

Based on these previous kinetic studies of UvrD-catalyzed unwinding we have conducted a series of pre-steady state, single turn-over experiments measuring UvrD-catalyzed unwinding in the presence of MutL to characterize further the stimulation of UvrD by MutL. Using a 24 bp partial duplex with a 40 nucleotide 3'-ssDNA tail, which is readily unwound by UvrD, the addition of MutL caused an increase in the amount of DNA unwound but did not appreciably alter the length of the lag phase in the pre-steady state. When the length of the duplex region was increased to 90 bp UvrD catalyzed no unwinding of the substrate under single turnover conditions consistent with the modest processivity ascribed to this helicase. However, this same substrate was readily unwound by UvrD in single turnover experiments in the presence of MutL. We also report experiments with partial duplex substrates of 41 bp and 60 bp in length. Taken together, the data support a model in which MutL stimulates the helicase activity of UvrD by increasing its processivity. The implications of this result on the mechanism of MMR are discussed.

Materials and Methods

Protein Purification – MutL and UvrD were expressed and purified as previously described (36, 37).

DNA Substrates – The synthetic oligonucleotides used for preparation of DNA substrates were purified by the supplier (IDT) and the sequences are listed in Table 4. All partial duplex DNA substrates contained a 40 nucleotide 3'-ssDNA tail composed of thymidine residues. Radioactively labeled substrates were prepared by incubating 10 pmols (molecules) of the appropriate oligonucleotide with 3 μM [γ-^{32}P]ATP and T4 polynucleotide kinase (New England Biolabs) at 37°C for 40 minutes followed by a 20 minute incubation at 65°C to inactivate the kinase enzyme. The unincorporated [^{32}P]ATP was removed using a 0.5 mL Sephadex G-50 spin column (Pharmacia). The labeled oligonucleotide and its complement were annealed to create the partial duplex substrate by combining the oligonucleotides at a 1:1 molar ratio in annealing buffer (50 mM NaCl, 10 mM Tris-HCl (pH 7.5), 1 mM $MgCl_2$) and heating to 90°C for 3 minutes followed by slow cooling to room temperature. The substrate was extensively dialyzed against TEN buffer (10 mM Tris-HCl (pH 7.5), 0.1 mM EDTA, 50 mM NaCl) and subsequently stored at 4°C to be directly used in helicase assays. Concentration was determined assuming 90% recovery of the oligonucleotide from the spin column.

A *Rsa*I restriction site was incorporated into the sequence of the 90 bp partial duplex such that digestion with *Rsa*I produced a 60 bp partial duplex. After digestion the partial duplex DNA was gel purified, dialyzed against TEN buffer as above and stored at 4°C. Similarly, the 41 bp partial duplex was constructed by digestion of the 90 bp partial duplex with *Hae*III followed by gel purification and dialysis. The 24 bp blunt duplex was constructed by labeling 10 pmols of the

24-mer as described above followed by annealing to its complement lacking the 3' $dT_{(40)}$ extension.

Protein Trap – A DNA hairpin flanked by a 30 base 3'-ssDNA tail (Table 4) was used as a protein trap for UvrD as previously described (11). The oligonucleotide was suspended in Tris-EDTA (10 mM Tris-HCl (pH 8.0), 1 mM EDTA), heated to 95°C for 3 minutes and then snap cooled on ice. The protein trap was used at a final concentration of 2 μM in all experiments.

Electrophoretic Mobility Shift Assays – Electrophoretic mobility shift assays were performed using the 24 bp partial duplex substrate. Reaction mixtures (20 μl) with UvrD contained 25 mM Tris-HCl (pH 7.5), 5 mM 2-mercaptoethanol, 10% glycerol, 0.2 mg/mL bovine serum albumin (BSA), 25 mM NaCl, 0.2 mM EDTA, 1 nM [^{32}P]DNA ligand, 3 mM AMP-PNP and were assembled on ice. UvrD was titrated from 0 to 26.1 nM with dilutions made in UvrD storage buffer (20 mM Tris-HCl (pH 7.5), 0.2 M NaCl, 50% (v/v) glycerol, 1 mM EDTA, 25 mM 2-mercaptoethanol). Reactions were initiated with the addition of the protein and incubated on ice for 20 minutes followed by the addition of 5 μL of 75% glycerol (v/v). Dyes were added to the sample containing no protein to monitor migration on the gel. Samples were loaded on an 8% polyacrylamide gel (32:1 crosslinking ratio) containing 1X TBE buffer (89 mM Tris base, 89 mM boric acid, 2 mM EDTA) and electrophoresed at 8 v/cm for 12 hours at 4°C. Gels were imaged after exposure to a phosphor storage screen using a Storm Phosphorimager (Amersham Biosciences) and the images were quantified using ImageQuant software.

Table 4. Oligonucleotides used in the MutL stimulation of UvrD study

Oligonucleotide Sequence
RQ24: 5′ -GCCCTGCTGCCGACCAACGAAGGT- 3′
Comp 24: 5′ -ACCTTCGTTGGTCGGCAGCAGGGC- 3′
RQ64: 5′ -ACCTTCGTTGGTCGGCAGCAGGGC (T_{40}) -3′
RQ90: 5′ -GCCCTGCTGCCGACCAACGAAGGTTACATTCCCCGTGCTGGCCGTTTG CGGTTGTCCTGTACCACTCGAAGTAGGAGGGGTGCTCACCGA -3′
RQ130: 5′ -TCGGTGAGCACCCCTCCTACTTCGAGTGGTACAGGACAACCGCAA ACGGCCAGCACGGGGAATGTAACCTTCGTTGGTCGGCAGCAGGGC (T_{40}) -3′
Hairpin Trap: 5′ -CCTCGCTGCTTTTTGCAGCGAGGC (T_{30}) -3′

Reaction mixtures (20 μl) containing both UvrD and MutL contained 25 mM Hepes-HCl (pH 7.5), 5 mM 2-mercaptoethanol, 10% glycerol, 0.2 mg/mL BSA, 25 mM NaCl, 0.2mM EDTA, 1 nM [^{32}P]DNA ligand, 25 nM UvrD and varying concentrations (0 to 125 nM) of MutL. For these experiments MutL, UvrD and the [^{32}P]DNA ligand were dialyzed against 10 mM Hepes-HCl (pH 7.5), 50 mM NaCl and 0.1 mM EDTA. Reactions were initiated with the addition of 3 mM AMP-PNP and incubated on ice for 20 min followed by the addition of glutaraldehyde to 0.1%. Samples were loaded onto on a 5% polyacrylamide gel containing 1 X TBE buffer and electrophoresed at 8 v/cm for 12 hours at 4°C. Gels were imaged and quantified as above.

Rapid-Quench Helicase Unwinding Assays – Helicase unwinding assays were performed using rapid chemical quench techniques to measure pre-steady state kinetics under single turnover conditions. All DNA substrates were at a final concentration of 1 nM. UvrD (50 nM) was mixed with 2 nM [^{32}P]DNA substrate, 3 mM ATP and Buffer L (25 mM Tris-HCl (pH 7.5), 5 mM 2-mercaptoethanol, 10% glycerol (v/v), 0.2 mg/mL BSA, 25 mM NaCl, and 0.2 mM EDTA) in one syringe and incubated on ice for 20 minutes. This solution was then warmed to ambient temperature (~19°C) for 5 minutes. EDTA was included in the protein-DNA-ATP incubation buffer to chelate any residual $MgCl_2$. This did not affect the unwinding reaction since the same amount of DNA was unwound at the same rate whether reactions were initiated with ATP (excluding EDTA from the protein-DNA mixture) or with $MgCl_2$ as described (data not shown). For reactions containing MutL, 150 nM MutL dimer was added to the reaction mixture. The second syringe contained 4 μM hairpin protein trap, 6 mM $MgCl_2$ and Buffer M (25 mM NaCl, 25 mM Tris-HCl (pH 7.5), 5 mM 2-mercaptoethanol and 10% glycerol (v/v)) and was incubated on ice for 20 minutes and then warmed to 19°C. Equal volumes from each syringe

were rapidly mixed to initiate the reaction and subsequently quenched with 0.5 M EDTA at the desired time point (ranging from 0.075 to 20 seconds). $MgCl_2$ (final concentration of 3 mM) was used to initiate all unwinding reactions. Quenched reactions were analyzed on 14% (24 bp partial duplex), 12% (41 bp partial duplex) or 10% (60 and 90 bp partial duplex DNAs) native polyacrylamide gels. The running buffer was 1X TBE + 0.1% SDS and gels were run at 25 volts/cm for 3 hours. Gels were imaged after exposure to a phosphor storage screen using a Storm Phosphorimager (Amersham Biosciences) and the images were quantified using ImageQuant software. Control experiments to test the effectiveness of the DNA hairpin as a protein trap for UvrD and MutL were conducted using the 24 bp partial duplex substrate.

The control samples for the rapid chemical quenched flow helicase assays were prepared in a similar manner to the unwinding reactions. The pre-incubated protein-DNA sample used for the unwinding reactions was mixed with an equal volume of a control initiation solution containing 3 mM hairpin protein trap and Buffer M (25 mM NaCl, 25 mM Tris-HCl (pH 7.5), 5 mM 2-mercaptoethanol and 10% glycerol (v/v)). The lack of $MgCl_2$ was sufficient to halt any detectable helicase activity. The control samples were allowed to interact with the protein-DNA complexes for the same amount of time as the longest duration unwinding time point. Once quenched, one aliquot from this control was heat denatured at 95°C, converting all DNA substrate to ssDNA and another sample was loaded without further treatment.

Results

Our initial efforts to elucidate the mechanism of stimulation by MutL led us to propose that MutL loads multiple molecules of UvrD onto a DNA substrate by an iterative process (Fig. 9B) (27). This model is consistent with the established processivity of UvrD as a helicase (40-50 bp) (18) and as a translocase on ssDNA (~250 bp) (30, 31). As the 'leading' dimer of UvrD

dissociates from the partially unwound substrate due to its intrinsic processivity it can be replaced by another UvrD dimer to ensure continued unwinding. Crystal structures of MutL in the presence of a non-hydrolyzable ATP analog (34, 35), along with the discovery that the ATP-bound form of MutL (38, 39) is required for stimulation of UvrD, have led us to propose an alternative model for stimulation of UvrD by MutL (Fig. 9C). In this model ATP-bound MutL physically interacts with UvrD to increase its processivity either by acting as a topological clamp to tether UvrD on the DNA or by stabilizing UvrD in an 'open' conformation allowing it to unwind by a strand displacement mechanism that relies on the processivity of UvrD as a translocase. Recent experiments with the 'hyper-helicase' UvrD303 (Chapter 2) have revealed this possibility. In either case, MutL would increase the processivity of the unwinding reaction catalyzed by UvrD. A series of kinetic experiments performed under single turnover conditions provide support for these models that posit an increase in UvrD unwinding processivity in the presence of MutL.

Rapid quench kinetic experiments under single turnover conditions have elucidated the stepwise mechanism (Scheme 2) used by many helicases, including UvrD, to unwind duplex DNA (9, 13, 18, 40). In these experiments the unwinding reaction is typically initiated by the addition of ATP after formation of a helicase-DNA complex. However, since the ATP-bound form of MutL is required to stimulate UvrD (38), initiation by the addition of ATP was not possible for the experiments reported below using both UvrD and MutL. Therefore, $MgCl_2$ was used to initiate unwinding reactions and ATP was added to the DNA-bound protein complexes prior to initiating the unwinding reaction. To ensure the formation of UvrD-MutL complexes on the partial duplex substrates used in kinetic assays in the presence of ATP and the absence of

$MgCl_2$, electrophoretic mobility shift assays using the 24 bp partial duplex DNA as a ligand were performed using UvrD and UvrD+MutL to evaluate complex formation.

A titration of UvrD was used to measure the binding of UvrD to the DNA substrate prior to the initiation of unwinding and in the absence of $MgCl_2$ (Fig. 10A). Under these conditions UvrD forms a stable complex with the DNA with an apparent K_d of approximately 3.4 nM. The apparent K_d observed in these experiments agrees well with the apparent K_d reported previously using a similar DNA substrate (14). Importantly, binding occurs in the absence of added $MgCl_2$. It has previously been shown that UvrD has a high affinity for the ssDNA overhang composed of thymidine residues and a ssDNA region of 40 bases is sufficient for optimal UvrD binding (14) consistent with the results shown here.

Gel mobility shift assays using MutL indicate that MutL by itself does not form a stable complex in the absence of added $MgCl_2$ (Fig. 10B). The DNA substrate in the lane containing MutL alone migrates similarly to the DNA in the absence of protein but is slightly smeared suggesting that MutL may interact with the DNA but that this interaction is unstable. However, a stable complex is formed on the 24 bp partial duplex substrate when both proteins (MutL + UvrD) are incubated together with the DNA (Fig. 10B). When MutL is added to the reaction in the presence of a saturating concentration of UvrD (25 nM) a large complex is formed that is distinct from that formed by UvrD alone. The formation of this complex is dependent on the concentration of MutL indicating that it contains both MutL and UvrD. At a concentration of approximately 50 nM MutL dimer all the DNA is present in the large complex. We conclude that under the established reaction conditions a MutL-UvrD complex is stably bound to the DNA prior to initiation of the unwinding reaction by $MgCl_2$.

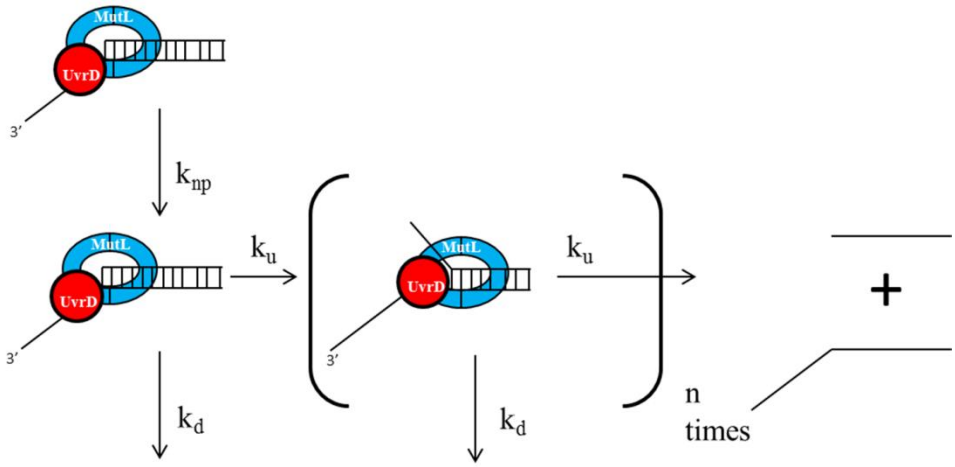

Scheme 2. The sequential n-step kinetic model. Preformed UvrD-MutL-DNA complexes undergo a conversion to partially unwound intermediates (see internal brackets) as the pathway progresses until a fully unwound ssDNA is generated. At each intermediate step the helicase may dissociate from the unwinding complex, k_d, or proceed with further unwinding, k_u. The processivity calculated using this model is representative of the probability that the helicase will proceed in the unwinding pathway. The model also predicts a slow, rate limiting step, k_{np}, which describes the conversion of nonproductive UvrD-MutL-DNA complexes into active unwinding complexes (18).

The rapid quench single turnover helicase unwinding experiments were done with an excess of both MutL and UvrD with respect to the DNA to ensure that all the substrate was bound by protein prior to the initiation of unwinding. The appropriate concentration of each protein was determined empirically using both electrophoretic mobility shift assays as discussed above and single turnover unwinding assays. A concentration of 25 nM UvrD was chosen based on the gel mobility shift assays to ensure that an excess of protein was present. This was validated using single turnover unwinding assays. When the UvrD concentration was reduced to 10 nM less DNA was unwound than in reactions using 25 nM UvrD suggesting that the DNA was not saturated at the start of the reaction. Since UvrD has optimal helicase activity as a dimer (11, 12) a concentration of 10 nM UvrD (monomer) may not be sufficient to ensure the DNA is bound by UvrD dimers. At concentrations of 40 nM and 80 nM UvrD the unwinding profiles for the 24 bp partial duplex were superimposable with those obtained using 25 nM UvrD suggesting that 25 nM UvrD was sufficient to saturate the DNA.

The appropriate concentration of MutL to use in the unwinding assays was determined similarly. At a concentration of 25 nM UvrD and 45 nM MutL dimer the DNA is completely bound by MutL-UvrD complexes (Fig. 10B). Thus, 75 nM MutL dimer was used in the experiments reported below to ensure an excess of protein. As above, rapid quench single turnover experiments were performed using a higher concentration of MutL to confirm assumptions based on the gel mobility shift assays. The addition of 125 nM MutL dimer did not change the amount of DNA unwound by 25 nM UvrD or the length of the lag phase in the pre-steady state using the 24 bp partial duplex substrate. We conclude that the DNA is saturated with MutL-UvrD complexes at 25 nM UvrD and 75 nM MutL dimer.

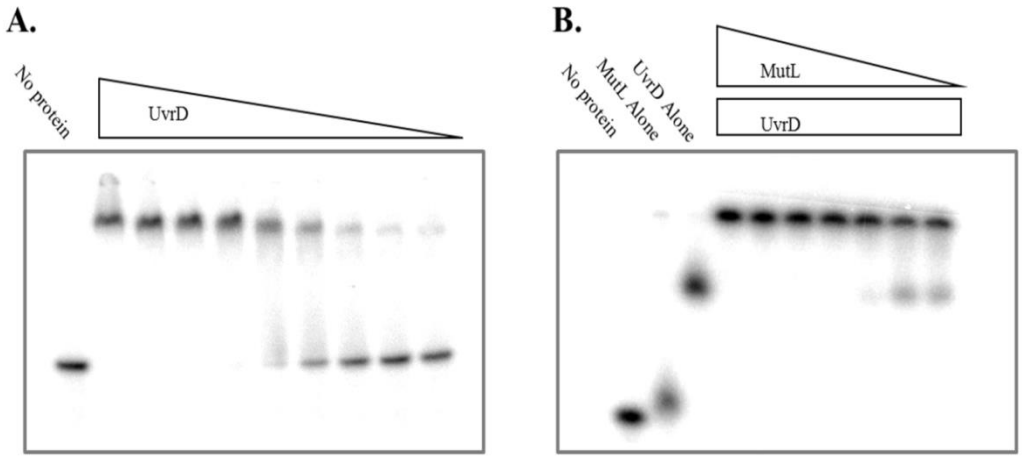

Figure 10. Panel A - Gel mobility shift assays with UvrD and the 24 base pair partial duplex substrate. Gel mobility shift assays were as described under "Materials and Methods" Concentrations of UvrD used were 26.1, 17.4, 11.6, 7.7, 5.1, 3.4, 2.3, 1.5, and 1 nM DNA ligand. Panel B - Gel mobility shift assay with MutL and UvrD. Gel mobility shift assays were as described under "Materials and Methods" using UvrD at a concentration of 25 nM monomer and the following concentrations of MutL: 125, 89.3, 63.8, 45.6, 32.5, 23.2, and 16.6 nM dimer.

UvrD has been shown to initiate unwinding on blunt-ended DNA in multiple turnover reactions. This reaction requires a higher concentration of UvrD than is needed to initiate unwinding on a 3'-ssDNA flanking region (14, 41). In addition, MutL has been demonstrated to stimulate UvrD-catalyzed unwinding of blunt ended DNA molecules in multiple turnover reactions (27). For these reasons it was important to demonstrate that unwinding of the substrates used here, and under the conditions reported, resulted from initiation on the 3'-ssDNA overhang. Control single turnover unwinding experiments using a 24 bp *blunt* duplex substrate resulted in no unwinding by 40 nM UvrD in the absence and in the presence of 80 nM MutL dimer (Fig. 11A). Therefore, initiation of unwinding at the blunt end of the partial duplex substrates does not contribute to the total DNA unwound as a result of MutL-stimulated UvrD unwinding under single turnover conditions.

To ensure that single turnover conditions were met, control experiments were performed using a hairpin DNA with a 30 nucleotide ssDNA tail as a protein trap. When the protein trap was included in the preincubation with DNA, UvrD, MutL and ATP at a concentration of 2 μM (2000-fold excess over the [^{32}P]DNA substrate) no unwinding was detected (Fig. 11B and 11C). We conclude that the trap concentration is sufficient to capture both unbound and dissociated UvrD and that single turnover conditions are met.

UvrD, at a concentration of 25 nM, unwinds approximately 50% of the 24 bp partial duplex under single turnover conditions (Fig. 12). A well-defined lag phase is seen in the pre-steady state phase of the reaction before a rapid burst of unwinding. Although the DNA is saturated with UvrD at this concentration, not all the UvrD-DNA complexes will initiate unwinding simultaneously. It has been observed that only a fraction, albeit a large fraction, of the UvrD complexes is productively bound to the DNA. Some fraction of the DNA molecules

are bound by UvrD in an unproductive state that must undergo a slow isomerization reaction to a productive state before an unwinding event can take place (14, 18). In addition, the gel-based assay for unwinding is an 'all-or-none' assay that does not provide any measurement of partially unwound molecules. Consequently, the lag represents both time for isomerization to a productive complex as well as the steps required for complete unwinding of the substrate molecule and both of these terms are part of the modeled value of k_{np}. The fraction of the DNA substrate unwound in the absence of MutL is in reasonable agreement with that previously reported in rapid quench single turnover experiments (18) although the burst amplitude is somewhat lower and the lag phase is somewhat longer. We attribute these differences to the fact that the experiments reported here were done at a lower temperature than those reported previously. The addition of 75 nM MutL dimer stimulated the UvrD-catalyzed unwinding reaction and approximately 80% of the DNA was unwound (Fig. 12). Since the DNA was saturated with UvrD at 25 nM in the absence of MutL and the reactions are performed under single turnover conditions, it seems unlikely that the increase in ssDNA product results from MutL repeatedly loading additional UvrD dimers onto the DNA. Instead the data suggest that MutL has increased the efficiency of UvrD-catalyzed unwinding without loading additional UvrD onto the DNA. This interpretation is consistent with the notion of an increase in processivity.

DNA unwinding catalyzed by UvrD occurs with a distinct lag phase in the pre-steady state in which no unwinding of DNA molecules is observed until the duplex DNA is completely unwound. This lag phase represents a series of partially unwound intermediates that are produced as the helicase unwinds using a step-wise mechanism and are not detected using this

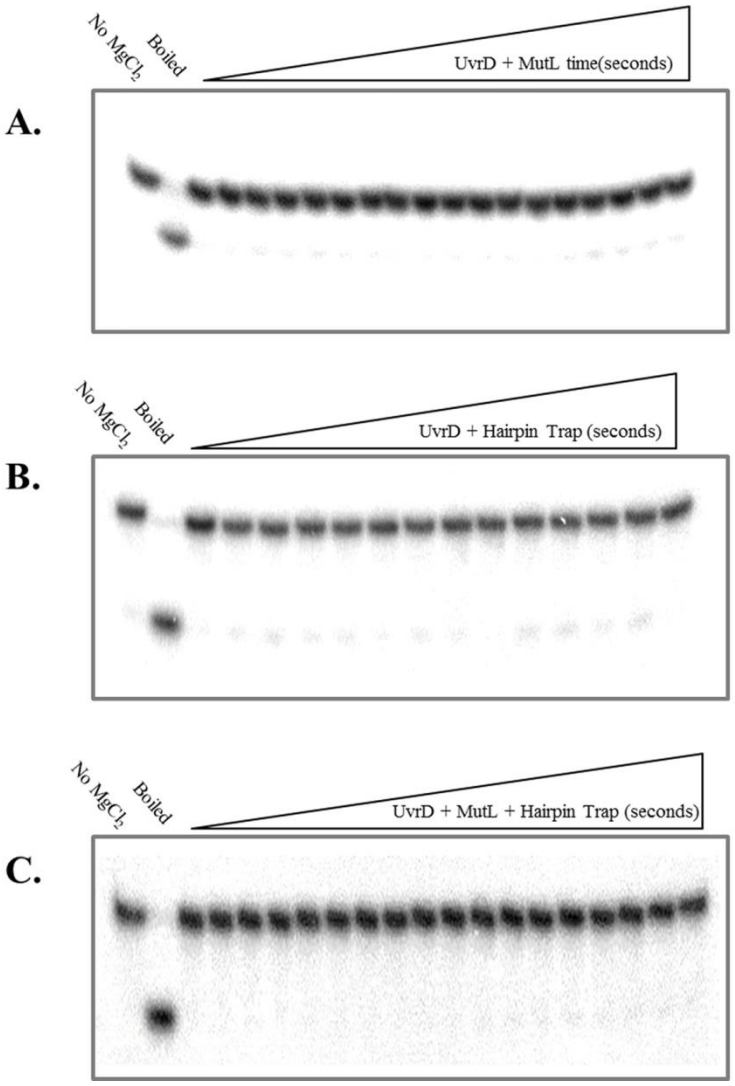

Figure 11**.** UvrD does not unwind a blunt DNA duplex under single turnover conditions nor will UvrD unwind in the presence of the hairpin trap. Panel A – Single turnover, rapid quench unwinding assay were as described under "Materials and Methods' using a 24 base pair blunt duplex substrate (1 nM), 40 nM UvrD (monomer) and 80 nM MutL (dimer). Reaction products were resolved on a 12% native polyacrylamide gel. The time course shown runs from 0.075 sec to 30 sec. Panel B – Rapid quench unwinding assays were as described under "Materials and Methods" using 80 nM UvrD, 1 nM 24 bp partial duplex substrate and 2 μM hairpin trap. Reactions were resolved on a 12% native polyacrylamide gel. The time course shown extends from 0.075 sec to 30 sec. Panel C – Reactions were as in (A) using 50 nM UvrD (monomer), 100 nM MutL (dimer), 1 nM 24 bp partial duplex substrate and 2 μM hairpin trap.

'all or none' gel-based assay of helicase activity (13, 40). For the 24 bp partial duplex, this lag phase lasts approximately 0.2-0.3 seconds under these conditions and is immediately followed by a rapid burst in the fraction of completely unwound DNA. A lag phase also exists when MutL is present in the reaction and the lag is essentially identical with that observed with UvrD alone. The rapid burst of unwinding that occurs in the presence of MutL mimics the unwinding burst with UvrD alone but terminates at a higher amplitude with a larger fraction of total DNA molecules unwound, supporting a model in which MutL-stimulated UvrD-catalyzed unwinding also occurs via a step-wise process. Since the lag phase with MutL persisted for approximately the same duration as the lag phase with UvrD alone, we infer that the unwinding mechanism of UvrD is stimulated, but otherwise unchanged. In addition, the exponential rise of the unwinding curves are similar, suggesting that MutL does not appreciably change the rate of UvrD-catalyzed unwinding of duplex DNA.

Three additional partial duplex substrates were constructed to determine the impact of MutL on UvrD-catalyzed unwinding using substrates with duplex regions that approach and exceed the processivity of UvrD. When using a 41 bp partial duplex substrate, no appreciable unwinding was detectable when UvrD was allowed to unwind this substrate under single turnover conditions (Fig. 13). The addition of MutL dramatically increased the burst amplitude resulting in nearly 70% of the substrate being unwound. As expected, the lag phase increased compared to that observed with the 24 bp partial duplex DNA. Thus, MutL dramatically stimulated UvrD-catalyzed unwinding of a substrate longer than the 24 bp partial duplex. Previous studies on the kinetics of UvrD unwinding show that the amplitude of the burst phase increases with decreasing length of duplex DNA and that the lag phase increases with increasing

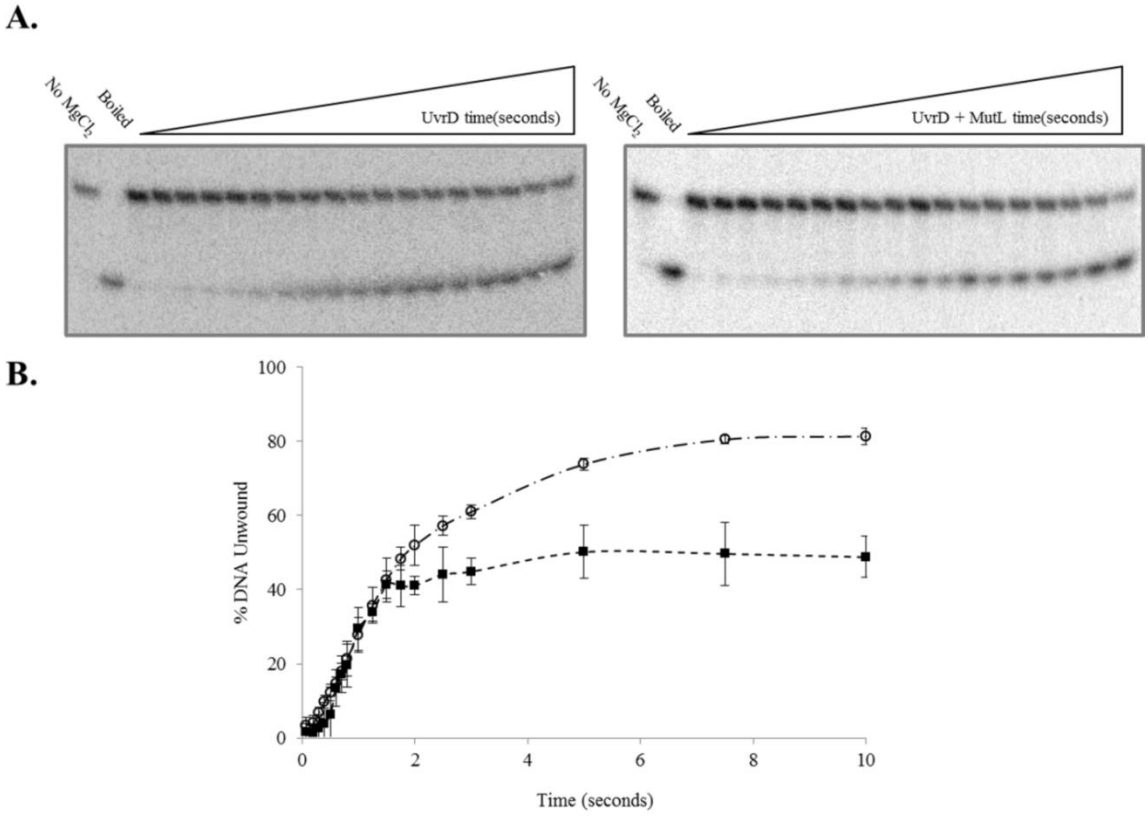

Figure 12. MutL stimulates UvrD-catalyzed unwinding activity in single turnover rapid quench reactions. Panel A – DNA helicase single turnover rapid quench reactions were performed as described under "Materials and Methods" using a 24 bp partial duplex substrate and increasing time. The first two lanes are controls for heat denatured substrate and no magnesium chloride ($MgCl_2$). The remaining lanes depict a time course from 0.075 to 10 seconds for both UvrD alone and UvrD+MutL. Panel B – Quantitative data from 3 experiments for UvrD (filled squares) and UvrD+MutL (open circles) were plotted as an average. Error bars represent the standard deviation about the mean.

length (14). Therefore, experimental results with this substrate are consistent with the result seen using the 24 bp partial duplex DNAs and provide additional evidence to support the idea that MutL does not alter the step-wise mechanism by which UvrD unwinds DNA, but is affecting the total amount of duplex DNA unwound per UvrD dimer binding event.

Finally, experiments were performed using a 60 bp and a 90 bp partial duplex DNA substrate; duplex lengths well outside the measured processivity of UvrD. As expected, UvrD catalyzed no measureable unwinding of these substrates in single turnover experiments (Fig. 14). However, the addition of MutL to the reaction mixture resulted in approximately 55% and 40% of the DNA substrates unwound, respectively.. As expected, the unwinding profile is characterized by a distinct lag phase followed by a rapid burst in unwinding, mimicking the unwinding curves on the 24 bp and 41 bp partial duplex substrates but with a longer lag phase indicating that more partially unwound DNA intermediates were required before a completely unwound population was detectable.

The increased helicase activity observed as a result of the stimulation of UvrD by MutL could indicate an increase in the processivity of the unwinding reaction. Applying the previously mentioned step-wise unwinding mechanism (see Scheme 2) to the single turnover data in conjunction with the kinetic modeling software Tenua (Bililite), the processivity of the MutL stimulated unwinding activity was calculated. Applying the model to our data, the resultant best fits are shown in Figure 15. These data indicate a striking increase in the processivity of the MutL-stimulated UvrD unwinding reaction. The processivity of UvrD alone was calculated to be 0.87 or 9 "steps" taken before the helicase dissociated from the DNA. These values are in very close agreement with the previously reported values of processivity and steps take, 0.9 and 9-10, respectively. The addition of MutL to the unwinding reaction increases the processivity

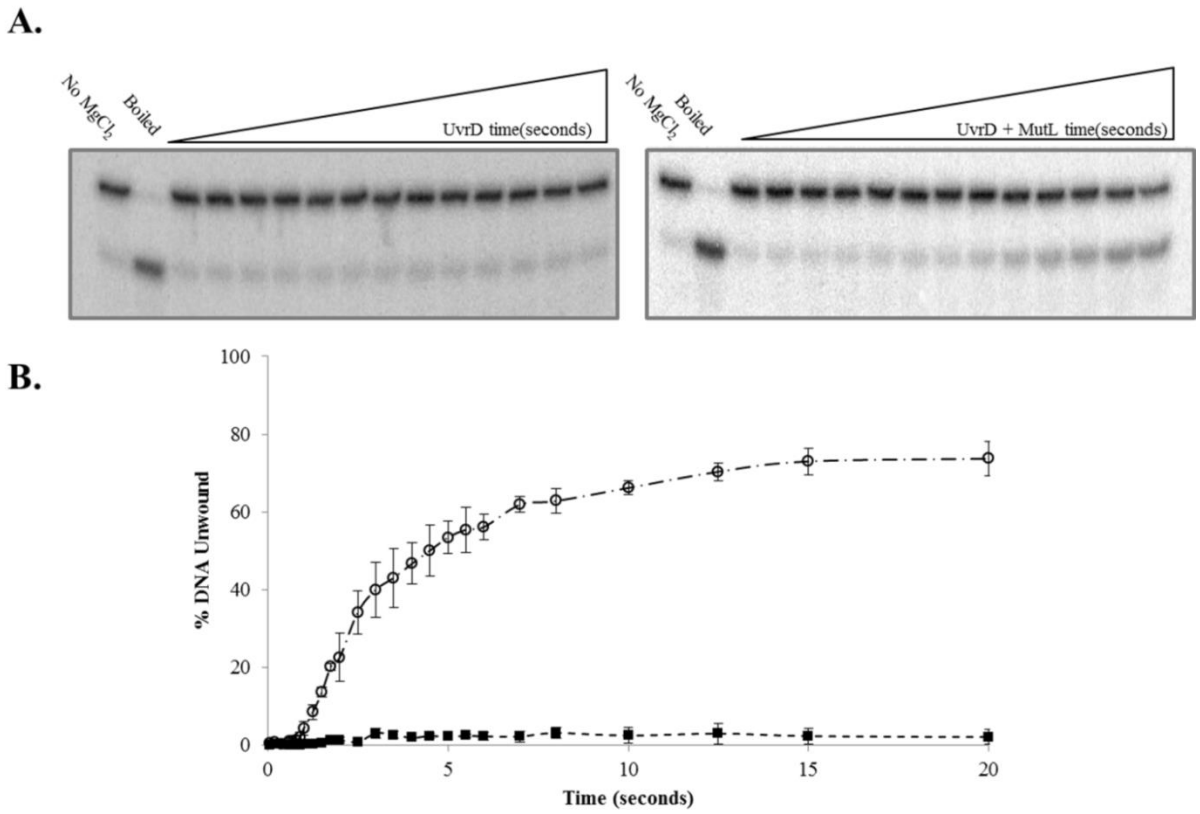

Figure 13. MutL stimulates UvrD-catalyzed unwinding activity in single turnover rapid quench reactions. Panel A – Single turnover rapid quench reactions were performed as described under "Materials and Methods" using a 41 bp partial duplex substrate and increasing time. The first two lanes are controls for heat denatured substrate and no magnesium chloride ($MgCl_2$). The remaining lanes depict a time course from 0.075 to 20 seconds for UvrD alone and UvrD+MutL. Panel B – Quantitative data from 3 experiments for UvrD (filled squares) and UvrD+MutL (open circles) were plotted as an average. Error bars represent the standard deviation about the mean.

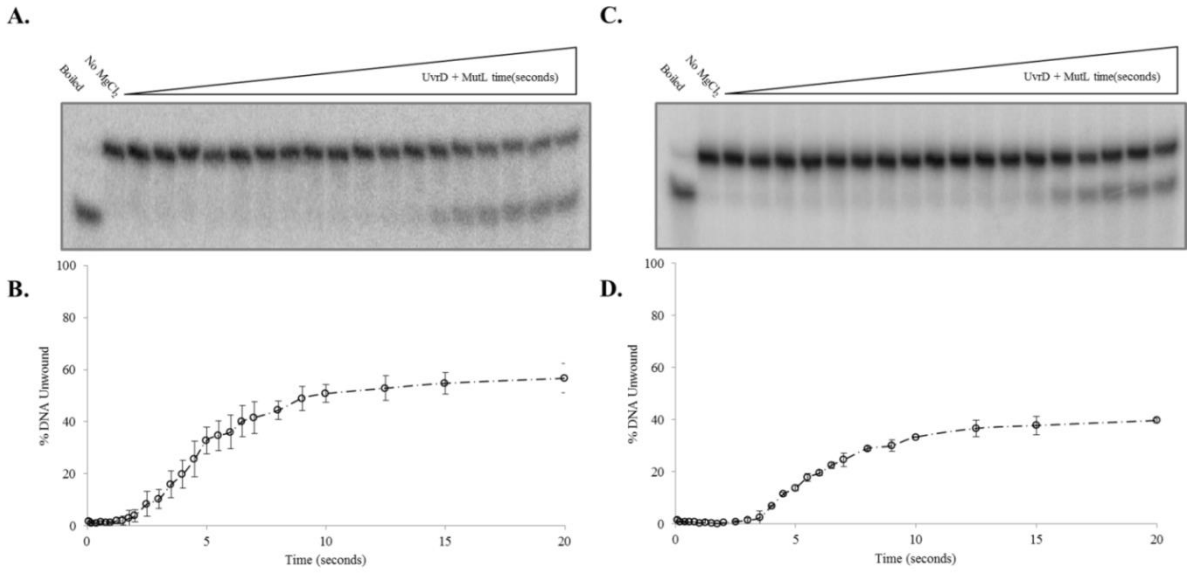

Figure 14. MutL stimulates UvrD-catalyzed unwinding activity in single turnover rapid quench reactions. Panel A – Single turnover rapid quench reactions were performed as described under "Materials and Methods" using a 60 bp partial duplex substrate and increasing time. The first two lanes are controls for heat denatured substrate and no magnesium chloride ($MgCl_2$). The remaining lanes depict a time course from 0.075 to 20 seconds for UvrD+MutL. Panel B – Quantitative data from 3 experiments for UvrD+MutL (open circles) were plotted as an average. Error bars represent the standard deviation about the mean. Panel C – Single turnover rapid quench reactions were performed as described under "Materials and Methods" using a 90 bp partial duplex substrate and increasing time. The first two lanes are controls for heat denatured substrate and no magnesium chloride ($MgCl_2$). The remaining lanes depict a time course from 0.075 to 20 seconds for UvrD+MutL. Panel D – Quantitative data from 3 experiments for UvrD+MutL (open circles) were plotted as an average. Error bars represent the standard deviation about the mean.

to 0.965 which correlates to approximately 29 steps taken. This increase in processivity correlates with a more than 3-fold increase in the average number of bp unwound in a single turnover, from 35 bp unwound by UvrD alone to 115 bp unwound by UvrD in the presence of MutL.

UvrD303 has been described as a 'hyper-helicase' due to its increased unwinding activity (42). We have recently shown that UvrD303 exhibits an increased processivity and may unwind duplex DNA via a strand displacement mechanism as compared with the 'wrench and inchworm' mechanism proposed for wild-type UvrD (see Chapter 2) (43). In addition, cells expressing UvrD303 exhibit an antimutator phenotype (42, 44) which may be due to the increased processivity exhibited by UvrD303. Since MutL interacts with UvrD (26) and this interaction is essential for MMR (28, 29) we were interested in evaluating the impact of MutL on UvrD303. As indicated above, MutL dramatically stimulates UvrD by increasing the processivity of the unwinding reaction. Surprisingly, MutL does not stimulate the unwinding reaction catalyzed by UvrD303 (Fig. 16). This is not due to a failure of MutL to interact with UvrD303 which was tested by far Western blot (see Chapter 4).

Discussion

Previously published data were used to propose a model in which the interaction between UvrD and MutL resulted in loading multiple molecules of UvrD onto the DNA in an iterative loading process (3, 5, 6) to ensure the unwinding of long regions of duplex DNA as required in MMR. This model was based on several facts. First, the distance between the nick that initiates the excision reaction and the base-base mispair varies and in some cases can be quite long (19). Second, UvrD has a very modest processivity of 40-50 bases unwound per binding event (18) .

A.

	UvrD	UvrD + MutL			
Duplex Size	24bp	24bp	41bp	60bp	90bp
Amplitude	0.48	0.81	0.74	0.57	0.4
Processivity	0.88	0.97	0.97	0.96	0.96
Step Size	5 bp	4.8 bp	4.56 bp	3.8 bp	3 bp
k_{np}	$1.09s^{-1}$	$0.7s^{-1}$	$0.33s^{-1}$	$0.24s^{-1}$	$0.11s^{-1}$
k_u	$6.70s^{-1}$	$5.8s^{-1}$	$6.0s^{-1}$	$5.7s^{-1}$	$5.6s^{-1}$
k_d	$0.41s^{-1}$	$0.37s^{-1}$	$0.35s^{-1}$	$0.6s^{-1}$	$0.67s^{-1}$

B.

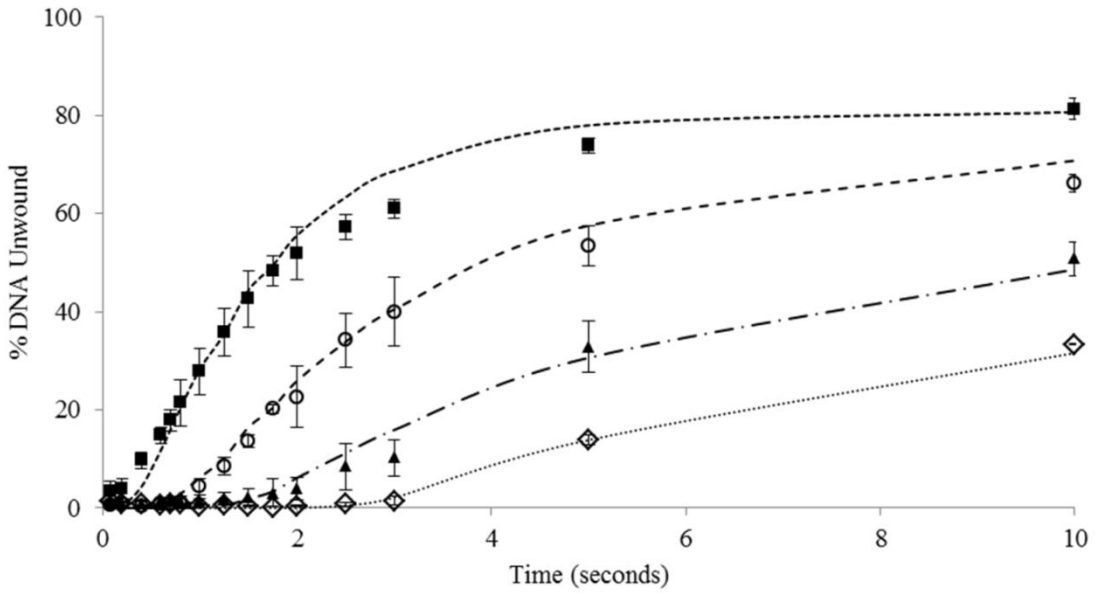

Figure 15. Modeled kinetics of MutL stimulated UvrD helicase activity. Panel A – Compiled data for kinetic parameters of the n-step model for UvrD and MutL-stimulated UvrD on the 24bp partial duplex, 41 bp partial duplex, 60 bp partial duplex, and 90 bp partial duplex. Panel B – Graphical fit of modeled data versus collected data. The hashed lines represent the unwinding predicted by the model while the markers depict the average data collected from single turnover rapid quench experiments for the 24 bp partial duplex (closed squares), the 41 bp partial duplex (open circles), the 60 bp partial duplex (closed triangles), and the 90 bp partial duplex (open diamonds). Error bars represent the standard deviation about the mean.

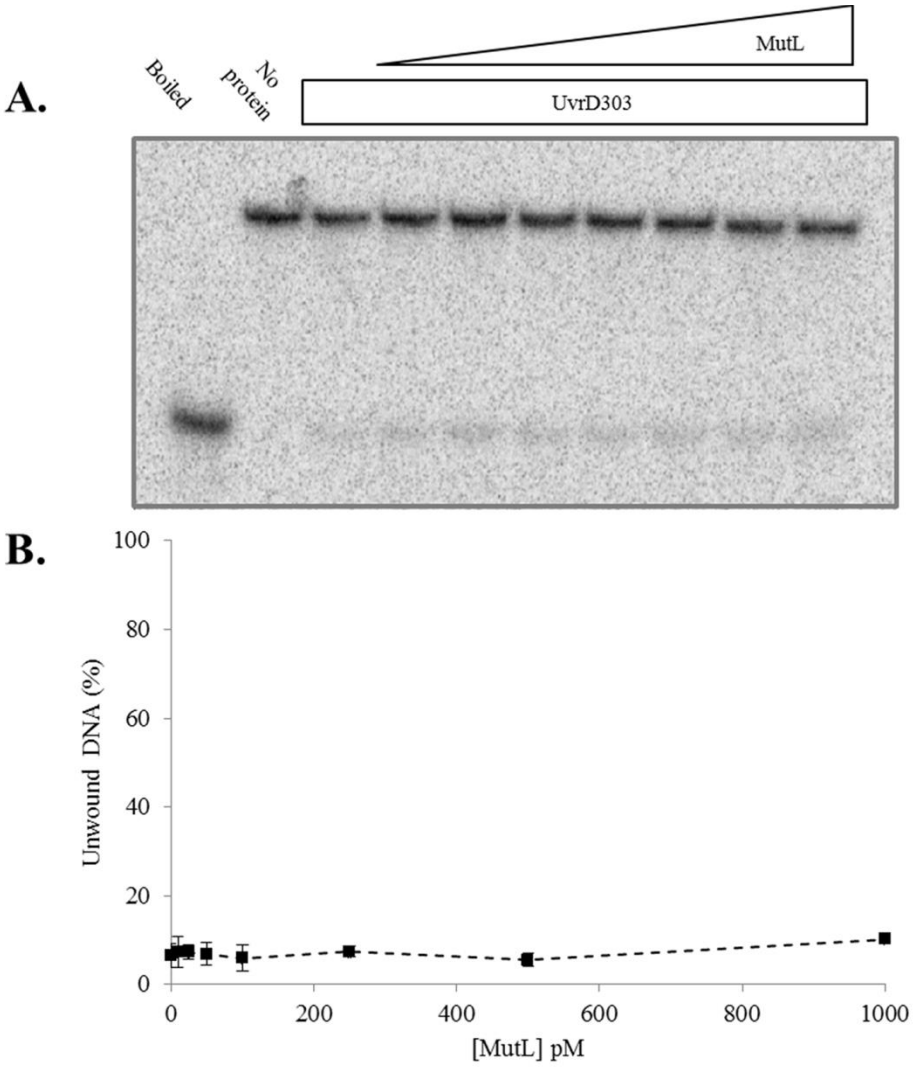

Figure 16. MutL does not stimulate the helicase activity of the UvrD303 mutant. Panel A – DNA helicase reactions were performed as described under "Materials and Methods" using the 24 bp partial duplex substrate, a fixed concentration of UvrD303 (75 pM) and increasing concentrations of MutL. Reactions were incubated at 37^{o}C for 5 min. The first two lanes are controls for no protein and heat denatured substrate DNA. The remaining lanes depict a protein titration of increasing concentration from 0 to1000 pM MutL. Panel B – Quantitative data from 2 experiments at the indicated concentrations of MutL (closed squares) were plotted as the average at each protein concentration. Error bars represent the standard deviation about the mean.

Third, the processivity of UvrD as a translocase is significantly greater than as a helicase (31, 18). Finally, MutL has a very significant stimulatory effect on UvrD that depends on the ATP-bound form of MutL but not MutL-catalyzed hydrolysis of ATP (27, 38, 39).

Here we have presented evidence in support of a revised model where MutL acts as a processivity factor for UvrD. In single turnover kinetic time courses UvrD is not able to catalyze complete unwinding of DNA duplexes exceeding its previously determined processivity of ~40 bp. This is evident using a 90 bp partial duplex (no detectable unwinding) and a 60 bp partial duplex (no detectable unwinding) substrates. However, when MutL is added to the reaction a significant amount of substrate is converted to ssDNA product by UvrD (~55% of 60 bp partial duplex unwound and ~40% of 90 bp partial duplex unwound) under single turnover reaction conditions. We suggest that MutL acts to increase the processivity of UvrD and in doing so increases the number of bp the productive unwinding complex can separate before dissociation from the DNA. In other words, MutL enables UvrD to take more 'steps' through duplex DNA as estimated by the n-step model of unwinding. Our model suggests that an average of ~35 bp is unwound in a single event by UvrD and an average of ~115 bp is unwound by a UvrD-MutL complex.

In addition, the model generated from our data shows that MutL does not change the step size of UvrD-catalyzed unwinding. The previously reported step size of 4-5 bases unwound in a single kinetic step for UvrD alone was also observed for the MutL-stimulated UvrD-catalyzed unwinding complex. Additionally, the lag phase was seen to increase with increasing duplex length, suggesting that the helicase has to take a greater number of steps to completely unwind the longer substrate. Therefore, MutL-catalyzed UvrD unwinding is likely occurring by the

same step-wise mechanism with the same average kinetic step size of 4 bases as determined previously for UvrD alone.

While the processivity of UvrD has been previously reported as ~40-50 bp (1), our data yields a slightly lower processivity. This may be due to an effect of temperature on processivity (19°C verses 25°C). We propose that MutL is acting a processivity factor by increasing the probability that UvrD will take more steps before dissociating from the DNA. One possibility is that MutL acts as a clamp, effectively tethering UvrD on the DNA and that MutL translocates along the duplex with UvrD until the unwinding reaction is terminated, effectively increasing its processivity.

We also note that in the pre-steady state phase of UvrD-catalyzed unwinding, the rapid burst in the unwinding curve has the same slope with and without MutL. Therefore, MutL does not appear to change the rate of UvrD-catalyzed unwinding. The increased amplitude of unwinding can be attributed to a greater number of molecules being able to completely translocate through the duplex region before dissociation.

A recent study of the hyper-helicase, UvrD303, suggested that a two amino acid substitution at positions 403 and 404 (both D→A) in the 2B subdomain resulted in a mutant enzyme with a dramatically increased processivity (see Chapter 2). When the impact of MutL on the activity of UvrD303 was examined, no detectable stimulation of UvrD303 helicase activity was observed (Fig. 16). The interaction sites between MutL and UvrD have not been fully defined and it was possible that the mutation in UvrD303 may have resulted in a loss of interaction between these two proteins. Using a far western blot we did observe an interaction between MutL and UvrD303 and concluded that the two proteins were capable of a physical interaction (see Chapter 4). If there is no detectable stimulation of UvrD303 by MutL, then

perhaps the mutation in UvrD303 is mimicking the effect of MutL on wild-type UvrD. It was previously suggested that the UvrD303 mutation may be forcing the 2B subdomain of UvrD into a more open conformation and that this open helicase unwinds duplex DNA via the "strand displacement" mechanism (see Chapter 2). It has been suggested that UvrD uses this strand displacement mechanism to translocate along ssDNA. It is possible that MutL stimulates the UvrD-catalyzed unwinding reaction by interacting with the 2B subdomain in a manner that induces an opening of the 2B subdomain, allowing the helicase to unwind the duplex in a more processive manner.

The experiments reported here cannot distinguish between the possibility of MutL acting as a clamp, topologically constraining UvrD on the DNA, or holding the 2B subdomain open as the helicase unwinds the DNA. Both possibilities would manifest in an increase in processivity. A more direct study of these two possibilities will be required to ascertain which is more likely.

The repair of mismatched bases in *E. coli* begins with the recognition of the mismatch by MutS, the recruitment of MutL and the introduction of a nick in the nascent DNA strand at the nearest hemi-methylated d(GATC) sequence by MutH. This is followed by resection of the DNA strand containing the mismatch, facilitated by the action of UvrD and appropriate exonucleases, and resynthesis of the DNA strand by DNA polymerase III. The distance between the mismatched base and the nearest hemi-methylated d(GATC) site can be up to, and in some cases, in excess of 1 kbp resulting in resynthesis repair tracts that are quite long in many cases (19). To effect repair, UvrD must unwind the nascent strand to provide the substrate for resection by the appropriate exonuclease. Yet UvrD has a modest processivity of only 40-50 bp. Since repair efficiency decreases with increased distance between the d(GATC) site at which repair is initiated and the mismatch, increasing the amount of duplex DNA that UvrD can unwind before

dissociation improves the likelihood that the duplex will be successfully unwound past the mismatch. The notion that MutL may clamp UvrD onto the DNA is consistent with the idea of MutL-directed UvrD loading onto the appropriate strand so that UvrD unwinds towards the mismatch. Since MMR has bidirectional capability, it is crucial that UvrD is loaded onto the DNA accurately and that it unwinds towards the mismatch or IDL with the appropriate polarity for successful restoration of the DNA duplex and if MutL clamps UvrD onto the DNA, this may act as a checkpoint.

As the 'master coordinator' of MMR, MutL interacts with all the major proteins in MMR, including MutS, MutH, and UvrD to modulate their activity. We have provided evidence in support of a model for a MutL-UvrD interaction in which MutL stimulates the unwinding activity of UvrD by increasing its processivity rather than continuously loading multiple molecules of UvrD onto the DNA until a termination signal is received. A more complete characterization of the interaction between MutL and UvrD is essential to further our understanding of the mechanism of MMR.

REFERENCES

1. Abdelhaleem, M. (2010) Helicases: an overview. Methods Mol.Biol. 587, 1-12

2. Matson, S.W., Bean, D.W., and George, J.W. (1994) DNA helicases: enzymes with essential roles in all aspects of DNA metabolism. Bioessays. 16, 13-22

3. Tuteja, N., and Tuteja, R. (2004) Prokaryotic and eukaryotic DNA helicases. Essential molecular motor proteins for cellular machinery. Eur.J.Biochem. 271, 1835-1848

4. Lohman, T.M., and Bjornson, K.P. (1996) Mechanisms of helicase-catalyzed DNA unwinding. Annu.Rev.Biochem. 65, 169-214

5. Matson, S.W., and Kaiser-Rogers, K.A. (1990) DNA helicases. Annu.Rev.Biochem. 59, 289-329

6. Croteau, D.L., Popuri, V., Opresko, P.L., and Bohr, V.A. (2014) Human RecQ Helicases in DNA Repair, Recombination, and Replication. Annu.Rev.Biochem.

7. Singleton, M.R., Dillingham, M.S., and Wigley, D.B. (2007) Structure and Mechanism of Helicases and Nucleic Acid Translocases. Annu.Rev.Biochem. 76, 23-50

8. Patel, S.S., and Donmez, I. (2006) Mechanisms of helicases. J.Biol.Chem. 281, 18265-18268

9. Lohman, T.M., Tomko, E.J., and Wu, C.G. (2008) Non-hexameric DNA helicases and translocases: mechanisms and regulation. Nat.Rev.Mol.Cell Biol. 9, 391-401

10. Eoff, R.L., and Raney, K.D. (2005) Helicase-catalysed translocation and strand separation. Biochem.Soc.Trans. 33, 1474-1478

11. Maluf, N.K., Fischer, C.J., and Lohman, T.M. (2003) A Dimer of Escherichia coli UvrD is the active form of the helicase in vitro. J.Mol.Biol. 325, 913-935

12. Maluf, N.K., Ali, J.A., and Lohman, T.M. (2003) Kinetic mechanism for formation of the active, dimeric UvrD helicase-DNA complex. J.Biol.Chem. 278, 31930-31940

13. Eoff, R.L., and Raney, K.D. (2006) Intermediates revealed in the kinetic mechanism for DNA unwinding by a monomeric helicase. Nat.Struct.Mol.Biol. 13, 242-249

14. Ali, J.A., Maluf, N.K., and Lohman, T.M. (1999) An oligomeric form of E. coli UvrD is required for optimal helicase activity. J.Mol.Biol. 293, 815-834

15. Lahue, R.S., and Modrich, P. (1988) Methyl-directed DNA mismatch repair in Escherichia coli. Mutat.Res. 198, 37-43

16. Kunkel, T.A., and Erie, D.A. (2005) DNA mismatch repair. Annu.Rev.Biochem. 74, 681-710

17. Iyer, R.R., Pluciennik, A., Burdett, V., and Modrich, P.L. (2006) DNA mismatch repair: functions and mechanisms. Chem.Rev. 106, 302-323

18. Ali, J.A., and Lohman, T.M. (1997) Kinetic measurement of the step size of DNA unwinding by Escherichia coli UvrD helicase. Science. 275, 377-380

19. Bruni, R., Martin, D., and Jiricny, J. (1988) d(GATC) sequences influence Escherichia coli mismatch repair in a distance-dependent manner from positions both upstream and downstream of the mismatch. Nuc Acids Res. 16, 4875-4890

20. Husain, I., Van Houten, B., Thomas, D.C., Abdel-Monem, M., and Sancar, A. (1985) Effect of DNA polymerase I and DNA helicase II on the turnover rate of UvrABC excision nuclease. Proc.Natl.Acad.Sci.U.S.A. 82, 6774-6778

21. Caron, P.R., Kushner, S.R., and Grossman, L. (1985) Involvement of helicase II (uvrD gene product) and DNA polymerase I in excision mediated by the uvrABC protein complex. Proc.Natl.Acad.Sci.U.S.A. 82, 4925-4929

22. Flores, M.J., Bidnenko, V., and Michel, B. (2004) The DNA repair helicase UvrD is essential for replication fork reversal in replication mutants. EMBO Rep. 5, 983-988

23. Flores, M.J., Sanchez, N., and Michel, B. (2005) A fork-clearing role for UvrD. Mol.Microbiol. 57, 1664-1675

24. Stambuk, S., and Radman, M. (1998) Mechanism and control of interspecies recombination in Escherichia coli. I. Mismatch repair, methylation, recombination and replication functions. Genetics. 150, 533-542

25. McGlynn, P. (2011) Helicases that underpin replication of protein-bound DNA in Escherichia coli. Biochem.Soc.Trans. 39, 606-610

26. Hall, M.C., Jordan, J.R., and Matson, S.W. (1998) Evidence for a physical interaction between the Escherichia coli methyl-directed mismatch repair proteins MutL and UvrD. EMBO J. 17, 1535-1541

27. Mechanic, L.E., Frankel, B.A., and Matson, S.W. (2000) Escherichia coli MutL loads DNA helicase II onto DNA. J.Biol.Chem. 275, 38337-38346

28. Yamaguchi, M., Dao, V., and Modrich, P. (1998) MutS and MutL activate DNA helicase II in a mismatch-dependent manner. J.Biol.Chem. 273, 9197-9201

29. Dao, V., and Modrich, P. (1998) Mismatch-, MutS-, MutL-, and helicase II-dependent unwinding from the single-strand break of an incised heteroduplex. J.Biol.Chem. 273, 9202-9207

30. Fischer, C.J., Maluf, N.K., and Lohman, T.M. (2004) Mechanism of ATP-dependent translocation of E.coli UvrD monomers along single-stranded DNA. J.Mol.Biol. 344, 1287-1309

31. Tomko, E.J., Fischer, C.J., and Lohman, T.M. (2012) Single stranded DNA translocation of E. coli UvrD monomer is tightly coupled to ATP hydrolysis. J.Mol.Biol.

32. Wessel, R., Muller, H., and Hoffmann-Berling, H. (1990) Electron microscopic analysis of DNA forks generated by Escherichia coli DNA helicase II. Eur.J.Biochem. 192, 695-701

33. Indiani, C., and O'Donnell, M. (2006) The replication clamp-loading machine at work in the three domains of life. Nat.Rev.Mol.Cell Biol. 7, 751-761

34. Ban, C., and Yang, W. (1998) Crystal structure and ATPase activity of MutL: implications for DNA repair and mutagenesis. Cell. 95, 541-552

35. Guarne, A., Ramon-Maiques, S., Wolff, E.M., Ghirlando, R., Hu, X., Miller, J.H., and Yang, W. (2004) Structure of the MutL C-terminal domain: a model of intact MutL and its roles in mismatch repair. EMBO J. 23, 4134-4145

36. Robertson, A., Pattishall, S.R., and Matson, S.W. (2006) The DNA binding activity of MutL is required for methyl-directed mismatch repair in Escherichia coli. J.Biol.Chem. 281, 8399-8408

37. Runyon, G.T., Wong, I., and Lohman, T.M. (1993) Overexpression, purification, DNA binding, and dimerization of the Escherichia coli uvrD gene product (helicase II). Biochemistry. 32, 602-612

38. Robertson, A.B., Pattishall, S.R., Gibbons, E.A., and Matson, S.W. (2006) MutL-catalzyed ATP hydrolysis is required at a post-UvrD loading step in methyl-directed mismatch repair. J.Biol.Chem.

39. Matson, S.W., and Robertson, A.B. (2006) The UvrD helicase and its modulation by the mismatch repair protein MutL. Nucleic Acids Res. 34, 4089-4097

40. Lucius, A.L., Maluf, N.K., Fischer, C.J., and Lohman, T.M. (2003) General methods for analysis of sequential "n-step" kinetic mechanisms: application to single turnover kinetics of helicase-catalyzed DNA unwinding. Biophys.J. 85, 2224-2239

41. Runyon, G.T., Bear, D.G., and Lohman, T.M. (1990) Escherichia coli helicase II (UvrD) protein initiates DNA unwinding at nicks and blunt ends. Proc.Natl.Acad.Sci.U.S.A. 87, 6383-6387

42. Zhang, G., Deng, E., Baugh, L., and Kushner, S.R. (1998) Identification and characterization of Escherichia coli DNA helicase II mutants that exhibit increased unwinding efficiency. J.Bacteriol. 180, 377-387

43. Lee, J.Y., and Yang, W. (2006/12/29) UvrD Helicase Unwinds DNA One Base Pair at a Time by a Two-Part Power Stroke. Cell. 127, 1349-1360

44. Centore, R.C., Leeson, M.C., and Sandler, S.J. (2009) UvrD303, a Hyperhelicase Mutant That Antagonizes RecA-Dependent SOS Expression by a Mechanism That Depends on Its C Terminus. J.Bacteriol. 191, 1429-1438

CHAPTER 4: THE UVRD 2B SUBDOMAIN IS NOT REQUIRED FOR HELICASE ACTIVITY

Abstract

DNA helicases use energy derived from nucleoside 5′-triphosphate hydrolysis to catalyze the separation of double-stranded DNA to form single stranded DNA (ssDNA) intermediates for replication, recombination, and repair. *Escherichia coli* helicase II (UvrD) functions in methyl-directed mismatch repair, nucleotide excision repair, and homologous recombination. Previous work with the similar Rep helicase (38% amino acid identity) has suggested that the 2B subdomain of the protein is involved in regulating the activity of the helicase. Similar studies with UvrD have not been reported due to an apparent lethality of UvrDΔ2B upon expression. I was able to express and partially purify UvrDΔ2B to examine the biochemical activity of the helicase *in vitro*. Using rapid quench, pre-steady state kinetic experiments we show the UvrDΔ2B helicase exhibits a decreased helicase activity relative to the wild-type protein, the opposite of what was observed with RepΔ2B. Cells expressing UvrDΔ2B exhibited increased sensitivity to ultraviolet light exposure and demonstrated a mutator phenotype similar to a UvrD deletion strain. This is consistent with the idea that the 2B subdomain may have a role in coordinating the activity of the helicase to perform vital roles in the cell. Unlike the closely related Rep helicase, deletion of the 2B subdomain of UvrD does not stimulate the helicase activity suggesting that the role of the 2B subdomain is more complex than simply regulating the unwinding activity of the helicase.

Introduction

DNA helicases are a ubiquitous class of motor proteins that derive energy from the hydrolysis of nucleoside 5′-triphosphates to catalyze the transient separation of double-stranded DNA (dsDNA) into its respective complementary strands. These enzymes are involved in nearly all aspects of DNA metabolism and are essential for many cellular processes including DNA replication, recombination, and repair (1-5). Mutations within the genes encoding human DNA helicases have been linked to a variety of genetic disorders and other diseases including as premature gaining disorders and various forms of cancer (6-8). Although many DNA helicases have been identified from a wide variety of organisms, our understanding of the mechanisms by which these enzymes perform their roles is not complete.

The *Escherichia coli* DNA helicase II (UvrD) has been shown to play vital roles in both methyl-directed mismatch repair (MMR) (9, 10) and nucleotide excision repair (NER) (11). As DNA polymerase III replicates the chromosome, misincorporated bases are removed by the 3′ to 5′ proofreading exonuclease activity of the polymerase. Occasionally, errors escape the proofreading activity of the polymerase and must be repaired in another manner. MMR is a DNA repair pathway that recognizes and facilitates the removal of the mispaired bases. The error containing strand is newly synthesized and has not yet been by methylated by deoxyadenine methyl-transferase, differentiating the nascent strand from the template. The hemimethlylated state of the DNA ensures that the repair process is targeted to the daughter strand. In MMR, a MutS homodimer recognizes the DNA damage and recruits MutL. MutL then activates the latent sequence and methylation specific endonuclease activity of the repair protein MutH to induce a nick in the unmethylated DNA strand 5′ to a target d(GATC) sequence. The repair process is bidirectional with the MutH-induced nick occurring either 5′ or 3′ to the

mismatch site. UvrD initiates unwinding from this nicked d(GATC) site and acts in conjunction with MutL to displace the newly synthesized error-containing DNA strand (9, 12). The distance from the site of UvrD loading and the mismatched base pair is variable and can be upwards of a thousand base pairs. As UvrD separates the duplex, the error-containing, nascent DNA strand is degraded by appropriate exonucleases. DNA polymerase III synthesizes a new DNA strand to fill the resulting gap and ligase seals the nick to complete the repair reaction. (13). NER is a repair process by which the cell can remove bulky lesions, such as pyrimidine dimers, from the DNA. In NER, UvrD acts in conjunction with the UvrABC excision nuclease to remove a short 12-13 base oligonucleotide containing the damaged DNA allowing DNA polymerase I to fill the resulting gap and ligase to complete the repair process. (11).

Both MMR and NER require the unwinding activity of UvrD to facilitate displacement of the error-containing DNA strand for efficient repair. *In vivo* studies have indicated that *E. coli* cells lacking the UvrD helicase exhibit both mutator and UV sensitive phenotypes, denoting deficiencies in both MMR and NER (14-16). Likewise, *in vitro* studies have determined that UvrD plays an integral role in both repair pathways (9-11). While these studies show that UvrD is required for execution of these repair pathways, less is known about UvrD functionality.

UvrD is a Superfamily 1 (SF1) helicase with well documented 3′ to 5′ helicase and translocase activities (17-19). Similar to other SF1 helicases, such as *E. coli* Rep and *Bacillius stearothermophilus* PcrA, UvrD contains seven conserved helicase motifs and two structural domains (1 and 2) which are then further divided into two subdomains (A and B) (20-24) (see Fig. 2, Chapter 2). Structural studies with both Rep and UvrD have shown that the 2B subdomain is highly mobile and capable of rotating 130° and160°, respectively, about a flexible linker between the 2A and 2B subdomains. When the 2B subdomain is stacked above the 2A

subdomain, the protein is referred to as being the in "open" conformation. As the 2B domain rotates and closes onto the 1B subdomain, the structure is referred to as the "closed" conformation (24-26, Figure 2, Chapter 2). Crystal structures for both UvrD and PcrA have shown a monomer of the helicase bound to a dsDNA with a 3′ ssDNA tail in the closed conformation (25, 27). In this conformation Lee et al. (25) have suggested the 2B subdomain engages the duplex DNA and the ssDNA is bound by the 1A subdomain. Previous work has shown that the subdomains 1A and 2A are the core of the helicase engine responsible for ATP binding and hydrolysis (20, 21, 25). The binding of ATP in the pocket created between the 1A and 2A subdomains induces a closing of this pocket. Structural studies of a UvrD/DNA co-crystal suggested that the closing of the pocket and subsequent hydrolysis of ATP is responsible for the separation of the dsDNA as it forces the separation pin of the 2A subdomain between the two strands of the duplex DNA (Fig. 17) (25). The 2B subdomain engages the duplex DNA via the so called GIG motif and, along with the ssDNA anchor of motif III, holds the DNA substrate while the separation pin and ssDNA gateway remain flexible allowing for unwinding. As the helicase cycles through the process of ATP hydrolysis these four contact points invert their roles allowing the helicase to act as a sort of "molecular ratchet" in the course of the unwinding reaction (25). Though these structural studies suggest that a monomer of SF1 helicases is the active unwinding form, the biochemical studies of these helicases support the view that a dimer or oligomer is required for helicase activity. SF1 helicases have been observed to be monomeric when in solution and binding to DNA induces a dimerization of the helicase. Previous studies of Rep have suggested

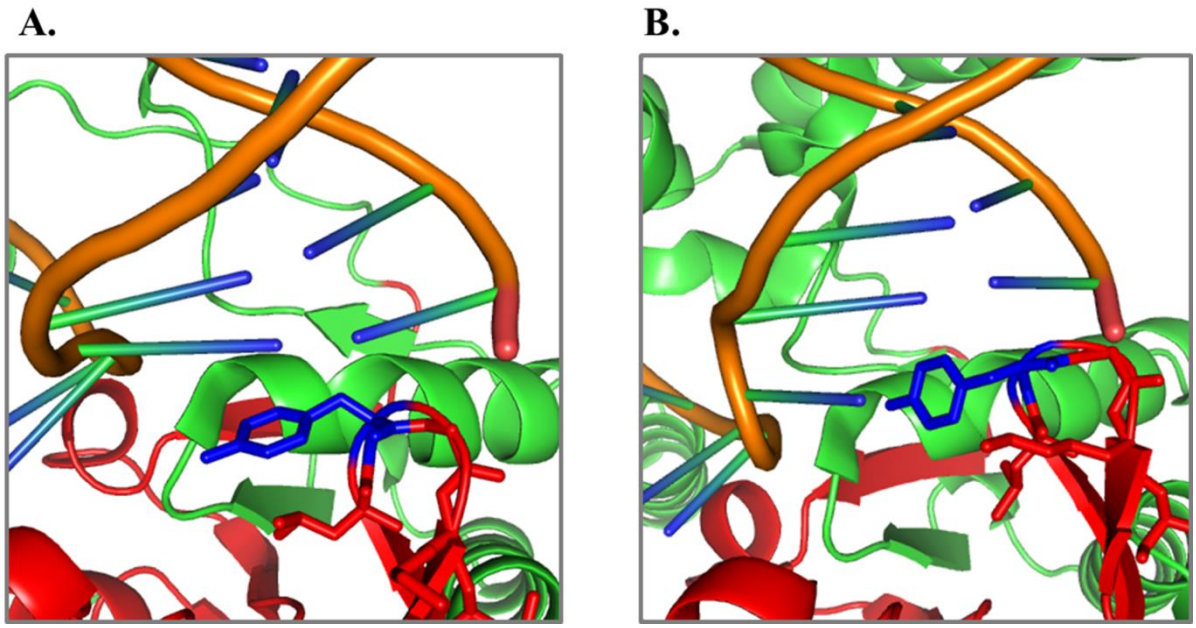

Figure 17. Models of the *E. coli* UvrD 2A subdomain and the role of the Y621 residue in facilitating the separation of dsDNA base pairs in an ATPdependent manner.. Panel A– Ribbon diagram of UvrD bound to partial duplex DNA in the closed conformation with no nucleotide bound (Protein Data Bank code 2IS2) (23). The 2A subdomain is shown in red and the rest of the helicase in green. Amino acids 620-625 are shown in stick representation with Y621 colored blue. Panel B – Ribbon diagram of UvrD bound to partial duplex DNA in the closed conformation bound with ADP-MgF_3 (Protein Data Bank Code 2IS6) (23). The 2A subdomain is shown in red and the rest of the helicase in green. Amino acids 620-625 are shown in stick representation with Y621 colored blue. Molecular images were generated with the PyMOL Molecular Graphics System, Version 1.3, Schrödinger, LLC. B.

that the 2B subdomain is involved in the dimerization of the helicase. The 2B subdomain has been observed in SF1 helicases to adopt two conformations, "open" and "closed", as previously mentioned. Previous work has demonstrated that the 2B subdomain of UvrD can alternate between open and closed conformations in response to substrate binding, nucleotide occupancy, and salt concentration (26). These results suggest that the 2B subdomain is more open while bound to DNA substrates, but closes during nucleotide binding and hydrolysis. In Rep helicase, the 2B subdomain was thought to be mobile in response to ssDNA binding, leading to the hypothesis that the 2B subdomain of Rep may be functionally relevant for helicase activity.

Among the SF1 helicases, UvrD shares ~38% amino acid identity with Rep helicase over the entirety of the protein and a 90% identity over the seven conserved motifs. Based on this high degree of similarity, Rep helicase has historically been used as a structural model for UvrD. Previous studies have shown that the 2B subdomain is not required for Rep helicase activity, and that the deletion of the 2B subdomain resulted in a protein with stimulated helicase activity (28, 29). These data suggest that the 2B subdomain may be fulfilling some regulatory role and exhibits an autoinhibitory effect on the unwinding activity of Rep helicase (23,30). The proposed autoregulatory activity of the 2B subdomain may prevent SF1 helicases from separating duplex DNA in an uncontrolled manner, generating vulnerable ssDNA intermediates.

The role of the 2B subdomain in the related UvrD helicase is less well studied. Recent work has examined the conformations adopted by the 2B subdomain under varying salt, nucleotide, and bound substrate conditions and found that the 2B subdomain is, at least, partially open while bound to ssDNA or duplex DNA with a 3′ ssDNA tail (26). These data suggest that there may be numerous intermediate conformations between completely open and completely closed. When the helicase binds ATP, the 2B subdomain is observed to be partially open, and,

by using nucleotides which mimic ATP hydrolysis intermediates, closes during hydrolysis (26). None of the seven conserved helicase motifs in UvrD are found within the 2B domain. In addition, the related SF2 helicases, such as the hepatitis C virus helicase NS3, lack the equivalent of the 2B subdomain. This may suggest that the 2B subdomain is not required for SF1 helicase activity. However, all previous attempts at directly examining a UvrDΔ2B mutant have failed due to an apparent lethality upon expression of the mutant helicase, presumably due to an unregulated unwinding activity exhibited by UvrD mutant.

This chapter presents a preliminary examination of UvrDΔ2B helicase and the possible roles the 2B subdomain plays in the regulation of MMR and possibly NER. Using single turnover rapid quench helicase assays, we have shown that deletion of the 2B subdomain results in a less active helicase and, contrary to the effect observed in Rep, does not activate the monomer activity of UvrD. Using mutation reversion assays we were also able to determine that the 2B subdomain is required for efficient MMR, possibly due to a direct interaction between UvrD and MutL via the 2B subdomain. Finally, we show that strains expressing UvrDΔ2B are unable to properly recover from UV irradiation suggesting that the mutant is unable to function in NER.

Materials and Methods

Helicase purification – pET11d-UvrD was constructed as previously described (36). Using pET11d-UvrD as a template, polymerase chain reaction (PCR) amplification was performed using a NcoI-site containing primer 5′-GGAGTATACCATGGACGTTTCTTACC-3′ and the Δ2B reverse primer 5′- TTTGGTACCCCCGCCGTAAATACGGTA -3′. A second PCR amplification was performed using the HindIII-site containing primer 5′-GACAGCTTATCATCGATAAGCTTGGGC -3′ and the Δ2B forward primer 5′-

TTTGGTACCGGGGGGCAGGCGGATACCTGG- 3′. The PCR products of these two reactions were blunt end ligated and used as a template for a third PCR amplification using the aforementioned NcoI and HindIII containing primers. This PCR product was digested with NcoI and HindIII and ligated into pET11d to generate pET11d-UvrDΔ2B. The resulting modified UvrD-encoding gene eliminated 165 of the 178 amino acids in the 2B subdomain fusing the first two amino acids of the 2B subdomain (G378 and G379) to G545, eliminating all but 13 amino acids within the 2B subdomain (Fig. 18).

The pET11d-UvrDΔ2B plasmid was digested with EcoRI and BsiWI to generate an 878 bp fragment that was cloned into pTYB4-His-UvrD (see chapter 2) that was digested using the same restriction enzymes replacing the 1364 bp fragment endogenous to this construct. The resulting plasmid, pTYB4-His-UvrDΔ2B was used to express and purify UvrDΔ2B. pTYB4-UvrDΔ2B-His was transformed into *E. coli* BL21DE3*uvrD*::Tn5*mutL*::Tn10 and a 20 mL culture was grown overnight at 37°C in ZY media (31). The overnight culture was introduced to 1 L of ZYM5052 autoinduction media (31) and grown at 16°C for 48 hours. The cells were harvested by centrifugation, washed once with 25 mL of STE buffer (10 mM Tris-HCl (pH8.0), 1 mM EDTA and 100 mM NaCl) and harvested again by centrifugation. The cells were stored at -80^{o}C until use. The cells were lysed and the protein was purified as previously described using a combination of Talon (Clone-tech) and Chitin (NEB) resins to take advantage of the two affinity tags present on the overexpressed fusion protein (32). Protein that eluted from the Chitin column was dialyzed against UvrD storage buffer (33) and stored at -20^{o}C. Wild-type UvrD was purified as previously described (33).

DNA Substrates – Partial duplex substrates were prepared by radiolabeling the 5'-end of oligonucleotides obtained from Integrated DNA Technologies (Coralville, Iowa) using

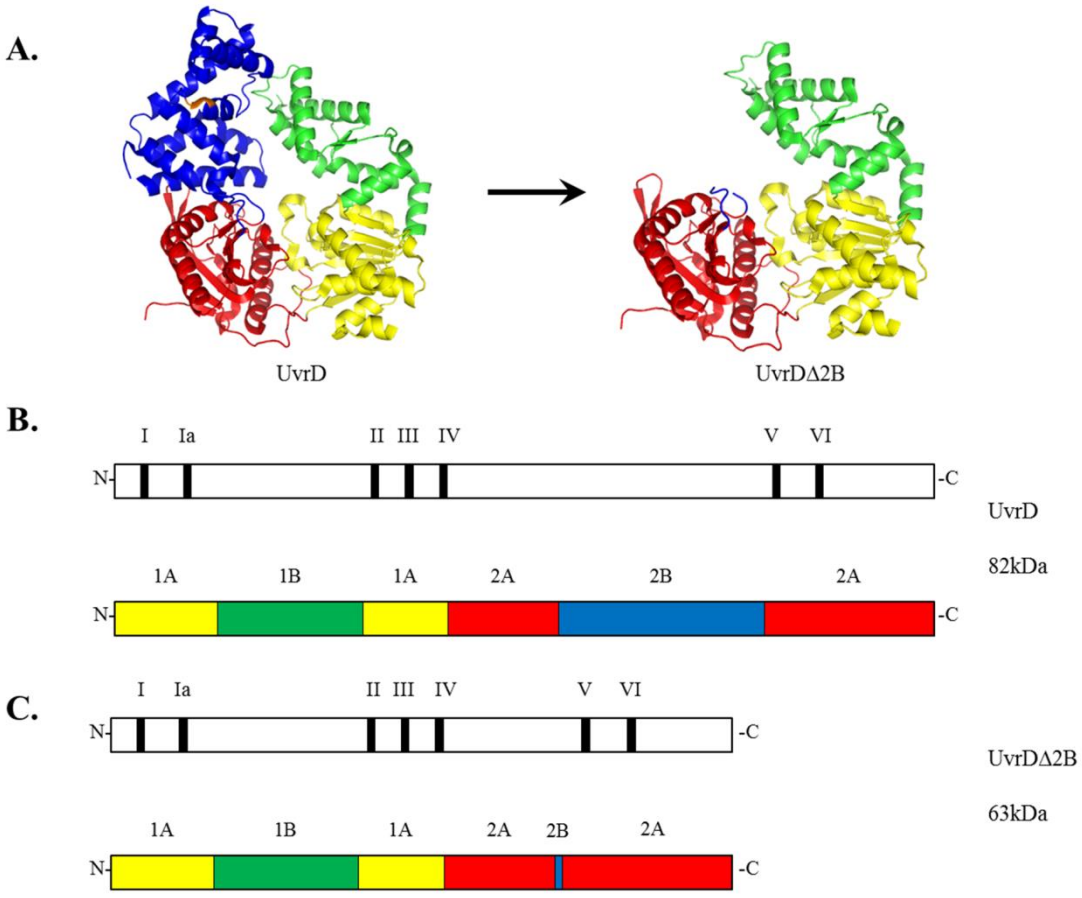

Figure 18. Models of *E. coli* UvrD helicase in the open conformation and the mutant UvrDΔ2B**.** A. Left – Ribbon diagram of the apo-structure of UvrD in the open conformation (Protein Data Bank code 3LFU). Right – Ribbon diagram of UvrDΔ2B generated in Pymol. Molecular images were generated with the PyMOL Molecular Graphics System, Version 1.3, Schrödinger, LLC. B. Top panel – A schematic representation of the seven conserved helicase motifs of UvrD. Bottom panel – A schematic representation of the four structural subdomains of UvrD. The two graphics are aligned such that the placement of the 2B subdomain can be seen with respect to the seven conserved motifs. C. Top panel – A schematic representation of the seven conserved helicase motifs of UvrD in UvrDΔ2B. Bottom panel – A schematic representation of the four structural subdomains of UvrD after the removal of the vast majority of the 2B subdomain. The two graphics are aligned such that the placement of the 2B subdomain can be seen with respect to the seven conserved motifs

[γ-^{32}P]ATP and T4 polynucleotide kinase (see Table 1 for oligonucleotide sequences). A 1.1-fold excess of an unlabeled complementary oligonucleotide was annealed to the labeled strand by heating the two strands to 95°C for 5 minutes and allowing them to slow cool to 25°C overnight. The partial duplex substrate was purified from free nucleotide using a Sephadex G50 spin column and dialyzed into TEN buffer (10 mM Tris-HCl (pH 7.5), 1 mM EDTA, 50 mM NaCl). This process was used to generate the 24/64 partial duplex substrate. The shorter DNA strand was radioactively labeled. The longer DNA strand contains a 40 base 3'-tail ssDNA tail to facilitate loading of UvrD.

Helicase Assays – Helicase reaction mixtures (16 μL) for steady-state experiments contained 25 mM Tris-HCl (pH7.5), 3 mM $MgCl_2$, 20 mM NaCl, 5 mM 2-mercaptoethanol (βME), 50 μg/mL bovine serum albumin, 3 mM ATP, helicase concentration as described, and approximately 0.2 nM radiolabeled partial duplex DNA substrate. The reactions were assembled on ice and the helicase was allowed to preincubate with the DNA substrate for several minutes. The reactions were initiated by the addition of ATP and incubated in a 37°C for 5 minutes before addition of 8 μL of stop solution, 37.5% (v/v) glycerol, 50 mM EDTA, 0.3% (w/v) SDS, 0.5x TBE and dyes. The reactions were resolved on 12% (w/v) non-denaturing polyacrylamide gels (19:1 crosslinking ratio) to separate duplex DNA substrate from ssDNA products and visualized by PhosphorImaging (Molecular Dynamics).

Rapid Quench Singe Turnover Assays and Modeling – Rapid quench single turnover assays were performed essentially as previously described (34), with minor modifications, at room temperature (~19^{o}C) using a computer controlled quenched-flow apparatus (KinTek RQF-3, University Park, PA). Helicase was allowed to incubate with the partial duplex substrate (100 nM helicase, 2 nM DNA substrate for single turnover assays or 150 nM DNA, 50 nM helicase

for monomer activity assays) in buffer L (25 mM Tris-HCl (pH 7.5), 200 μg/mL bovine serum albumin, 200 μM EDTA, 10% (v/v) glycerol, 5 mM βME) plus 3 mM ATP on ice for 15 min, and then loaded into the D loop. The opposite E loop was loaded with 6 mM $MgCl_2$ and 3 μM DNA hairpin trap in buffer M (25 mM Tris-HCl (pH 7.5), 25 mM NaCl, 10% (v/v) glycerol, 5 mM βME). Reactions were initiated by rapidly mixing equal volume aliquots of the solutions from loops D and E, and were quenched with 200 mM EDTA and 0.2% (w/v) SDS. Samples were resolved on non-denaturing polyacrylamide gels and visualized by PhosphorImaging (Molecular Dynamics).

Far Western Blots– Far western blots were performed by spotting approximately 20 pmols of either MutL or helicase protein onto a Protran nitrocellulose transfer membrane (Whatman) and incubated at room temperature (~19°C) for 5 minutes. The membrane was blocked using 2% (w/v) non-fat powdered milk in TBST (10 mM Tris-HCl (pH7.5), 150 mM NaCl, 0.1% (v/v) Tween-20) for 5 minutes. The membrane was removed from the milk and allowed to air dry slightly for no more than two minutes before spotting approximately 20 pmols of MutL atop each of the initial samples. The proteins were incubated together on the membrane at room temperature for 5 minutes before the membrane was washed three times for five minute each with 0.2% (w/v) non-fat powdered milk in TBST. The membrane was then incubated with an anti-MutL primary antibody from rabbit (1:15,000 fold dilution) for one hour. The membrane was washed as described above before being incubated with an anti-rabbit IgG secondary antibody from goat conjugated to alkaline phosphatase. After a final wash the membrane was developed with approximately 10 mL of Western Blue (Promega) for 2 minutes to visualize binding of the secondary antibody. The alkaline phosphatase reaction was stopped by extensive washing with ddH_2O.

Immunoprecipitation of MutL/UvrD complexes – Approximately 5 μg of MutL and an equal amount of UvrD were incubated together at 4°C for 60 min. in a final volume of 50 μL under the same conditions as the helicase reactions described above. After the initial incubation, anti-MutL primary antibody from rabbit was added (1:50 fold dilution) and incubated for 60 minutes at 4°C. Approximately 50 μL of protein A/G coated beads (Sigma-Aldrich) slurry was added to the tube and allowed to incubate for 30 minutes. The beads were pelleted in a microfuge at 2000 rpm for 3 minutes and the supernatant was removed. The beads were washed five times in 500 μL wash buffer (50 mM Tris-HCl (pH8.0), 500 mM NaCl, 10% (v/v) glycerol) and suspended in 25 μL of 2x SDS gel loading buffer (200 mM Tris-HCl (pH6.8), 20% (v/v) glycerol, 3.2% (w/v) SDS, 1.15 M βME). The bead slurry was heated in a 95°C water bath for five minutes then spun down at 1500rpm for 1 minute to pellet the beads. The supernatant was removed and resolved on a 10% SDS-polyacrylamide gel.

Spontaneous Mutation Rate Determination – pET11d-UvrDΔ2B and pET11d-UvrD were transformed into the strains GE1752 *metE*::cam and GE1752Δ*uvrD metE*$^{+}$ Δ*uvrD*::tet^{r} (Table 5). Three isolates of each strain containing pET11D-UvrDΔ2B were grown overnight at 37°C in LB (5 g/L NaCl, 5 g/L yeast extract, 10 g/L tryptone) containing the appropriate antibiotics. The number of cells in each culture was estimated using a spectrophotometer (LKB Biochrom Ulstraspec II) to measure optical density via A_{600}. The cultures were diluted, if necessary, to an absorbance of 0.75. The cultures were serially diluted and plated in triplicate onto rifampicin containing LB plates. The plates were incubated at37°C incubator for 16-20 hours and scored for colonies which showed resistance to rifampicin. The colony counts were used in conjunction with the Leah-Coulson model (35) to determine mutation rates.

Ultraviolet Sensitivity Determination –pET11d-UvrDΔ2B and pET11d-UvrD were transformed into the strains GE1752 *metE*::cam and GE1752Δ*uvrD metE*::cam Δ*uvrD*::tet^r Three isolates of each strain containing pET11D-UvrDΔ2B were grown overnight at 37°C in LB containing the appropriate antibiotics. The number of cells in each culture was estimated using a spectrophotometer (LKB Biochrom Ulstraspec II) to measure optical density via A_{600}. The cultures were diluted, if needed, to an absorbance reading of 0.75. The cultures were streaked onto LB plates and exposed to short wavelength (254 nM) ultraviolet light for 0-50 seconds. The irradiated plates were incubated at 37°C for 16-20 hours and evaluated for cell growth.

Results

Three SF1 helicases, PcrA, UvrD, and Rep are all structurally similar, containing four subdomains: 1A, 1B, 2A, and 2B. All three also have shown large rotations of the 2B subdomain, displaying both open and closed conformations (25, 27, 28). Previous crystal structures have suggested that these helicases bind to a 3′-ssDNA/dsDNA junction as monomers in the closed conformation (25, 27). These crystal structures show an extensive interaction between the 2B subdomain and the dsDNA suggesting that the closed monomer is the active form of the helicase and that the 2B subdomain is essential for activity. There is substantial evidence, however, that the monomeric forms of PcrA, UvrD, and Rep are not active helicases (28, 29, 34). In addition, deletion of the 2B subdomain in the Rep helicase results in a protein with increased helicase activity (28).

Taken together, these data suggest the observed 2B subdomain/duplex DNA interaction is not required for the unwinding activity of these helicases. Brendza et al (29) have suggested an alternate role for the 2B subdomain. Their work with Rep helicase suggested that the 2B subdomain may be fulfilling an autoregulatory role, possibly coordinating various activities of

the enzyme. Similarly, mutations within the UvrD 2B subdomain have been shown to have a direct impact on the unwinding activity of the helicase (see Chapter 2). However, there have been no direct studies of a UvrD 2B deletion mutant.

Previous work has studied the effects of a 2B subdomain deletion in Rep helicase. The resulting RepΔ2B exhibits an increased unwinding activity compared to the wild-type protein. Cheng et al. (28) calculated the rate of unwinding to be over 6-fold higher in the RepΔ2B compared to wild-type Rep. It was later suggested that RepΔ2B was capable of catalyzing unwinding as a monomeric helicase. Brendza et al. (29) proposed a mechanism based on these data by which the DNA unwinding activity of the helicase was regulated through the 2B subdomain. Given that previous studies have reached differing conclusions regarding the role of the 2B subdomain, a study of a UvrD 2B deletion mutant might shed additional light on the role of the 2B subdomain and confirm its role as a regulatory region in SF1 helicases.

UvrDΔ2B was cloned into pTYB4-His as described under "Materials and Methods". This expression vector allows for a simple and rapid purification of the desired protein. Although expression was robust from this vector (Fig. 19A), recovery of the protein was challenging. Although cleavage of the intein tag in the presence of 50 mM DTT is observed for wild-type UvrD and other helicases, a very small amount of UvrDΔ2B was recovered after the cleavage step. In addition, the protein that was recovered was not homogeneous (Fig. 19B). Of the many preparations that were performed, the best purity yield was estimated to be no more than 50% pure.

To begin to characterize the helicase activity of partially purified UvrDΔ2B, we compared the helicase activity of wild-type UvrD to that of UvrDΔ2B using a 24 base pair (bp) partial duplex DNA substrate with a 3′-$(dT)_{40}$ tail under steady state, multiple turnover

conditions. Previous studies have shown that a 40 nucleotide ssDNA tail is the optimal length for helicase activity for UvrD (34). The proteins were incubated with the DNA substrate and the reaction was initiated with the addition of ATP. The activity of UvrD and UvrDΔ2B were essentially identical (Fig. 20). Importantly, deletion of the 2B subdomain did not appear to stimulate the activity of UvrD in contrast to the results obtained using Rep protein, nor did it eliminate the helicase activity of the protein (Fig. 20). We can be confident that the UvrDΔ2B preparation was not contaminated by wild-type UvrD, as the mutant was purified form an *E. coli* strain that has the endogenous *uvrD* gene deleted. However, we note these results have been obtained using a protein preparation that is not homogeneous. Consequently, these results must be interpreted with caution.

While the multiple turnover unwinding experiments confirm that UvrDΔ2B is indeed active as a helicase, they do not offer much insight into how deletion of the 2B subdomain impacts the unwinding activity. A similar deletion of the 2B subdomain in Rep helicase exhibited a stimulated helicase activity under single turnover (STO) conditions (28). We performed a similar STO assay using a rapid chemical quenched flow protocol. Excess helicase (50 nM final concentration), the partial duplex substrate (1 nM final concentration) and ATP were pre-incubated to allow formation of the enzyme-substrate complex, and then rapidly mixed with $MgCl_2$ and a 1500-fold excess of a DNA hairpin trap to initiate unwinding. The excess trap ensures the sequestering of any free or dissociated helicase and prevents any reinitiation of unwinding. It is important to note that these STO quenched-flow assays are “all or none” DNA unwinding assays and incapable of detecting partially unwound substrates. Using the 24 bp partial duplex, both UvrD and UvrDΔ2B were capable of converting the substrate to ssDNA

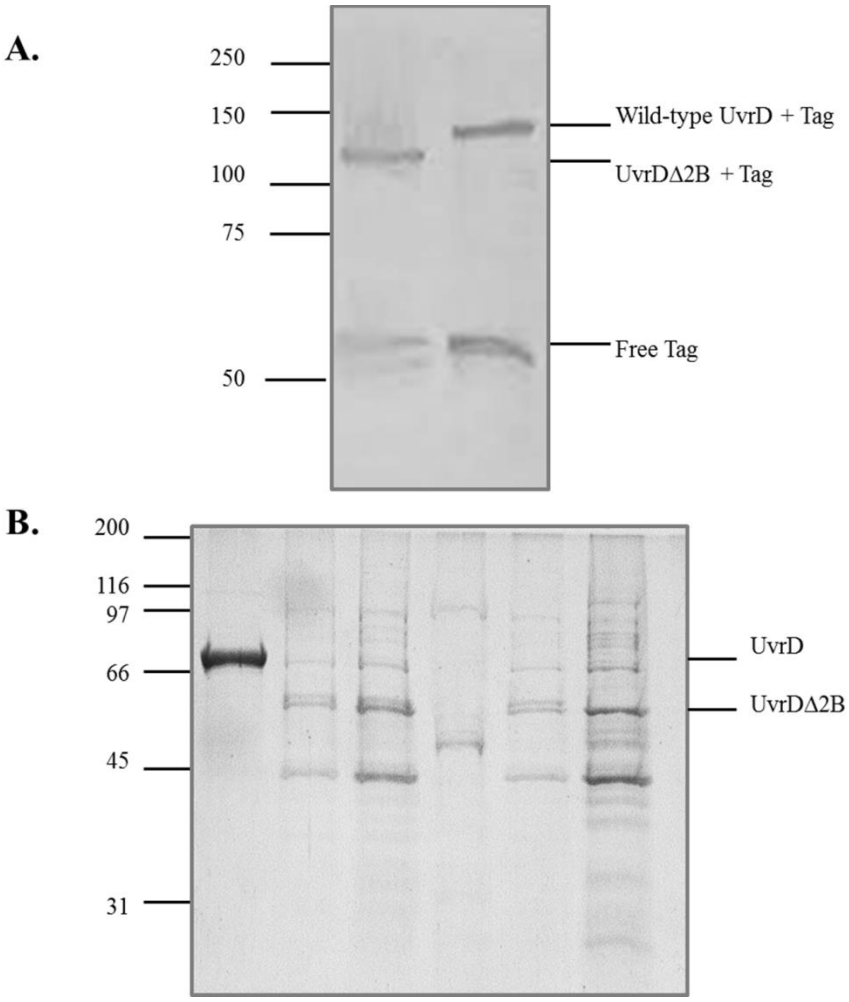

Figure 19. Expression and purification of UvrDΔ2B. Panel A. Cultures of autoinduced BL21(DE3)Δ*uvrD*,Δ*mutL E. coli* expressing wild-type UvrD or UvrDΔ2B from the pTYB4-His vector were lysed. Equal amounts of crude lysate were analyzed by Western blotting for protein expression using α-His primary antibody. Species observed were either helicase/intein tag fusions or free intein tag. Panel B. Multiple preparations of UvrDΔ2B were compared to purified wild-type UvrD by Coomassie stain. The first lane from the left contained ~3μg of >95% pure wild-type UvrD.

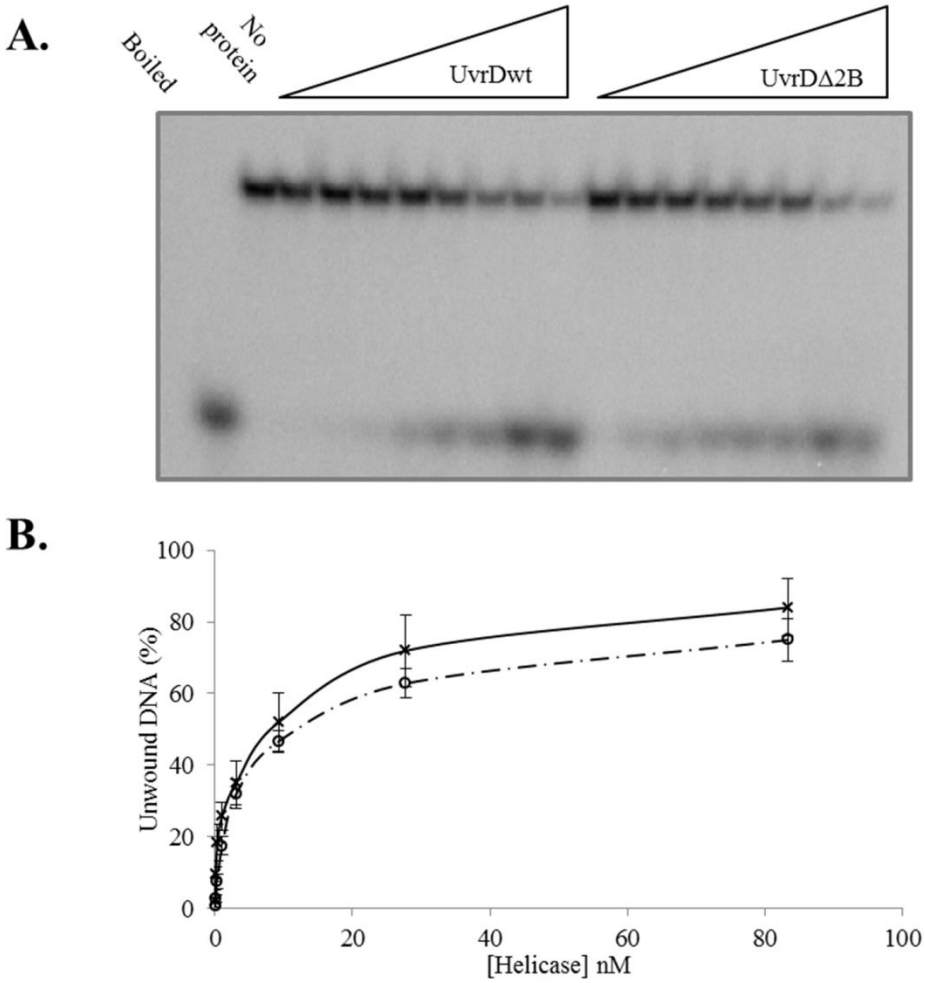

Figure 20. UvrD and UvrDΔ2B exhibit comparable helicase activity under multiple turnover conditions. Panel A – DNA helicase reactions were performed as described under "Materials and Methods" using the 24 bp partial duplex substrate and increasing concentrations of UvrD or UvrDΔ2B. The first two lanes are controls for no protein and heat denatured substrate DNA. The remaining lanes depict a protein titration of increasing concentration from 0.05 to 85 nM UvrD or UvrDΔ2B. Panel B – Quantitative data from 2 experiments at the indicated concentrations of UvrD (open circles) and UvrDΔ2B (crosses) were plotted as the average at each protein concentration. Error bars represent the standard deviation about the mean.

(Fig. 21). Under these conditions UvrD unwinds approximately 60% of the substrate while UvrDΔ2B only unwound 40%. These results show that under STO conditions UvrDΔ2B exhibits a somewhat less robust helicase activity than the wild-type UvrD. This result was, perhaps, unexpected since deletion of the 2B subdomain of Rep helicase resulted in a dramatically stimulated helicase activity under similar conditions (24).

Deletion of the 2B subdomain stimulated the Rep protein helicase activity and activated the unwinding ability of the Rep monomer. Although a similar deletion in UvrD was not seen to stimulate unwinding, it was of interest to determine if there was an impact on the monomer activity. To assess the helicase activity of the UvrD monomer a series of STO DNA unwinding experiments were performed. In these experiments 150 nM of the 24 bp partial duplex and 50 nM UvrDΔ2B were premixed in the presence of ATP. The excess DNA ensures that no more than one UvrDΔ2B monomer is bound per DNA substrate molecule. The preformed enzyme-substrate complexes were then rapidly mixed with $MgCl_2$ and a 1500-fold excess of a DNA hairpin trap to initiate unwinding. Under these conditions, the UvrDΔ2B monomer was not observed to have any measurable unwinding activity (Fig. 22). Taken together, these results clearly demonstrate that UvrDΔ2B is active as a helicase, but it remains unknown if UvrDΔ2B is functional in the cell.

A preliminary genetic characterization of the *uvrDΔ2B* allele was initiated by transforming plasmids containing *uvrD* (pET11d-UvrD), or *uvrDΔ2B* (pET11d-UvrDΔ2B) into *E. coli* GE1752 and GE1752Δ*uvrD*. Expression of the relevant *uvrD* gene is driven by the T7 RNA polymerase promoter in these plasmid constructs. Work by previous lab members has demonstrated the ability of these constructs to express protein at levels approximate to those observed from the chromosome in strains lacking the λ DE3 lysogen (36). Although UvrD is not

essential for the viability of *E. coli* under lab growth conditions, UvrD plays an integral role in MMR. Therefore, the ability of UvrDΔ2B to support mismatch repair *in vivo* was tested using spontaneous mutation assays. As summarized in Table 6, an elevated mutation rate is observed in GE1752*ΔuvrD*, confirming the importance of the helicase in the repair process. When pET11d-UvrD was transformed into GE1752*ΔuvrD*, the mutation rate returned to approximately wild-type levels. Thus, UvrD expressed from pET11d-UvrD under these conditions can complement the loss of helicase II in GE1752*ΔuvrD*. In contrast, pET11d- UvrDΔ2B exhibited a mutation frequency that is not statistically significantly different from that of GE1752*ΔuvrD*. These results suggest thatUvrDΔ2B cannot function in MMR. In an effort to determine the relationship between the wild-type UvrD and UvrDΔ2B, GE1752 was transformed with pET11d-UvrDΔ2B and the mutation rate was measured. In this case, both wild-type UvrD and UvrDΔ2B should be present. The mutation rate of GE1752/pET11d- UvrDΔ2B was not significantly different from that of GE1752 (P value > 0.05), suggesting no dominant negative interaction between the wild-type and UvrDΔ2B alleles.

Despite being shown to be an active in the above *in vitro* assays, UvrDΔ2B did not complement the loss of the wild-type enzyme in the mutation assays. It is possible that the deletion of the 2B subdomain renders UvrD unable to interact with the appropriate MMR proteins required to facilitate repair. It has been suggested that MutL recruits UvrD to the nicked d(GATC) site during MMR to initiate unwinding *in vivo* and direct evidence shown that MutL stimulates the unwinding activity of UvrD *in vitro* (37). The effect of MutL on the helicase activity of UvrD and UvrDΔ2B was examined (Fig. 23). MutL stimulates the unwinding activity of wild-type UvrD as shown previously. However, MutL does not have any effect on the helicase activity of UvrDΔ2B.

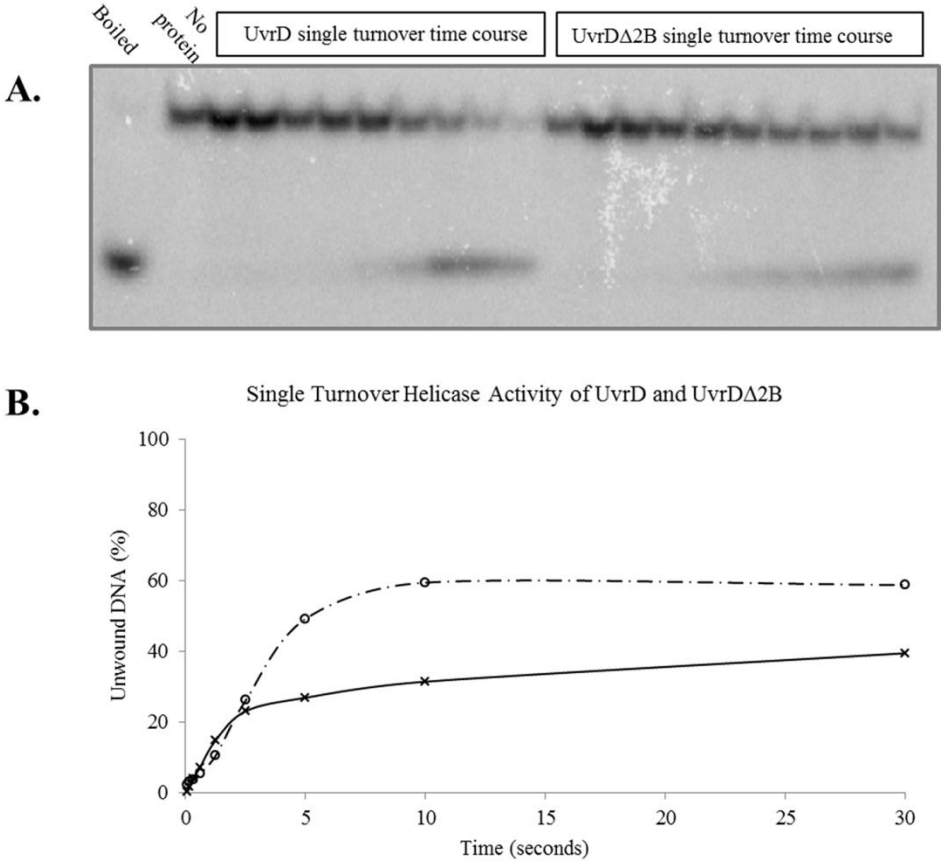

Figure 21. UvrDΔ2B exhibits a decreased helicase activity in single turnover, rapid quench reactions. Panel A – DNA helicase single turnover rapid quench reactions were performed as described under "Materials and Methods" using a 24 bp partial duplex substrate and increasing time. The first two lanes are controls for heat denatured substrate and for no magnesium chloride ($MgCl_2$). The remaining lanes depict a time course from 0.075 to 30 seconds for both UvrD and UvrDΔ2B. Panel B – Quantitative data from 3 experiments for UvrD (open circles) and UvrDΔ2B (crosses) were plotted as an average.

Table 5. Strains examined in the UvrDΔ2B study

Strain	Relevant Genotype	Source
GE1752	*metE*::cam	G. Weinstock
GE1752ΔuvrD	GE1752 *metE*$^{+}$ ΔuvrD::tet^{r}	This laboraatory

Table 6. Spontaneous mutation rates of strains expressing UvrD or UvrDΔ2B

Strain	Mutation Rate (x 10^{-8})	Relative Mutability
GE1752	2.13	1.0
GE1752ΔuvrD	54.2	25.5
GE1752ΔuvrD, pET11d-UvrD	6.41	3.0
GE1752ΔuvrD, pET11d-UvrDΔ2B	37.6	17.6
GE1752, pet11d-UvrDΔ2B	0.76	0.36

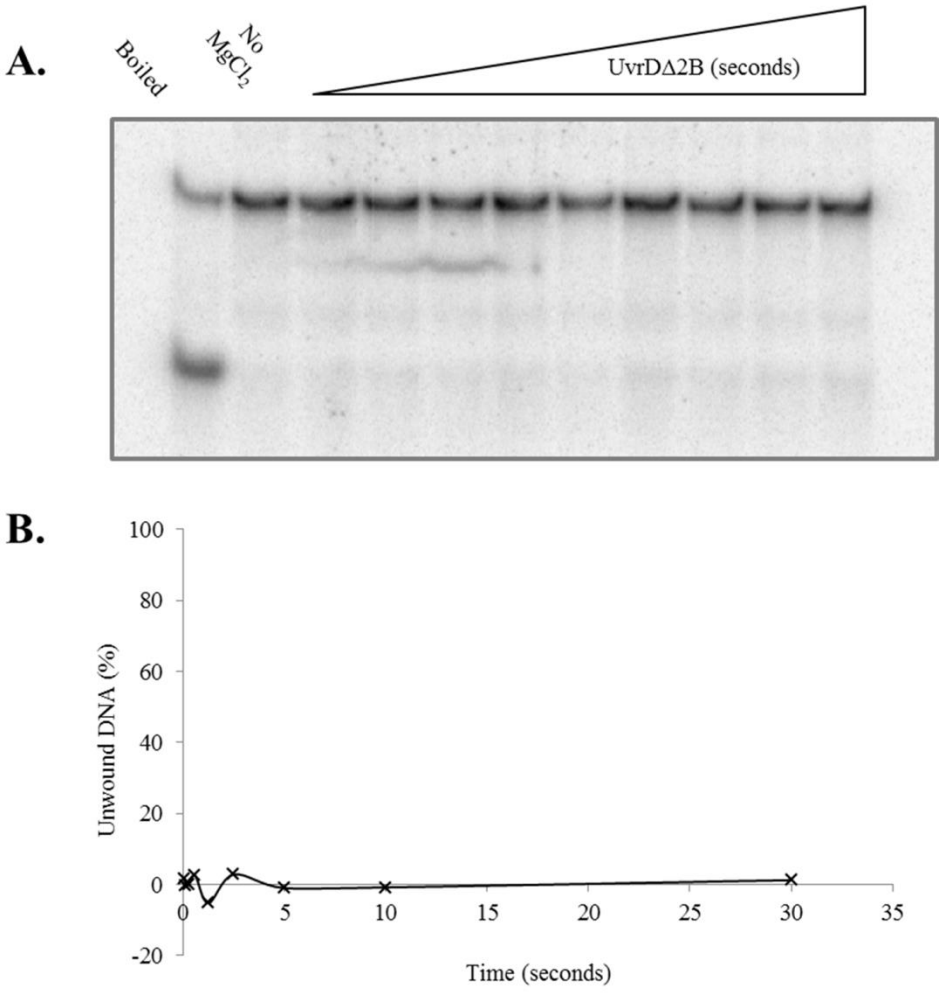

Figure 22. UvrDΔ2B does not exhibit helicase activity as a monomer. Panel A – DNA helicase single turnover rapid quench reactions were performed as described under "Materials and Methods" using a 24 bp partial duplex substrate and increasing time. The first two lanes are controls for heat denatured substrate and for no magnesium chloride ($MgCl_2$). The remaining lanes depict a time course from 0.075 to 30 seconds for UvrDΔ2B. Panel B – Quantitative data from 2 experiments for UvrDΔ2B (crosses) were plotted as an average.

A physical interaction between UvrD and MutL has been observed *in vitro*, but little is known about the interaction sites between the two proteins. The interaction between MutL and UvrD is also thought to be crucial for mismatch repair *in vivo*. The increased spontaneous mutation rate observed in the strain expressing UvrDΔ2B and the lack of MutL-stimulated helicase activity may suggest that the 2B subdomain is required for interaction with MutL. The interaction between MutL and UvrDΔ2B was examined using both far western blotting and immunoprecipitation (Fig. 24). Both techniques demonstrated that the interaction between MutL and UvrDΔ2B was either abolished or severely weakened. These data are consistent with the idea that the 2B subdomain is required for physical interaction between these proteins. This observation also indicates that UvrDΔ2B may be unable to participate in mismatch repair due to an inability to stably interact with MutL.

To investigate the activity of UvrDΔ2B in another DNA repair pathway requiring UvrD activity, NER, a UV sensitivity assay was performed. Plasmids containing *uvrD* (pET11d-UvrD), or *uvrDΔ2B* (pET11d-UvrDΔ2B) were transformed into *E. coli* GE1752 and GE1752Δ*uvrD* and used to qualitatively measure the UV sensitivity of the cells. The strains were stuck out onto LB plates and exposed to short wavelength UV light for 0-50 seconds. The GE1752 and GE1752*ΔuvrD*/pET11D-UvrD strains recovered from the UV exposure, the GE1752*ΔuvrD* and GE1752*ΔuvrD*/pET11d-UvrDΔ2B strains did not (Fig. 25)

Discussion

Expression and purification of a UvrDΔ2B mutant was previously reported to be difficult, due to an apparent lethality upon expression of the helicase. In the creation of the RepΔ2B

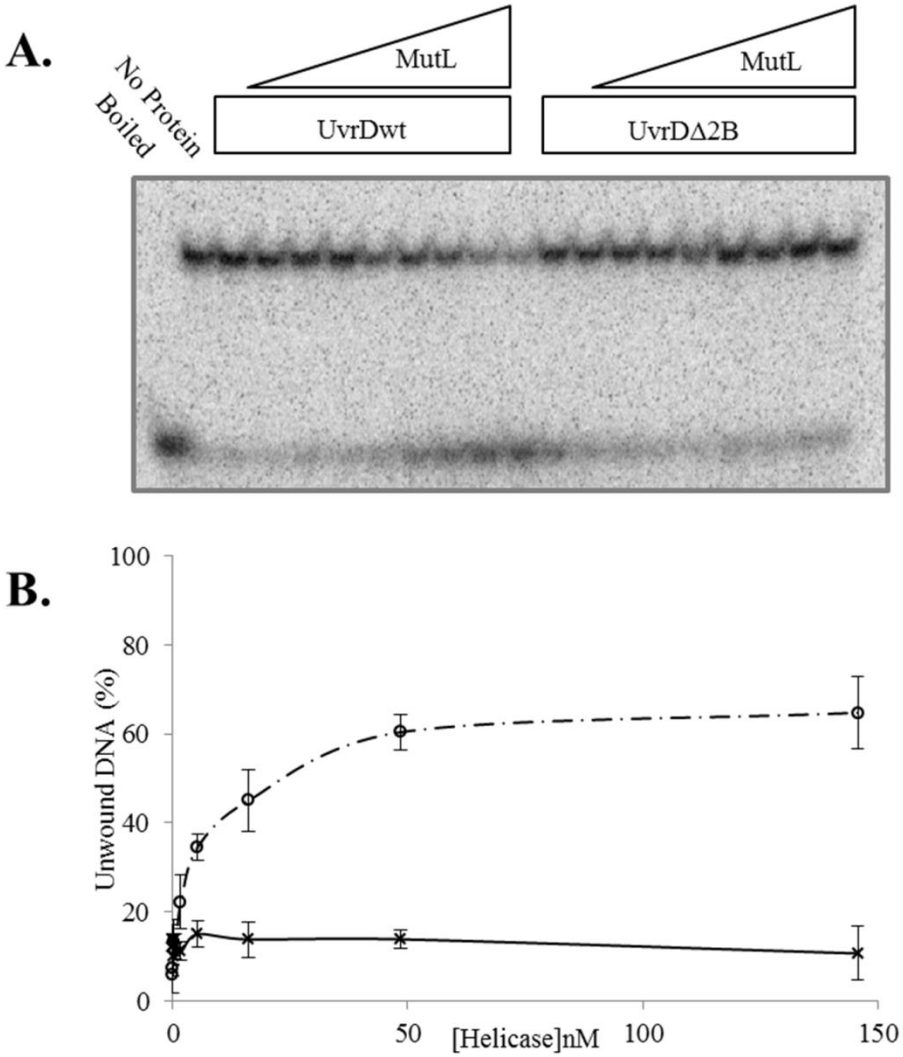

Figure 23. MutL does not stimulate the helicase activity of the UvrDΔ2B mutant. Panel A – DNA helicase reactions were performed as described under "Materials and Methods" using the 24 bp partial duplex substrate, a fixed concentration of wild-type UvrD or UvrDΔ2B (0.5 nM) and increasing concentrations of MutL. The first two lanes are controls for no protein and heat denatured substrate DNA. The remaining lanes depict a protein titration of increasing concentration from 0 to145 nM MutL dimer. Panel B – Quantitative data from 2 experiments at the indicated concentrations of MutL (closed squares) were plotted as the average at each protein concentration. Error bars represent the standard deviation about the mean.

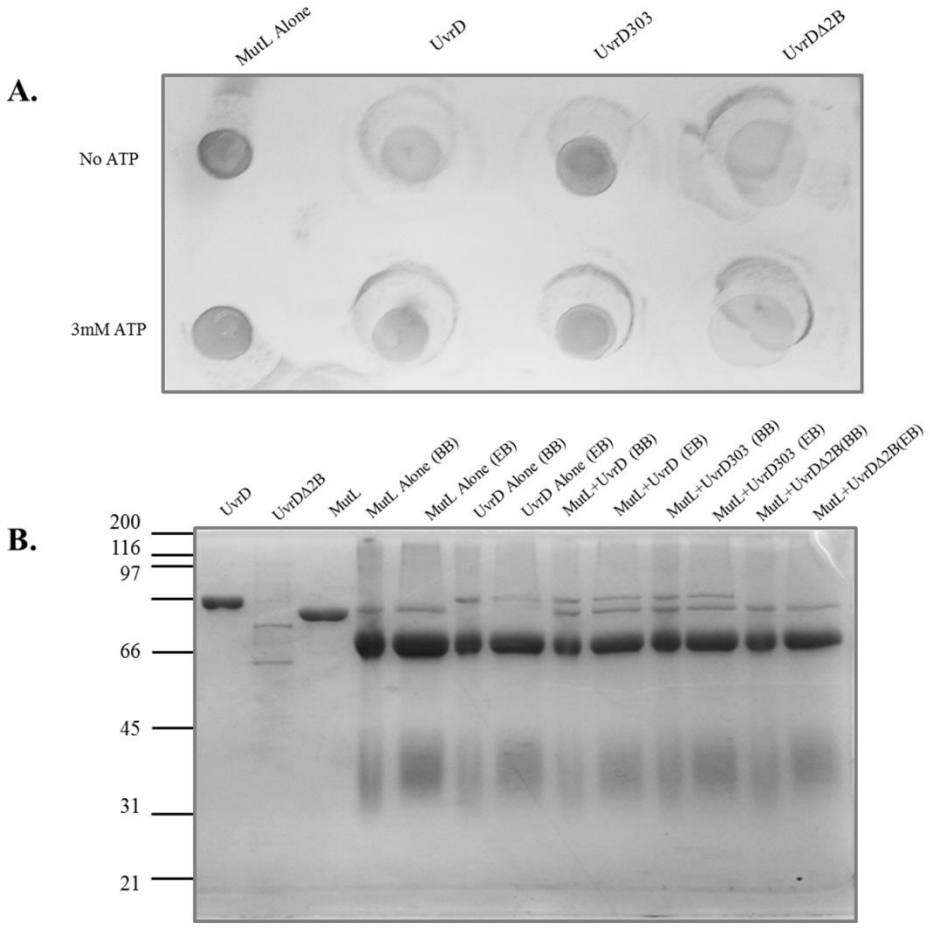

Figure 24. UvrDΔ2B exhibits a much weaker physical interaction with MutL. Panel A – Interaction between UvrD, UvrD303 and UvrDΔ2B was assayed for using a far western blot as described under "Material and Methods." The interaction between MutL and the helicases was assayed in both the presence and absence of ATP (3 mM). Panel B – Immunoprecipitation of MutL/UvrD complexes was performed as described under "Materials and Methods." The first 3 lanes depict wild-type UvrD, UvrDΔ2B, and MutL. The remaining lanes are the result of eluting the MutL/UvrD complexes from the protein A/G coated beads (eluted from beads, EB) or boiling the beads after elution (boiled beads, BB).

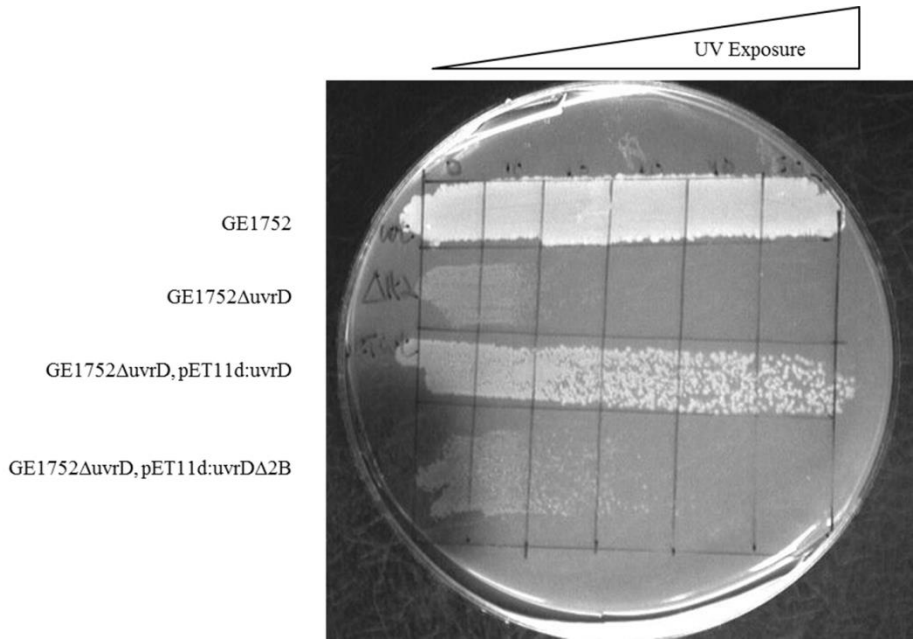

Figure 25. Expression of UvrDΔ2B results in UV sensitive phenotype. The indicated strains were exposed to short wavelength UV light as indicated under "Materials and Methods."

mutant, the entirety of the 2B subdomain was removed by replacing the 375th -542nd amino acids with three glycines. We modeled the UvrD 2B deletion mutant described here on the RepΔ2B mutant described previously (28, 29) and connected the two consecutive glycines (G378, G379) at the N-terminus of the 2B subdomain to G545, removing ~93% of the 2B subdomain (see Fig. 18). Based on observations made with Rep protein, it was suggested that the removal of the 2B subdomain from UvrD might produce an unregulated helicase, and that this unregulated activity might somehow be responsible for the apparent lethality of cells expressing UvrDΔ2B. However, we observed robust expression of UvrDΔ2B under our conditions (see Fig. 19). Perhaps the expression vector used here, pTYB4-His, which fuses a ~55kDa C-terminal intein tag to the helicase (25) provides an explanation. The tag on the fusion construct expressed in the cell may be large enough to prevent the helicase from performing unregulated activities that result in cell death. Alternatively, we expressed UvrDΔ2B using an autoinduction method (31). Autoinduction is thought to cause expression of the intended protein more slowly than an IPTG induction and perhaps this slower expression abated any lethal effects of UvrDΔ2B. We cannot formally exclude the possibility that by retaining the 13 amino acids from the 2B subdomain, the resulting helicase is somehow able to be expressed although this seems unlikely since more than 90% of the 2B subdomain has been removed. These explanations are all speculative and, whatever the reason, expression of UvrDΔ2B has been achieved.

Unfortunately, purification of the protein proved much more challenging than its expression. For reasons that are not clear, efficient cleavage of the intein to remove the affinity tags was very inefficient and the preparations of the protein used for biochemical studies are not pure. Nevertheless, we sought to gain some new information from biochemical studies using the protein preparations in hand.

Previous studies with UvrD have shown that a dimer or higher ordered oligomer is required to for helicase activity *in vitro* (34). The region(s) of UvrD involved in the oligomerization are not known. It is clear from the single turnover and multiple turnover helicase assays that excess UvrDΔ2B is able to catalyze unwinding of the substrate DNA. These data may suggest that the 2B subdomain is not required for the oligomerization of UvrDΔ2B into an active complex. Deletion of the 2B subdomain in Rep activates the monomeric helicase activity in Rep (29), but no monomeric helicase activity was observed partially purified preparations of UvrDΔ2B. While the 2B subdomain may be acting in an autoinhibitory manner in Rep, attenuating the helicase activity of the wild-type protein and preventing the monomeric form of the helicase from initiating unwinding, neither of these effects were observed when investigating UvrDΔ2B. In fact, UvrDΔ2B was observed to be a somewhat more anemic helicase than wild-type UvrD and the monomer form of UvrDΔ2B exhibited no unwinding activity. These data may suggest that, although these two helicases are similar in their structure and amino acid composition, they possess different methods of regulating their helicase activity.

It was shown that RepΔ2B was capable of supporting ϕX174 phage replication comparable to wild-type Rep, indicating that the 2B subdomain was not crucial for Rep helicase to perform this role in the cell (28). UvrDΔ2B, on the other hand, was unable to substitute for wild-type UvrD in both post-replicative MMR and in NER. Mutations within the UvrD 2B subdomain have been shown to impact DNA repair efficiency in previous studies (38, 39). Strains expressing the UvrD303 hyper-helicase exhibit UV sensitivity not because of an inability to interact with the UvrABC complex, but due to an error in RecA-mediated recombination repair (38). While it is currently unclear whether UvrDΔ2B is able to interact with the UvrABC

complex or RecA, it is clear that strains expressing UvrDΔ2B are more sensitive to UV light exposure than wild-type strains.

One possible explanation for the loss of efficient MMR is the apparent loss of the interaction between UvrD and MutL. These two proteins have been shown to physically interact *in vitro* and *in vivo*, but the site of their interaction has never been fully elucidated (37, 40). Two different assays, far western and immunoprecipitation, suggest that the UvrD 2B subdomain may be critical for effective or stable interaction with MutL. Moreover, MutL has been shown to have a significant stimulatory effect on the helicase activity of UvrD (Chapter 3). This stimulation is thought to be necessary, enabling UvrD to unwind the long stretches of DNA required for efficient mismatch repair. However, MutL was not able to stimulate the helicase activity of UvrDΔ2B. In addition, MutL has been shown to have no stimulatory effects on UvrD303, which contains a mutation in the 2B subdomain (Chapter 3). However, the 303 mutation does not abolish the interaction between UvrD and MutL. We suggest that the 2B subdomain may be necessary for effective interaction between MutL and UvrD.

The role of the 2B subdomain in SF1 is, as yet, not clear. Data presented here are consistent with the idea this subdomain of UvrD is necessary for interactions with other proteins. Data presented previously with Rep helicase (28, 29) suggested an autoregulatory role. While both investigations converge on the idea of a regulatory role, more work needs to be done to fully appreciate the role of the 2B subdomain and the significance of the closed and open conformations of these helicases.

REFERNCES

1. Matson SW, Bean DW, George JW. DNA helicases: Enzymes with essential roles in all aspects of DNA metabolism. Bioessays 1994 Jan;16(1):13-22.

2. Egelman EH. Bacterial helicases. J Struct Biol 1998 Dec 15;124(2-3):123-8.

3. Bochman ML, Schwacha A. The mcm complex: Unwinding the mechanism of a replicative helicase. Microbiol Mol Biol Rev 2009 Dec;73(4):652-83.

4. Abdelhaleem M. Helicases: An overview. Methods Mol Biol 2010;587:1-12.

5. Bachrati CZ, Hickson ID. RecQ helicases: Guardian angels of the DNA replication fork. Chromosoma 2008 Jun;117(3):219-33.

6. Gupta R, Brosh RM,Jr. DNA repair helicases as targets for anti-cancer therapy. Curr Med Chem 2007;14(5):503-17.

7. Chu WK, Hickson ID. RecQ helicases: Multifunctional genome caretakers. Nat Rev Cancer 2009 Sep;9(9):644-54.

8. Brosh RM,Jr, Bohr VA. Human premature aging, DNA repair and RecQ helicases. Nucleic Acids Res 2007;35(22):7527-44.

9. Yamaguchi M, Dao V, Modrich P. MutS and MutL activate DNA helicase II in a mismatch-dependent manner. J Biol Chem 1998 Apr 10;273(15):9197-201.

10. Lahue RS, Au KG, Modrich P. DNA mismatch correction in a defined system. Science 1989 Jul 14;245(4914):160-4.

11. Husain I, Van Houten B, Thomas DC, Abdel-Monem M, Sancar A. Effect of DNA polymerase I and DNA helicase II on the turnover rate of UvrABC excision nuclease. Proc Natl Acad Sci U S A 1985 Oct;82(20):6774-8.

12. Dao V, Modrich P. Mismatch-, MutS-, MutL-, and helicase II-dependent unwinding from the single-strand break of an incised heteroduplex. J Biol Chem 1998 Apr 10;273(15):9202-7.

13. Bruni R, Martin D, Jiricny J. D(GATC) sequences influence escherichia coli mismatch repair in a distance-dependent manner from positions both upstream and downstream of the mismatch. Nucleic Acids Res 1988 Jun 10;16(11):4875-90.

14. Washburn BK, Kushner SR. Construction and analysis of deletions in the structural gene (uvrD) for DNA helicase II of escherichia coli. J Bacteriol 1991 Apr;173(8):2569-75.

15. Siegel EC. Ultraviolet-sensitive mutator strain of escherichia coli K-12. J Bacteriol 1973 Jan;113(1):145-60.

16. Ogawa H, Shimada K, Tomizawa J. Studies on radiation-sensitive mutants of E. coli. I. mutants defective in the repair synthesis. Mol Gen Genet 1968 May 3;101(3):227-44.

17. Matson SW. Escherichia coli helicase II (urvD gene product) translocates unidirectionally in a 3' to 5' direction. J Biol Chem 1986 Aug 5;261(22):10169-75.

18. Hickson ID, Arthur HM, Bramhill D, Emmerson PT. The E. coli uvrD gene product is DNA helicase II. Mol Gen Genet 1983;190(2):265-70.

19. Matson SW, George JW. DNA helicase II of escherichia coli. characterization of the single-stranded DNA-dependent NTPase and helicase activities. J Biol Chem 1987 Feb 15;262(5):2066-76.

20. Matson SW, Kaiser-Rogers KA. DNA helicases. Annu Rev Biochem 1990;59:289-329.

21. Gorbalenya AE, Koonin EV. Helicases: Amino acid sequence comparisons and structure-function relationships. Curr Opin Struct Biol 1993;3(3):419 <last_page> 429.

22. Iyer LM, Leipe DD, Koonin EV, Aravind L. Evolutionary history and higher order classification of AAA+ ATPases. J Struct Biol 2004 Apr-May;146(1-2):11-31.

23. Velankar SS, Soultanas P, Dillingham MS, Subramanya HS, Wigley DB. Crystal structures of complexes of PcrA DNA helicase with a DNA substrate indicate an inchworm mechanism. Cell 1999 Apr 2;97(1):75-84.

24. Korolev S, Hsieh J, Gauss GH, Lohman TM, Waksman G. Major domain swiveling revealed by the crystal structures of complexes of E. coli rep helicase bound to single-stranded DNA and ADP. Cell 1997 Aug 22;90(4):635-47.

25. Lee JY, Yang W. UvrD helicase unwinds DNA one base pair at a time by a two-part power stroke. Cell 2006 Dec 29;127(7):1349-60.

26. Jia H, Korolev S, Niedziela-Majka A, Maluf NK, Gauss GH, Myong S, Ha T, Waksman G, Lohman TM. Rotations of the 2B sub-domain of E. coli UvrD helicase/translocase coupled to nucleotide and DNA binding. J Mol Biol 2011 Aug 19;411(3):633-48.

27. Velankar SS, Soultanas P, Dillingham MS, Subramanya HS, Wigley DB. Crystal structures of complexes of PcrA DNA helicase with a DNA substrate indicate an inchworm mechanism. Cell 1999 Apr 2;97(1):75-84.

28. Cheng W, Brendza KM, Gauss GH, Korolev S, Waksman G, Lohman TM. The 2B domain of the escherichia coli rep protein is not required for DNA helicase activity. Proc Natl Acad Sci U S A 2002 Dec 10;99(25):16006-11.

29. Brendza KM, Cheng W, Fischer CJ, Chesnik MA, Niedziela-Majka A, Lohman TM. Autoinhibition of escherichia coli rep monomer helicase activity by its 2B subdomain. Proceedings of the National Academy of Sciences 2005;102(29):10076.

30. Lohman TM, Tomko EJ, Wu CG. Non-hexameric DNA helicases and translocases: Mechanisms and regulation. Nat Rev Mol Cell Biol 2008 May;9(5):391-401.

31. Studier FW. Protein production by auto-induction in high density shaking cultures. Protein Expr Purif 2005 May;41(1):207-34.

32. Tahmaseb K, Matson SW. Rapid purification of helicase proteins and in vitro analysis of helicase activity. Methods 2010 Jul;51(3):322-8.

33. Runyon GT, Wong I, Lohman TM. Overexpression, purification, DNA binding, and dimerization of the escherichia coli uvrD gene product (helicase II). Biochemistry 1993 Jan 19;32(2):602-12.

34. Ali JA, Maluf NK, Lohman TM. An oligomeric form of E. coli UvrD is required for optimal helicase activity. J Mol Biol 1999 Nov 5;293(4):815-34.

35. Lea DE, Coulson CA. The distribution of the numbers of mutants in bacterial populations. J Genet 1949 Dec;49(3):264-85.

36. George JW, Brosh RM,Jr, Matson SW. A dominant negative allele of the escherichia coli uvrD gene encoding DNA helicase II. A biochemical and genetic characterization. J Mol Biol 1994 Jan 14;235(2):424-35.

37. Mechanic LE, Frankel BA, Matson SW. Escherichia coli MutL loads DNA helicase II onto DNA. J Biol Chem 2000 Dec 8;275(49):38337-46.

38. Centore RC, Leeson MC, Sandler SJ. UvrD303, a hyperhelicase mutant that antagonizes RecA-dependent SOS expression by a mechanism that depends on its C terminus. J Bacteriol 2009 Mar;191(5):1429-38.

39. Zhang G, Deng E, Baugh L, Kushner SR. Identification and characterization of escherichia coli DNA helicase II mutants that exhibit increased unwinding efficiency. J Bacteriol 1998 Jan;180(2):377-87.

40. Hall MC, Jordan JR, Matson SW. Evidence for a physical interaction between the escherichia coli methyl-directed mismatch repair proteins MutL and UvrD. EMBO J 1998 Mar 2;17(5):1535-41.

CHAPTER 5: CONCLUDING REMARKS

The research presented in this thesis has provided a greater understanding of the role of the 2B subdomain in Superfamily 1 helicases. Using UvrD as a model, this thesis provides new information supporting that the 2B subdomain is responsible for regulating the unwinding activity of this class of helicases.

The dichotomy in unwinding activity and DNA repair roles of UvrD is not well understood. That such a poorly processive helicase evolved to responsible for the potentially lengthy repair events of MMR seems contradictory. That UvrD can be stimulated to exhibit more robust helicase activity seemingly in line with one of its biological function may offer insights into the regulation of SF1 helicases. Other members of this family, such as Rep, regulate their activity with the 2B subdomain, but the role of the 2B subdomain in UvrD is not known. When the 2B subdomain is closed, the helicase may exhibit a modest unwinding processivity. This level of unwinding appears to be sufficient to complete short unwinding events, such as the ~12 bp unwinding required for effective repair in NER (18, 19). The work presented here suggests that, if the 2B subdomain is opened, perhaps even only partially, the helicase activity can be dramatically stimulated. The enhanced unwinding observed may serve to enable UvrD to unwind DNA duplexes of sufficient length to facilitate repair of post-replicative mismatches, as is required for MMR.

In Chapter 2, I reported that a mutant variant of UvrD (UvrD303), containing a previously discovered two amino acid substitution of residues 403 and 404 (both D→A) in the 2B subdomain (1) exhibits a dramatically stimulated helicase activity. The data reported in

Chapter 2 demonstrate that several of the biochemical characteristics of UvrD303, such as DNA binding and ATPase activity, are modestly increased compared to the wild-type helicase. My investigation shows that this increase in helicase activity stems from an increase in the enzyme's processivity. Taken together the data in this study is consistent with the idea that the 2B subdomain may regulate the activity of the helicase and govern the extent to which UvrD can unwind DNA.

The studies in Chapter 3 focused on two *E. coli* proteins, MutL and UvrD, and how MutL stimulates the helicase activity of UvrD. Previous work suggests that MutL plays a role in loading UvrD onto the DNA at the nicked d(GATC) site to facilitate displacement of the error containing DNA strand (2-7). This study offers additional data to suggest that MutL increases the processivity of UvrD, enabling the helicase to unwind longer tracts of DNA than it could alone. The data presented in Chapter 3 shows that MutL stimulates the processivity of UvrD by more than 3-fold under single turnover conditions. These data suggest that the MutL-mediated stimulation of UvrD assists in unwinding stretches of DNA of the required length to faithfully complete repair in the MMR pathway.

Finally, in Chapter 4 I present *in vitro* and *in vivo* evidence of the activity of UvrDΔ2B helicase, a UvrD variant that lacks the 2B subdomain. Previous work had suggested that the expression of this protein was lethal, perhaps due to some anticipated unregulated helicase activity (8). Unlike the closely related Rep helicase, which exhibited an increase in helicase activity when the 2B subdomain was removed (8, 9), UvrDΔ2B exhibited a decrease in helicase activity. Strains expressing UvrDΔ2B in place of the wild-type helicase exhibited a mutator phenotype similar to a *ΔuvrD* strain, possibly due to an inability of UvrDΔ2B to perform in

MMR. Lastly, strains expressing the UvrDΔ2B protein also exhibit a UV sensitive phenotype, although it is unclear as to what aspect of this repair process is defective.

As with many scientific endeavors, often more information leads to more questions. Although these studies have yielded some additional insights into the role of the 2B subdomain in UvrD, there is still much that is unknown about the precise function of this subdomain in regulating and coordinating the activity of UvrD. The following sections will present approaches and hypotheses concerning the activity of the 2B subdomain and the role it plays in modulating UvrD helicase activity.

Mutations within the 2B subdomain stimulate the helicase activity of UvrD

The data presented in the Chapter 2 offers an explanation as to how the 303 mutation conveys a so called "hyper-helicase" activity. Although UvrD303 exhibits an increased processivity, it is unclear if this mutation alters the mechanism by which the helicase unwinds DNA. It has been documented that the 2B subdomain is capable of adopting two different conformations, open and closed (10, 11). It has been suggested that when the 2B subdomain is in the open conformation, the helicase may be capable of unwinding DNA via a strand displacement mechanism (10), much like a train on a track, "plowing through" the duplex and separating the complementary strands. Previous work has shown that the 2B subdomain is in a more open conformation when bound to ssDNA (11). Additionally, the processivity of UvrD as a translocase is nearly identical to that of the helicase processivity of UvrD303 (12). One interpretation of these results hypothesizes thatUvrD303 employs this strand displacement mechanism for unwinding duplex DNA in contrast to the "wrench and inchworm" unwinding mechanism that has been suggested for wild-type UvrD (10). I speculate that UvrD303 may be using this alternate unwinding mechanism due to the mutation preventing the 2B subdomain of

the helicase from adopting a closed conformation. Perhaps the mutant 2B subdomain is unable to make or maintain contacts with the 1B subdomain. If this were the case, it should be possible to generate a mutant of UvrD that contains mutations within the 1B subdomain that would be equally capable of disrupting the closed conformation of UvrD and recapitulating the hyper-helicase phenotype exhibited by UvrD303.

Both the 403rd and 404th amino acids must be mutated to achieve the hyper-helicase activity observed in UvrD303 (1). A careful examination of the UvrD crystal structure resulted in the prediction that the 403rd amino acid might have a role in stabilizing the previously reported interaction site between subdomains 2B and 1B via amino acids R396 and D118 (10). Additionally, I determined that the 404th amino acid was in a position to interact with amino acid R183 in the 1B subdomain. Unfortunately, neither double mutant exhibited hyper-helicase activity. Although my attempts at localizing the "contact points" of the 2B and 1B subdomains have not been successful, it may be possible to construct a helicase that exhibits UvrD303-like hyper-helicase activity via mutations in the 1B subdomain.

Previous work has attempted to ascertain the positioning of the 2B subdomain under various conditions such as DNA binding and nucleotide occupancy using intramolecular fluorescence resonance energy transfer (FRET) (11). In these experiments, the 2B subdomain and either the 2A or 1B subdomains were labeled with a dye pair that could report on the relative position of the 2B subdomain. By using a salt titration the helicase could be forced into a completely open conformation (at 600 mM NaCl) or a completely closed conformation (20 mM NaCl). The wild-type helicase was observed to adopt an intermediate conformation (~60% open) upon binding to ssDNA and to duplex DNA with a 3′ ssDNA tail (11). If these experiments could be performed with UvrD303, the results would directly examine the

positioning of the mutant 2B subdomain compared to the wild-type protein. Additionally, it may be possible to determine if the UvrD303 2B subdomain is even capable of adopting the closed conformation.

The position of the 2B subdomain may play a direct role in the regulation of DNA repair pathways like MMR. It has been shown that strains expressing the UvrD303 helicase from either the chromosome or plasmid exhibit an antimutator phenotype (1, 13), suggesting an increase in the effectiveness of the MMR system. It has been reported that the efficient repair of mismatches decreases as the distance from the site of unwinding initiation to the mismatch increases (14). It stands to reason that the increased processivity of UvrD303 enables the helicase to unwind to more distant mismatches, facilitating their repair. These data may suggest some balance between an "appropriate" amount of stimulated unwinding and an excessive amount. The mutation in UvrD303 may result in an unregulated helicase, unwinding farther than is required. The interaction of UvrD by MutL increases the helicase activity only about half that of the 303 mutation, in a single turnover (Chapter 3). This regulated amount of DNA unwinding may serve to maintain the integrity of the *E. coli* genome while also allowing for a measured amount of variation, which can be beneficial to future generations, i.e. adaptation. A greater understanding of the 303 mutation and its effects on DNA repair will provide insight into the mechanism of how the 2B subdomain is capable of impacting helicase activity.

MutL stimulates the helicase activity of UvrD by increasing the processivity

The interaction between MutL and UvrD has been previously examined with respect to mismatch repair in the cell. Studies have demonstrated a physical interaction between MutL and UvrD, and that MutL stimulates the helicase activity of UvrD *in vitro* (2-7). UvrD has been shown to have an unwinding activity on the order of ~35bp unwound in a single unwinding event

in vitro (15, Chapter 2). However, in MMR UvrD is required to displace an error containing strand that can be upwards of 1 kilobase away from the site of unwinding initiation (3). It would make sense that UvrD would benefit from a partner to enhance its ability to unwind DNA. The work presented here offers evidence to suggest that MutL stimulates the unwinding activity of UvrD by increasing the processivity of UvrD more than 3-fold in a single unwinding event.

There were two hypothesized mechanism for the stimulation of UvrD by MutL presented in Chapter 3. MutL may recruit UvrD molecules to the DNA so that as one unwinding unit dissociates, another would be poised to continue the unwinding process. Alternatively, MutL could be acting as a processivity factor, clamping UvrD on the DNA. Other processivity factors, such as PCNA or the β-clamp, tether DNA polymerases to the DNA to increase the efficiency of DNA replication (17). MutL may act in a similar manner and translocate with UvrD as it unwinds the DNA. The data from our single turn over experiments seems to indicate that the latter would be possible, since any free UvrD molecules would be sequestered by the trap and no longer be available for recruitment by MutL. These results may indicate that MutL can translocate with UvrD during an unwinding event, but does not exclude the iterative loading model. Both models may operate in conjunction, and combined yield sufficient unwinding activity to reach mismatches upwards of 1 kilobase from unwinding initiation site.

The stimulatory effect of MutL is not observed with the mutant helicase UvrD303. This lack of stimulation was not due to the inability of the two proteins to interact, as far westerns confirmed the interaction between MutL and UvrD303. These data may suggest that whatever impact the interaction of MutL has on UvrD helicase activity, it is mimicked by the UvrD303 mutation. If MutL were acting as a clamp, it would be logical that MutL would still be able to constrain UvrD303 onto the DNA and produce a more processive helicase. Since that outcome

was not observed, it may be that MutL alters the conformation of the 2B subdomain enabling the wild-type helicase to become more processive in a manner similar to the effect of the 303 mutation.

The 2B subdomain of UvrD is required for effective DNA repair, but not for helicase activity

The role of the 2B subdomain in UvrD has never been fully examined due to an apparent lethality of expressing a UvrDΔ2B mutant (8). In the closely related Rep helicase, the deletion of the 2B subdomain has a dramatic impact on the helicase activity of Rep, stimulating the helicase activity compared to the wild type helicase. Additionally, the RepΔ2B mutant was able to catalyze DNA separation as a monomer, something the wild-type Rep cannot do (8, 9). These data have led to the supposition that the 2B subdomain plays an autoinhibitory role in regulating the helicase activity of Rep and perhaps all SF1 helicases (8, 9). As stated in Chapter 4, the experimental data indicate that UvrDΔ2B does not possess a stimulated helicase activity. In single turnover reactions, the helicase activity of UvrDΔ2B was only about half as robust as that of the wild-type UvrD. These data may suggest that while the 2B subdomain might not be required for the helicase activity of UvrD, it is apparently beneficial.

The removal of the 2B subdomain from UvrD resulted in a mutator and UV sensitive phenotype when the mutant was expressed, indicating that UvrDΔ2B is defective in its ability to perform in DNA repair. When investigated, UvrDΔ2B expressing strains exhibited a mutation rate similar to that of a *ΔuvrD* strain. This apparent defect in MMR may be due to UvrDΔ2B's apparent inability to interact with MutL. The results from the far western and the immunoprecipitation suggest a lack of physical interaction between MutL and the mutant helicase. The observed lack of MutL mediated stimulation of the helicase activity may indicate

that without the increase in unwinding conveyed by MutL, UvrDΔ2B cannot sufficiently unwind DNA to perform MMR. The UV sensitivity of a UvrDΔ2B strain could be due to an inability of the mutant helicase to perform in NER. This may be due to a lack of interaction with the UvrABC complex, but there is no data to confirm this hypothesis. Alternatively, it was observed that UvrD303 strains also exhibit UV sensitivity, but the defect lies not in NER, but in RecA mediated recombination (13). A similar recombination defect may be occurring in UvrDΔ2B and merits further investigation.

Through these studies, significant advancements to understanding how the 2B subdomain functions to regulate the helicase activity of UvrD have been made. These data paint a clear picture that the 2B subdomain is integral not only for proper unwinding facilitated by UvrD, but the proper organization of UvrD with other DNA repair partners. Further study of the 2B subdomain in other SF1 helicase may reveal more information about the role of this structure in DNA helicase activity. Does the 2B subdomain function in an autoinhibitory manner in other SF1 helicases as it does in Rep? Is the 2B subdomain used in the coordination of the helicase and other DNA repair proteins to facilitate the repair of damaged DNA as it might in UvrD? As none of the seven conserved helicase motifs are found within the 2B subdomain in SF1 helicases, it may be the case that this subdomain is not directly involved in the unwinding of the duplex DNA, but used to target the SF1 helicase to the correct substrate and regulate its activity once there. A more detailed examination of this subdomain may yield new data pertaining to how this class of helicases performs its roles in the cell.

REFERENCES

1. Zhang G, Deng E, Baugh L, Kushner SR. Identification and characterization of Escherichia coli DNA helicase II mutants that exhibit increased unwinding efficiency. J Bacteriol 1998 Jan;180(2):377-87.

2. Hall MC, Jordan JR, Matson SW. Evidence for a physical interaction between the Escherichia coli methyl-directed mismatch repair proteins MutL and UvrD. EMBO J 1998 Mar 2;17(5):1535-41.

3. Modrich P, Lahue R. Mismatch repair in replication fidelity, genetic recombination, and cancer biology. Annu Rev Biochem 1996;65:101-33.

4. Robertson AB, Pattishall SR, Gibbons EA, Matson SW. MutL-catalyzed ATP hydrolysis is required at a post-UvrD loading step in methyl-directed mismatch repair. J Biol Chem 2006 Jul 21;281(29):19949-59.

5. Mechanic LE, Frankel BA, Matson SW. Escherichia coli MutL loads DNA helicase II onto DNA. J Biol Chem 2000 Dec 8;275(49):38337-46.

6. Dao V, Modrich P. Mismatch-, MutS-, MutL-, and helicase II-dependent unwinding from the single-strand break of an incised heteroduplex. J Biol Chem 1998 Apr 10;273(15):9202-7.

7. Yamaguchi M, Dao V, Modrich P. MutS and MutL activate DNA helicase II in a mismatch-dependent manner. J Biol Chem 1998 Apr 10;273(15):9197-201.

8. Cheng W, Brendza KM, Gauss GH, Korolev S, Waksman G, Lohman TM. The 2B domain of the Escherichia coli rep protein is not required for DNA helicase activity. Proc Natl Acad Sci U S A 2002 Dec 10;99(25):16006-11.

9. Brendza KM, Cheng W, Fischer CJ, Chesnik MA, Niedziela-Majka A, Lohman TM. Autoinhibition of Escherichia coli rep monomer helicase activity by its 2B subdomain. Proceedings of the National Academy of Sciences 2005;102(29):10076.

10. Lee JY, Yang W. UvrD helicase unwinds DNA one base pair at a time by a two-part power stroke. Cell 2006 Dec 29;127(7):1349-60.

11. Jia H, Korolev S, Niedziela-Majka A, Maluf NK, Gauss GH, Myong S, Ha T, Waksman G, Lohman TM. Rotations of the 2B sub-domain of E. coli UvrD helicase/translocase coupled to nucleotide and DNA binding. J Mol Biol 2011 Aug 19;411(3):633-48.

12. Tomko EJ, Fischer CJ, Lohman TM. Single-stranded DNA translocation of E. coli UvrD monomer is tightly coupled to ATP hydrolysis. J Mol Biol 2012 Apr 20;418(1-2):32-46.

13. Centore RC, Leeson MC, Sandler SJ. UvrD303, a hyperhelicase mutant that antagonizes RecA-dependent SOS expression by a mechanism that depends on its C terminus. J Bacteriol 2009 Mar;191(5):1429-38.

14. Bruni R, Martin D, Jiricny J. D(GATC) sequences influence Escherichia coli mismatch repair in a distance-dependent manner from positions both upstream and downstream of the mismatch. Nucleic Acids Res 1988 Jun 10;16(11):4875-90.

15. Ali JA, Lohman TM. Kinetic measurement of the step size of DNA unwinding by Escherichia coli UvrD helicase. Science 1997 Jan 17;275(5298):377-80.

16. Burgers PM. Saccharomyces cerevisiae replication factor C. II. formation and activity of complexes with the proliferating cell nuclear antigen and with DNA polymerases delta and epsilon. J Biol Chem 1991 Nov 25;266(33):22698-706.

17. Stukenberg PT, Studwell-Vaughan PS, O'Donnell M. Mechanism of the sliding beta-clamp of DNA polymerase III holoenzyme. J Biol Chem 1991 Jun 15;266(17):11328-34.

18. Caron PR, Kushner SR, Grossman L. Involvement of helicase II (uvrD gene product) and DNA polymerase I in excision mediated by the UvrABC protein complex. Proc Natl Acad Sci U S A 1985 Aug;82(15):4925-9.

19. Grossman L, Caron PR, Mazur SJ, Oh EY. Repair of DNA-containing pyrimidine dimers. FASEB J 1988 Aug;2(11):2696-701.